Application to Food Standards Australia New Zealand for the Inclusion of Corn MON 87419 in *Standard 1.5.2 - Food Derived from Gene Technology*

Submitted by:

Monsanto Australia Limited
Level 12 / 600 St Kilda Road,
Melbourne Victoria 3004

7 August 2015

TABLE OF CONTENTS

LIST OF FIGURES

LIST OF TABLES

UNPUBLISHED REPORTS BEING SUBMITTED

[redacted]. Nature of 14C-Dicamba Residues in Corn Raw Agricultural Commodities Following Preemergence or Postemergence Application to Dicamba-Glufosinate Tolerant Corn. **MSL0025703**. Monsanto Company.

[redacted]. 2014. Amended Report for MSL0025770: Bioinformatics Evaluation of MON 87419 Utilizing the AD_2014, TOX_2014 and PRT_2014 Databases. **MSL0026123**. Monsanto Company. **Confidential Commercial Information**

[redacted] 2014. Amended Report for MSL0026186: Effect of Heat Treatment on the Functional Activity of *Escherichia coli* (*E. coli*)-Produced MON 87419 Phophinothricin N-acetyltransferase Protein. **MSL0026345**. Monsanto Company.

[redacted]. 2015. Amended Report for MSL0025998: Assessment of the *in vitro* Digestibility of Phosphinothricin N-Acetyltransferase (*pat*) Protein by Pepsin and Pancreatin. **MSL0026362**. Monsanto Company.

[redacted] 2014. Assessment of DMO and PAT Protein Levels in Leaf, Root, Forage, and Grain Tissues Collected from Maize MON 87419 Produced in United States Field Trials during 2013. **MSL0025758**. Monsanto Company.

[redacted]. 2014. Amended Report for MSL0025997: Assessment of the *in vitro* Digestibility of *Escherichia coli*- Produced MON 87419 DMO Protein by Pepsin and Pancreatin. **MSL0026364**. Monsanto Company.

[redacted]. 2014. Amended Report for MSL0025438: Molecular Characterization of Herbicide Tolerant Corn MON 87419. **MSL0025902.** Monsanto Company. **Confidential Commercial Information**

[redacted]. 2014. Characterization of the Phosphinothricin N-Acetyltransferase Protein Purified from the Maize Grain of MON 87419 and Comparison of the Physiochemical and Functional Properties of the Plant-Produced and *Escherichia coli* (*E. coli*)-Produced Phosphinothricin N-Acetyltransferase Proteins. **MSL0026031**. Monsanto Company.

[redacted]. 2014. Segregation Analysis of the T-DNA Insert in Herbicide Tolerant Corn MON 87419 Across Three Generations. **MSL0025519**. Monsanto Company.

[redacted]. 2014. Bioinformatics Evaluation of the DMO and PAT Proteins Utilizing the AD_2014, TOX_2014 and PRT_2014 Databases. **MSL0025907**. Monsanto Company. **Confidential Commercial Information**

[redacted]. 2014. Bioinformatics Evaluation of DNA Sequences Flanking the 5' and 3' Junctions of Inserted DNA in MON 87419: Assessment of Putative Polypeptides. **MSL0025920**. Monsanto Company. **Confidential Commercial Information**

[redacted]. 2014. Compositional Analyses of Maize Forage and Grain from Dicamba and Glufosinate Treated MON 87419 Grown in the United States during 2013. **MSL0025559**. Monsanto Company.

[redacted]. 2014. Amended Report for MSL0025999: Characterization of the Dicamba Mono-Oxygenase Protein Purified from the Maize Grain of MON 87419 and Comparison of the Physicochemical and Functional Properties of the

Plant-Produced and *Escherichia coli* (*E.coli*)-Produced Dicamba Mono-Oxygenas Proteins. **MSL0026361**. Monsanto Company.

[redacted]. 2015. Analyticial Method for the Determination of Dicamba and Major Metabolites in Raw Agricultural Commodities by LC-MS/MS. **MSL0026344**. Monsanto Company.

[redacted]. 2012. An Acute Toxicity Study of *E. coli*-produced MON 88701 DMO Administered by Oral Gavage Route to Mice. **CRO-2011-035**. Monsanto Company.

[redacted]. 2012. An Acute Toxicity Study of *E. coli*-produced Phosphinothricin N-acetyltransferase (PAT[*bar*]) Protein Administered by Oral Gavage Route to Mice. **CRO-2011-007**. Monsanto Company.

[redacted]. 2015. Summary of the Magnitude of Residues of Dicamba in Dicamba Glufosinate Tolerant Maize Grain (MON87419) after Application of Dicamba-Based Formulation. **MSL0026819**. Monsanto Company.

[redacted]. 2014. Effect of Heat Treatment of the Functional Activity of *Escherichia coli*-Produced MON 87419 DMO Protein. **MSL0025906**. Monsanto Company.

CHECKLIST

General Requirements (3.1)	Reference
3.1.1 Form of application	
☑ Executive Summary	*Executive Summary*
☑ Relevant sections of Part 3 identified	
☑ Pages sequentially numbered	
☑ Electronic + 1 hard copies	
☑ Electronic and hard copies identical	
☑ Hard copies capable of being laid flat	
☑ All references provided	
3.1.2 Applicant details	*Page 1*
3.1.3 Purpose of the application	*Page 1*
3.1.4 Justification for the application	*Page 2*
3.1.5 Information to support the application	*Volumes 1 - 4*
3.1.6 Assessment procedure	*Page 4*
☑ General	
☐ Major	
☐ Minor	
3.1.7 Confidential Commercial Information	
☑ Confidential material separated in both electronic and hard copy	
☑ Justification provided	
3.1.8 Exclusive Capturable Commercial Benefit	*Page 4*
3.1.9 International and Other National Standards	*Page 4*
3.1.10 Statutory Declaration	*Page 159*
3.1.11 Checklist/s provided with Application	
☑ Checklist	
☑ Any other relevant checklists for Sections 3.2 – 3.7	*Checklist 3.5.1*

Foods Produced using Gene Technology (3.5.1)	
☑ A.1 Nature and identity of GM food	*Page 5*
☑ A.2 History of use of host and donor organisms	*Page 7*
☑ A.3 Nature of genetic modification	*Page 12*
☑ A.4 Analytical method for detection	*Page 50*
☑ B.1 Equivalence studies	*Page 55*
☑ B.2 Antibiotic resistance marker genes (if used)	*Page 87*
☑ B.3 Characterisation of novel protein(s)/substances	*Page 88*
☑ B.4 Potential toxicity of novel protein(s)/substances	*Page 101*
☑ B.5 Potential allergenicity of novel protein(s)	*Page 127*
☑ B.6 Toxicity of novel herbicide metabolites	*Page 132*
☑ B.7 Compositional Analyses	*Page 140*
☑ C.1 Nutritional impact of GM food	*Page 161*
☑ C.2 Animal feeding studies (if available)	*Page 161*

ABBREVIATIONS AND DEFINITIONS[1]

~	approximately
AA	Amino Acid
ADF	Acid Detergent Fiber
APHIS	Animal and Plant Health Inspection Service (USDA)
bar	coding sequence of the phosphinothricin N-acetyltransferase gene from Streptomyces hygroscopicus
bp	base pair
CFR	Code of Federal Regulations
CTAB	hexadecyltrimethylammonium bromide
CTP	chloroplast transit peptide
CTP2	Chloroplast Transit Peptide, isolated from *Arabidopsis thaliana* EPSPS
CTP4	Chloroplast Transit Peptide, isolated from Petunia hybrida EPSPS
Da	Dalton
DCSA	3,6 dichlorosalicylic acid also known as 3,6-dichloro-2-hydroxybenzoic acid
dmo	coding sequence of the dicamba mono-oxygenase gene from Stenotrophomonas maltophilia encoding DMO
DMO	Dicamba mono-oxygenase protein
DNA	deoxyribonucleic acid
dw	dry weight of tissue
E. coli	*Escherichia coli* bacteria
e.g.	Exempli gratia, meaning “for example”
EDTA	Ethylenediaminetetraacetic acid
EFSA	European Food Safety Authority
EPA	Environmental Protection Agency
EPSPS	5-Enolpyruvylshikimate-3-phosphate synthase
E-score	Expectation score
et al.	et alii, et aliae, or et alia, meaning "and others"
ETS	Excellence Through Stewardship
FA	Fatty acid
FAO	Food and Agriculture Organization of the United Nations
FDA	Food and Drug Administration (U.S.)
FFDCA	Federal Food, Drug and Cosmetic Act
FLt	Full-Length transcript
FOIA	Freedom of Information Act
FSANZ	Food Standards Australia and New Zealand
fw	fresh weight of tissue
GM	Genetically modified
GRAS	Generally recognized as safe
HPLC	High Performance Liquid Chromatography
ILSI	International Life Science Institute

[1] Alred, G.J., C.T. Brusaw, and W.E. Oliu. 2003. Handbook of Technical Writing, 7th edn., pp. 2-7. Bedford/St. Martin's, Boston, MA.

ILSI-CCDB	International Life Sciences Institute – Crop Compositional Database
ILSI-CERA	International Life Sciences Institute - Center for Environmental Risk Assessment
JSA	Junction Sequence Analysis
JSC	Junction Sequence Class
kb	Kilobase
kDa	Kilodalton
kg	kilogram
LOQ	Limit of Quantitation
NDF	Neutral Detergent Fiber
ng	nanogram
NGS	Next Generation Sequencing
OECD	Organisation for Economic Co-operation and Development
ORF	open reading frame
pat	coding sequence of the phosphinothricin N-acetyltransferase gene from Streptomyces viridochromogenes
PAT	full-length phosphinothricin N-acetyltransferase protein
PBN	Premarket Biotechnology Notice
PCR	polymerase chain reaction
ppm	parts per million
RO	reverse osmosis
ROP	Repressor of Primer
S. hygroscopicus	*Streptomyces hygroscopicus*
S. maltophilia	*Stenotrophomonas maltophilia*
S. viridochromogenes	*Streptomyces viridochromogenes*
SDS	sodium dodecyl sulfate
SDS-PAGE	Sodium Dodecyl Sulfate-Polyacrylamide Gel Electrophoresis
SE	Standard Error
TDF	Total Dietary Fiber
T-DNA	Transfer DNA
Tris	Tris(hydroxymethyl)aminomethane
Tween-20	Polyoxyethylenesorbitan monolaurate
µg	microgram
U.S.	United States
U.S. EPA	United States Environmental Protection Agency
USDA	United States Department of Agriculture
USDA-APHIS	United States Department of Agriculture – Animal and Plant Health Inspection Service
UV	Ultraviolet
v/v	volume to volume ratio
VOI	Verification of Identity
w/v	weight to volume ratio
WHO	World Health Organization

PART 1 GENERAL INFORMATION

1.1 Applicant Details

(a) Applicant's name/s	[redacted]
(b) Company/organisation name	Monsanto Australia Limited
(c) Address (street and postal)	Level 12 / 600 St Kilda Road, Melbourne, Victoria, 3004 PO Box 6051, St Kilda Road Central, Victoria, 8008
(d) Telephone number	[redacted]
(e) Email address	[redacted]
(f) Nature of applicant's business	Technology Provider to the Agricultural and Food Industries
(g) Details of other individuals, companies or organisations associated with the application	

1.2 Purpose of the Application

This application is submitted to Food Standards Australia New Zealand by Monsanto Australia Limited on behalf of Monsanto Company.

The purpose of this submission is to make an application to vary **Standard 1.5.2** – *Food Produced Using Gene Technology* of the *Australia New Zealand Food Standards Code* to seek the addition of maize line MON 87419 and products containing maize line MON 87419 (hereafter referred to as MON 87419) to the Table to Clause 2 (see below).

Food derived from gene technology	Special requirements
Food derived from maize line MON 87419	None

1.3 Justification for the Application

1.3(a) The need for the proposed change

Monsanto Company has developed MON 87419 maize that is tolerant to dicamba (3,6-dichloro-2-methoxybenzoic acid) and glufosinate (2-amino-4-(hydroxymethylphosphinyl) butanoic acid) herbicides. MON 87419 contains a demethylase gene from *Stenotrophomonas maltophilia* that expresses a dicamba mono-oxygenase (DMO) protein to confer tolerance to dicamba herbicide and the phosphinothricin N-acetyltransferase (*pat*) gene from *Streptomyces viridochromogenes* that expresses the PAT protein to confer tolerance to glufosinate herbicide.

1.3(b) The advantages of the proposed change over the status quo, taking into account any disadvantages

MON 87419 will offer maize growers multiple choices for effective weed management including tough to control and herbicide resistant broadleaf weeds. The combination of these two unique herbicide mechanisms-of-action provides an effective weed management system for maize production. Dicamba provides effective control of over 95 annual and biennial weed species, and suppression of over 100 perennial broadleaf and woody plant species. Glufosinate, a broad-spectrum contact herbicide, provides nonselective control of approximately 120 broadleaf and grass weeds. Additionally, dicamba and glufosinate provide control of herbicide-resistant weeds, including glyphosate-resistant biotypes of Palmer amaranth (*Amaranthus palmeri*), marestail (*Conyza canadensis*), common ragweed (*Ambrosia artemisiifolia*), giant ragweed (*Ambrosia trifida*) and waterhemp (*Amaranthus tuberculatus*).

MON 87419 will likely be combined, through traditional breeding methods, with other deregulated events (*e.g.,* glyphosate-tolerant). The in-crop use of dicamba and glufosinate herbicides, in addition to glyphosate herbicide, provides improved weed management options in maize to control a broad spectrum of grass and broadleaf weed species and effective control of weeds resistant to several herbicide families. Additionally, MON 87419 combined with glyphosate-tolerant maize systems will provide: 1) an opportunity for an efficient, effective weed management system for hard-to-control and herbicide-resistant weeds; 2) a flexible system for two additional herbicide mechanisms-of-action for in-crop application in current maize production systems as recommended by weed science experts to manage future weed resistance development; 3) an option to delay or prevent further resistance to glyphosate and other critically important maize herbicides; 4) crop safety to dicamba, glufosinate and glyphosate; and 5) additional weed management tools to enhance weed management systems necessary to maintain or improve maize yield and quality to meet the growing needs of the food, feed, and industrial markets.

1.4 Regulatory Impact Information

1.4(a) Costs and benefits

If the draft variation to permit the sale and use of food derived from MON 87419 is approved, possible affected parties may include consumers, industry sectors and government. The

consumers who may be affected are those particularly concerned about the use of biotechnology. Industry sectors affected may be food importers and exporters, distributors, processors and manufacturers. Lastly, government enforcement agencies may be affected.

A cost/benefit analysis quantified in monetary terms is difficult to determine. In fact, most of the impacts that need to be considered cannot be assigned a dollar value. Criteria would need to be deliberately limited to those involving broad areas such as trade, consumer information and compliance. If the draft variation is approved:

Consumers:

- There would be benefits in the broader availability of corn products.
- There is unlikely to be any significant increase in the prices of foods if manufacturers are able to use comingled corn products.
- Consumers wishing to do so will be able to avoid GM corn products as a result of labeling requirements and marketing activities.

Government:

- Benefit that if corn MON 87419 was detected in food products, approval would ensure compliance of those products with the Code. This would ensure no potential for trade disruption on regulatory grounds.
- Approval of corn MON 87419 would ensure no potential conflict with WTO responsibilities.
- In the case of approved GM foods, monitoring is required to ensure compliance with the labeling requirements, and in the case of GM foods that have not been approved, monitoring is required to ensure they are not illegally entering the food supply. The costs of monitoring are thus expected to be comparable, whether a GM food is approved or not.

Industry:

- Sellers of processed foods containing corn derivatives would benefit as foods derived from corn MON 87419 would be compliant with the Code, allowing broader market access and increased choice in raw materials. Retailers may be able to offer a broader range of corn products or imported foods manufactured using corn derivatives.
- Possible cost to food industry as some food ingredients derived from corn MON 87419 would be required to be labelled

1.4(b) Impact on international trade

If the draft variation to permit the sale and use of food derived from MON 87419 was rejected it would result in the requirement for segregation of any corn derived products containing MON 87419 from those containing approved corn, which would be likely to increase the costs of imported corn derived foods.

It is important to note that if the draft variation is approved, corn MON 87419 will not have a mandatory introduction. The consumer will always have the right to choose not to use/consume this product.

1.5 Assessment Procedure

Monsanto Australia is submitting this application in anticipation that it will fall within the General Procedure category.

1.6 Exclusive Capturable Commercial Benefit

This application is likely to result in an amendment to the Code that provides exclusive benefits and therefore Monsanto intends to pay the full cost of processing the application.

1.7 International and Other National Standards

1.7(a) International standards

Monsanto makes all efforts to ensure that safety assessments are aligned, as closely as possible, with relevant international standards such as the Codex Alimentarius Commission's *Principles for the Risk Analysis of Foods Derived from Modern Biotechnology* and supporting *Guideline for the Conduct of Food Safety Assessment of Foods Derived from Recombinant-DNA Plants* (Codex Alimentarius, 2009).

In addition, the composition analysis is conducted in accordance with OECD guidelines and includes the measurement of OECD-defined corn nutrients and anti-nutrients based on conventional commercial corn varieties (OECD, 2002c).

1.7(b) Other national standards or regulations

Monsanto has submitted a food and feed safety and nutritional assessment summary for MON 87419 to the United States Food and Drug Administration (FDA) and has also requested a Determination of Nonregulated Status for MON 87419, including all progenies derived from crosses between MON 87419 and other corn, from the Animal and Plant Health Inspection Service (APHIS) of the U.S. Department of Agriculture (USDA).

Consistent with our commitments to the Excellence Through Stewardship® (ETS) Program[2], regulatory submissions have been or will be made to countries that import significant maize or food and feed products derived from U.S. maize and have functional regulatory review processes in place.

[2] Excellence Through Stewardship is a registered trademark of Excellence Through Stewardship, Washington, DC. (http://www.excellencethroughstewardship.org)

PART 2 SPECIFIC DATA REQUIREMENTS FOR SAFETY ASSESSMENT

A. TECHNICAL INFORMATION ON THE GM FOOD

A1 Nature and Identity of the Genetically Modified Food

A1(a) A description of the new GM organism

Monsanto Company has developed MON 87419 maize that is tolerant to dicamba (3,6-dichloro-2-methoxybenzoic acid) and glufosinate (2-amino-4-(hydroxymethylphosphinyl) butanoic acid) herbicides. MON 87419 contains a demethylase gene from *S. maltophilia* that expresses DMO protein to confer tolerance to dicamba herbicide and the phosphinothricin N-acetyltransferase (*pat*) gene from *S. viridochromogenes* that expresses the PAT protein to confer tolerance to glufosinate herbicide.

MON 87419 will offer maize growers multiple choices for effective weed management including tough to control and herbicide resistant broadleaf weeds. The combination of these two unique herbicide mechanisms-of-action provides an effective weed management system for maize production. Dicamba provides effective control of over 95 annual and biennial weed species, and suppression of over 100 perennial broadleaf and woody plant species. Glufosinate, a broad-spectrum contact herbicide, provides nonselective control of approximately 120 broadleaf and grass weeds. Additionally, dicamba and glufosinate provide control of herbicide-resistant weeds, including glyphosate-resistant biotypes of Palmer amaranth (*Amaranthus palmeri*), marestail (*Conyza canadensis*), common ragweed (*Ambrosia artemisiifolia*), giant ragweed (*Ambrosia trifida*) and waterhemp (*Amaranthus tuberculatus*).

MON 87419 will likely be combined, through traditional breeding methods, with other deregulated events (e.g., glyphosate-tolerant). The in-crop use of dicamba and glufosinate herbicides, in addition to glyphosate herbicide, provides improved weed management options in maize to control a broad spectrum of grass and broadleaf weed species and effective control of weeds resistant to several herbicide families. Additionally, MON 87419 combined with glyphosate-tolerant maize systems will provide: 1) an opportunity for an efficient, effective weed management system for hard-to-control and herbicide-resistant weeds; 2) a flexible system for two additional herbicide mechanisms-of-action for in-crop application in current maize production systems as recommended by weed science experts to manage future weed resistance development; 3) an option to delay or prevent further resistance to glyphosate and other critically important maize herbicides; 4) crop safety to dicamba, glufosinate and glyphosate; and 5) additional weed management tools to enhance weed management systems necessary to maintain yield and quality to meet the growing needs of the food, feed, and industrial markets.

A1(b) Name, number or other identifier of each new line or strain

In accordance with OECD's "Guidance for the Designation of a Unique Identifier for Transgenic Plants" MON 87419 has been assigned the unique identifier MON-87419-8.

A1(c) The name the food will be marketed under (if known)

Maize containing the transformation event MON 87419 will be produced in North America. There are currently no plans to produce this product in Australia and New Zealand. A commercial trade name for the product has not been determined at the time of this submission and will be available prior to commercial launch of the product in North America.

A1(d) The types of products likely to include the food or food ingredient

Maize is widely used for a variety of food and feed purposes, and it is intended that MON 87419 will be utilized in the same manner and for the same uses as conventional maize. Maize grain and its processed products are consumed in a multitude of human food and animal feed products. Maize forage (as silage) is extensively consumed as an animal feed by ruminants.

A2 History of Use of the Host and Donor Organisms

A2(a) Description of all donor organism(s)

A2(a)(i) Common and scientific names and taxonomic classification

The *dmo* gene is derived from the bacterium *S. maltophilia* strain DI-6, isolated from soil at a dicamba manufacturing plant (Krueger *et al.*, 1989). *S. maltophilia* was originally named *Pseudomonas maltophilia*, and then transferred to the genus *Xanthomonas* before it was given its own genus (Palleroni and Bradbury, 1993). The taxonomy of *S. maltophilia* is (Palleroni and Bradbury, 1993; Ryan *et al.*, 2009):

Kingdom: Bacteria

Phylum: Proteobacteria

Class: Gammaproteobacteria

Order: Xanthomonadales

Family: Xanthomonadaceae

Genus: Stenotrophomonas

The *pat* gene is derived from the bacterium *S. viridochromogenes* . The taxonomy of *S. viridochromogenes* is (Waksman and Henrici, 1943):

Kingdom: Bacteria

Phylum: Actinobacteria

Class: Actinobacteria

Order: Actinomycetales

Family: Streptomycetaceae

Genus: Streptomyces

A2(a)(ii) Information on pathogenicity, toxicity, allergenicity

S. maltophilia is an aerobic, environmentally ubiquitous, gram-negative bacterium commonly present in aquatic environments, soil and plants. *S. maltophilia* is ubiquitously associated with plants and has been isolated from the rhizosphere of wheat, maize, grasses, beet, cucumber, potato, strawberry, sugarcane, and rapeseed (Berg *et al.*, 1996; Berg *et al.*, 1999; Berg *et al.*, 2002; Denton *et al.*, 1998; Echemendia, 2010; Juhnke and des Jardin, 1989; Juhnke *et al.*, 1987; Lambert *et al.*, 1987). *S. maltophilia* has also been isolated from cottonseed, bean pods, and coffee (Nunes and de Melo, 2006; Swings *et al.*, 1983); thus, *S. maltophilia* can be found in a variety of foods and feeds. *S. maltophilia* is also widespread in the home environment and can be found around sponges, flowers, plants, fruits, vegetables, frozen fish, milk and poultry (Berg *et al.*, 1999; Denton and Kerr, 1998; Echemendia, 2010). Strains of *S. maltophilia* have been found in the transient flora of hospitalized patients as a commensal organism (Echemendia, 2010). *S. maltophilia* can be found in healthy individuals without causing any harm to human health (Denton *et al.*, 1998) and infections in humans caused by *S. maltophilia* are extremely uncommon (Cunha, 2009). Similar to the

indigenous bacteria of the gastrointestinal tract, *S. maltophilia* can be an opportunistic pathogen (Berg, 1996). As such, *S. maltophilia* is of low virulence in immuno-compromised patients where a series of risk factors (severe debilitation, the presence of indwelling devices such as ventilator tubes or catheters, for prolonged periods of time and prolonged courses of antibiotics) must occur for colonization by *S. maltophilia* in humans (Ryan *et al.*, 2009). Therefore, infections by *S. maltophilia* almost exclusively occur in hospital settings, in which case they are only present in a minimal percentage of infections (Ryan *et al.*, 2009). Finally, *S. maltophilia* has not been reported to be a source of allergens.

S. viridochromogenes is a saprophytic, soil-borne bacterium with no known safety issues. *Streptomyces* species are widespread in the environment and present no known allergenic or toxicity issues (Kämpfer, 2006; Kutzner, 1981), though human exposure is quite common (Goodfellow and Williams, 1983). *S. viridochromogenes* is not considered pathogenic to plants, humans or other animals (Cross, 1989; Goodfellow and Williams, 1983; Locci, 1989). *S. viridochromogenes* history of safe use is discussed in Hérouet et al., (2005) and this organism has been extensively reviewed during the evaluation of several glufosinate-tolerant events with no safety or allergenicity issues identified by FDA or other regulatory agencies.

A2(a)(iii) History of use of the organism in food supply or human exposure

The ubiquitous presence of *S. maltophilia* in the environment, the presence in healthy individuals without any harm to human health, the incidental presence in foods without any adverse safety reports, and the lack of reported allergenicity establish the safety of the donor organism.

The ubiquitous presence of *S. viridochromogenes* in the environment, the widespread human exposure without any adverse safety or allergenicity reports, and the successive reviews of several glufosinate-tolerant events by regulators that have not identified particular safety or allergenicity issues further establishes the safety of the donor organism.

A2(b) Description of the host organism

A2(b)(i) Phenotypic information

Maize (*Zea mays* L.) is a member of the tribe Maydae, which is included in the subfamily Panicoideae of the grass family Gramineae.

Family - Gramineae
- Subfamily - Panicoideae
  - Tribe - Maydae
    - Western Hemisphere:
      - Genus - *Zea*
        - A. Subgenus - *Luxuriantes*
          1. *Zea luxurians* (2n = 20)
          2. *Zea perennis* (2n = 40)
          3. *Zea diploperennis* (2n = 20)
        - B. Subgenus - *Zea*
          1. *Zea mays* (2n = 20)
             Subspecies
             1. *Z. mays parviglumis* (2n = 20)

2. *Z. mays huehuetenangensis* (2n = 20)
3. *Z. mays mexicana* (Schrad.) (2n = 20)

The genera included in the tribe Maydae include *Zea* and *Tripsacum* in the Western Hemisphere, and *Coix*, *Polytoca*, *Chionachne*, *Schlerachne*, and *Trilobachne* in Asia. Although some researchers have implicated the Asian genera in the origin of maize, the evidence for them is not as extensive and convincing as for the genera located in the Western Hemisphere.

The genus *Zea* includes two sub-genera: *Luxuriantes* and *Zea*. Maize (*Zea mays* L.) is a separate species within the subgenus *Zea,* along with three subspecies. All species within the genus *Zea*, except maize, are different species of teosinte. Until recently, the teosinte species were included in the genus *Euchlaena* rather than the genus *Zea*.

Maize is grown in nearly all areas of the world and is the largest cultivated crop in the world followed by wheat (*Triticum* sp.) and rice (*Oryza sativa* L.) in total global metric ton production. From 2009 to 2013, worldwide maize grain production averaged approximately 875 million metric tons (MMT) per year (USDA-FAS, 2013b). During this same period, the top maize grain producers were the United States, China, Brazil, and the European Union (EU), accounting for 71% of average annual global maize production (USDA-FAS, 2013a). Also during this period, maize production trended upwards from 825 MMT in 2009 to over 960 MMT in 2013 (USDA-FAS, 2013b).

In industrialized countries maize has two major uses: (1) as animal feed in the form of grain, forage or silage; and (2) as a raw material for wet- or dry-milled processed products such as high fructose maize syrup, oil, starch, glucose, dextrose and ethanol. By-products of the wet- and dry- mill processes are also used as animal feed. These processed products are used as ingredients in many industrial applications and in human food products. Most maize produced in industrialized countries is used as animal feed or for industrial purposes, but maize remains an important food staple in many developing regions, especially sub-Saharan Africa and Central America, where it is frequently the mainstay of human diets (Morris, 1998).

Maize is a very familiar plant that has been rigorously studied due to its use as a staple food/feed and the economic opportunity it brings to growers. The domestication of maize likely occurred in southern Mexico between 7,000 and 10,000 years ago (Goodman, 1988). While the putative progenitor species of maize have not been recovered, it is likely that teosinte played an important role in contributing to the genetic background of maize. Although grown extensively throughout the world, maize is not considered a persistent weed or a plant that is difficult to control. Maize, as we know it today, cannot survive in the wild because the female inflorescence (the ear) is covered by a husk thereby restricting seed dispersal, it has no seed dormancy, and is a poor competitor in an unmanaged ecosystem. The transformation from a wild, weedy species to one dependent on humans for its survival most likely evolved over a long period of time through plant breeding by the indigenous inhabitants of the Western Hemisphere. Today, virtually all the maize grown in the U.S. is a hybrid, a production practice that started in the 1930's (Wych, 1988). Maize hybrids are

developed and used based on the positive yield increases and plant vigor associated with heterosis, also known as hybrid vigor.

Conventional plant breeding results in desirable characteristics in a plant through the unique combination of genes already present in the plant. However, there is a limit to genetic diversity with conventional plant breeding. Biotechnology, as an additional tool to conventional breeding, offers access to greater genetic diversity than conventional breeding alone, resulting in expression of highly desirable traits that are profitable to growers.

A2(b)(ii) How the organism is propagated for food use

Maize is wind-pollinated, and the distances that viable pollen can travel depend on prevailing wind patterns, humidity, and temperature. Pollen is shed from the tassel and is viable for approximately 10 to 30 minutes as it is rapidly desiccated in the air (Kiesselbach, 1980). Maize plants shed pollen for up to 14 days.

The reproductive phase begins when one or two auxiliary buds, present in the leaf axils, develop and form the pistillate inflorescence of female flower. The auxiliary bud starts the transformation to form a long 'cob' on which the flowers will be borne. From each flower a style begins to elongate towards the tip of the cob in preparation for fertilization. These styles form long threads, known as silks. The base of the silk is unique, as it elongates continuously until fertilization occurs. Styles may reach a length of 30 centimetres, the longest known in the plant kingdom. Individual maize kernels, or fruit, are unique in that mature seed is not covered by floral bracts (glumes, lemmas, and paleas) as in most other grasses, but rather the entire structure is enclosed and protected by large modified leaf bracts, collectively referred to as the ear. The mature female flowers will remain ready for fertilization for up to two weeks, at which point if fertilization has not occurred, the nucleus will de-organize and fertilization will no longer be possible.

The pollen of maize, a protandrous plant, matures before the female flower is receptive. This may have been an ancient mechanism to ensure cross-pollination, but is no longer considered conducive to modern agricultural practices. However, decades of conventional selection and improvement have produced many maize varieties with similar maturities for both male and female flowers, to ensure seed set for agricultural purposes.

Under natural conditions, maize reproduces only by seed production. Pollination occurs with the transfer of pollen from the tassels to the silks of the ear. About 95% of the ovules are cross-pollinated and about 5% are self-pollinated, although plants are completely self-compatible. Maize, as a thoroughly domesticated plant, has lost all ability to disseminate its seeds and relies entirely on the aid of man for its distribution.

A2(b)(iii) What part of the organism is used for food

Maize has been a staple of the human diet for centuries, and its processed fractions are consumed in a multitude of food and animal feed products. In the U.S. the demand for maize is driven by the demand for feed and fuel. In 2013, animal feed accounted for almost 40% of maize consumption, 30% for ethanol, approximately 11% for food and industrial uses, 8% was used as dried distillers grain with the remainder being exported (NCGA, 2014). Recent

increases in meat consumption in emerging economic countries, particularly China, coupled with biofuels production has increased global demand for maize (Edgerton, 2009).

Food uses include sweet corn, popcorn, and processed field maize, which are all varieties/hybrids of *Zea mays* subsp. *mays*. The majority of maize used for food and industrial purposes is processed by wet milling to produce starch and sweetener products (e.g., high fructose corn syrup) for use in foodstuffs. Non-food products such as industrial starches, maize gluten feed and maize gluten meal are also manufactured through the wet mill process (May, 1987; Watson, 1988). The primary products derived from the dry milling process are corn meal, corn flour, and ethanol.

Due to its high starch and low fiber contents, maize is considered a valuable energy source in animal feed for livestock such as cattle, pigs and poultry. Whole maize is usually ground and mixed with a high-protein feed compound and with vitamin and mineral supplements to balance the ratio according to the nutritional requirements of the animals being fed (Leath and Hill, 1987). Maize is also used for processing and the production of derivatives, which have a wide range of food, feed and industrial applications. Some of the processed fractions are used for animal feed, such as maize gluten, a resource that is rich in maize protein. Ethanol production from the dry mill process provides dried distiller's grain solubles (DDGS) which are another source of animal feed (RFA, 2010).

A2(b)(iv) Whether special processing is required to render food safe to eat

Maize grain contains 82% endosperm, 12% germ, 5% bran, and 1% tip cap. In addition, 2.2% of the bran fraction is made up of crude fiber (Earle and Curtis, 1946; Perry, 1988). Food uses include sweet corn, popcorn, and processed field maize, which are all varieties/hybrids of *Zea mays* subsp. *mays*.

Maize processing methods include wet milling, dry milling, and fermentation. The milling process separates the maize kernel into three basic parts; endosperm, pericarp, and the germ (Watson, 1988).

Products from wet milling: The majority of the maize used for food and industrial purposes is processed by wet milling to produce starch and sweetener products for use in foodstuffs. Starch is used as a food ingredient in: dairy and ice cream; batters and breading; baked goods; soups, sauces and gravies; salad dressings; meat and poultry; confections; and, in drinks. Starch can also be converted to a variety of sweetener and fermentation products including high fructose maize syrup and ethanol (Watson, 1988).

Products from dry milling: The primary food products derived from the dry milling process are maize grits, maize meal, and maize flours. Maize grits are derived from endosperm of the maize kernel, with less than 1 % oil content. Maize grits are consumed in the U.S. as side dish for breakfast. Maize meal, however, has larger particles than maize grits and is often enriched with thiamine, riboflavin, niacin, and iron to produce baked products such as maize bread and muffins. Maize flour consists of fine endosperm particles, and is often used as a binder in processed meats, as well as in producing several snack foods (Rooney and Serna-Saldivar, 1987).

Products from fermentation: Starch produced from the wet milling process can also be used in producing ethanol and distilled beverages through fermentation (Rooney and Serna-Saldivar, 1987).

A2(b)(v) The significance to the diet in Australia and New Zealand of the host organism

Maize has been a staple of the human diet for centuries, and its processed fractions are consumed in a multitude of food. Estimates of maize consumption are available from the WHO Global Environmental Monitoring System - Food Contamination Monitoring and Assessment Programme (GEMS/Food) (www.who.int/foodsafety/chem/gems). The GEMS/Food programme has developed 13 Cluster Diets which are considered to be representative of the major food consumption patterns exhibited by regional and cultural groups around the world. Australia is included in Cluster M, along with United States and Canada and several other countries.

A3 The Nature of the Genetic Modification

A3(a) Method used to transform host organism

MON 87419 was developed through *Agrobacterium tumefaciens* mediated transformation of immature maize embryos based on the method described by (Sidorov and Duncan, 2009) utilizing PV-ZMHT507801. Immature embryos were excised from a post-pollinated maize ear of LH244. After co-culturing the excised immature embryos with *Agrobacterium* carrying the plasmid vector, the immature embryos were placed on selection medium containing glyphosate and carbenicillin disodium salt in order to inhibit the growth of untransformed plant cells and excess *Agrobacterium*, respectively. Once transformed callus developed, the callus was placed on media conducive to shoot and root development. The rooted plants (R_0) with normal phenotypic characteristics were selected and transferred to soil for growth and further assessment.

The R_0 plants generated through the transformation process described above had already been exposed to glyphosate in the selection medium and demonstrated glyphosate tolerance. The R_0 plants were self-pollinated to produce R_1 seed and the unlinked insertions of T-DNA I and T-DNA II were segregated. Subsequently, R_1 plants that were positive for the *dmo* and *pat* expression cassettes (T-DNA I) and did not contain the *cp4 epsps* expression cassette (T-DNA II) were identified by a polymerase chain reaction (PCR) based analysis. The R_1 plants homozygous for T-DNA I were selected for further development and their progenies were subjected to further molecular and phenotypic assessments. As is typical of a commercial event production and selection process, thousands of different transformation events (regenerants) were generated in the laboratory using PV-ZMHT507801. After many months of careful selection and evaluation of these thousands of events in the laboratory, greenhouse and field, MON 87419 was selected as the lead event based on superior agronomic, phenotypic, and molecular characteristics (Prado *et al.*, 2014). Studies on MON 87419 were initiated to further characterize the genetic insertion and the expressed product, and to establish the food, feed, and environmental safety relative to commercial maize. The major steps involved in the development of MON 87419 are depicted in Figure

1. The result of this process was the production of MON 87419 maize with the *dmo* and *pat* expression cassettes and without the *cp4 epsps* expression cassette.

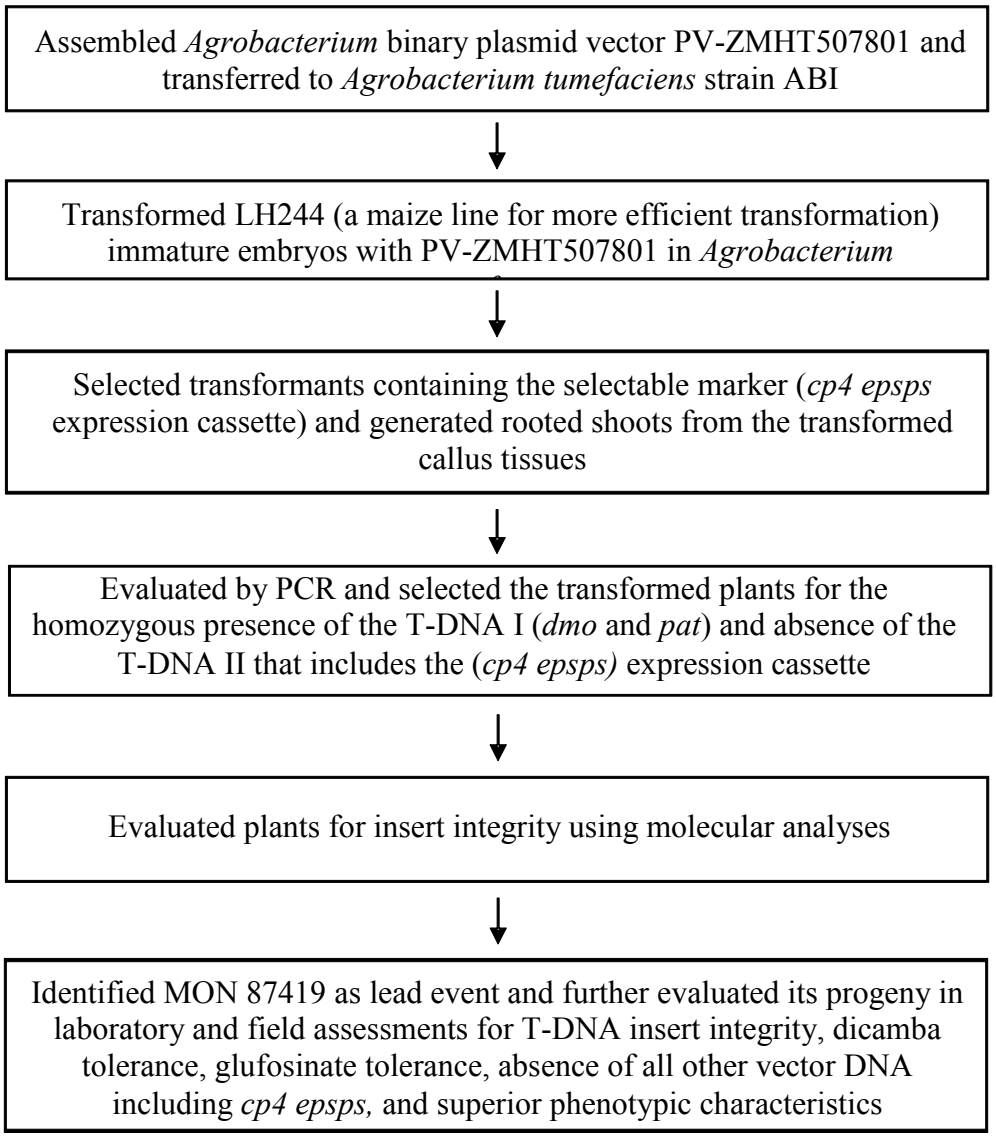

Figure 1. Schematic of the Development of MON 87419

A3(b) Intermediate hosts (*e.g.* bacteria)

A disarmed strain of *Agrobacterium tumefaciens* was the intermediate host used to transfer the plasmid PV-ZMHT507801 into maize cells. PV-ZMHT507801 contains one T-DNA containing the *dmo* and *pat* expression cassette. Following transformation, self-pollination, breeding, and segregation methods were used to produce MON 87419.

A3(c) Gene construct including size, source and function of all elements

A3(c)(i) Gene construct including size, source and function of all elements

MON 87419 was developed through *Agrobacterium tumefaciens*-mediated transformation of maize immature embryos from line LH244 utilizing PV- ZMHT507801.

PV-ZMHT507801

Plasmid vector PV ZMHT507801 was used in the transformation of maize to produce MON 87419 and its plasmid map is shown in Figure 4. The elements included in this plasmid vector are described in Table 1. Plasmid vector PV-ZMHT507801 is approximately 14.6 kb in length and contains two separate T-DNAs, each delineated by Left and Right Border regions. The first T-DNA, designated as T-DNA I, contains the *dmo* and *pat* expression cassettes. The *dmo* expression cassette is regulated by the peanut chlorotic streak caulimovirus (*PClSV*) promoter, the 5′ untranslated leader sequence of the *Cab* gene from *Triticum aestivum*, the *Ract1* intron from *Oryza sativa*, the *CTP4* chloroplast targeting sequence from *Petunia hybrida* and the 3′ untranslated region of heat shock protein 17 (*Hsp17*) from *Triticum aestivum.* The *pat* expression cassette is regulated by the *Ubq* promoter from *Andropogon gerardii*, the *Ubq* 5′ untranslated leader sequence from *Andropogon gerardii*, the *Ubq* intron from *Andropogon gerardii* and the 3′ untranslated region of the *Ara5* gene from *Oryza sativa*. The second T-DNA, designated as T-DNA II, contains the *cp4 epsps* expression cassette. The *cp4 epsps* expression cassette is regulated by the *Ract1* promoter from *Oryza sativa*, the *Ract1* 5′ untranslated leader from *Oryza sativa,* the *Ract1* intron from *Oryza sativa*, the *CTP2* chloroplast targeting sequence from *Arabidopsis thaliana*, and the *nos* 3′ untranslated region from *Agrobacterium tumefaciens*. During transformation, both T-DNAs were inserted into the maize genome. Subsequently, traditional breeding, segregation, selection and screening were used to isolate those plants that contain the *dmo* and *pat* expression cassettes (T-DNA I) and do not contain the *cp4 epsps* expression cassette (T-DNA II).

The backbone region of PV-ZMHT507801, located outside of the T-DNAs, contains two origins of replication for maintenance of the plasmid vector in bacteria (*ori V, ori pBR322*), a bacterial selectable marker gene (*aadA*), and a coding sequence for repressor of primer (ROP) protein for maintenance of plasmid vector copy number in *Escherichia coli* (*E. coli*). A description of the genetic elements and their prefixes (*e.g.* B, P, L, I, TS, CS, T, and OR) in PV-ZMHT507801 is provided in Table 1.

The *dmo* Coding Sequence and the DMO Protein

The *dmo* expression cassette encodes for 412 amino acids (340 amino acids encoded by the *dmo* gene and 72 amino acids encoded by the *CTP4* gene). MON 87419 expresses two

forms of DMO protein due to alternative processing of chloroplast transit peptide (CTP). One form, referred to as MON 87419 DMO+12 consists of 352 amino acids, which includes 340 amino acids encoded by the *dmo* gene and 12 amino acids encoded by the *CTP4* gene. The other form of the protein, referred to as MON 87419 DMO+7 consists of 347 amino acids, which includes 340 amino acids encoded by the *dmo* gene and seven amino acids encoded by the *CTP4* gene. MON 87419 DMO+7 does not contain the first five amino acids of MON 87419 DMO+12. Both forms of DMO protein expressed in MON 87419 are indistinguishable by Coomassie stain of SDS-PAGE and western blot analysis because the difference in molecular weight between these two forms is small. Therefore, a ~39.5 kDa MON 87419 DMO protein band is observed by Coomassie stain of SDS-PAGE and western blot analysis. The *dmo* open reading frame in the expression cassette includes a codon optimized sequence from *S. maltophilia* that encodes the DMO protein (Herman *et al.*, 2005; Palleroni and Bradbury, 1993; Wang *et al.*, 1997). The expression of MON 87419 DMO protein confers tolerance to dicamba herbicide.

```
  1  MAQINNMAQG IQTLNPNSNF HKPQVPKSSS FLVFGSKKLK NSANSMLVLK
 51  KDSIFMQKFC SFRISASVAT ACMLTFVRNA WYVAALPEEL SEKPLGRTIL
101  DTPLALYRQP DGVVAALLDI CPHRFAPLSD GILVNGHLQC PYHGLEFDGG
151  GQCVHNPHGN GARPASLNVR SFPVVERDAL IWIWPGDPAL ADPGAIPDFG
201  CRVDPAYRTV GGYGHVDCNY KLLVDNLMDL GHAQYVHRAN AQTDAFDRLE
251  REVIVGDGEI QALMKIPGGT PSVLMAKFLR GANTPVDAWN DIRWNKVSAM
301  LNFIAVAPEG TPKEQSIHSR GTHILTPETE ASCHYFFGSS RNFGIDDPEM
351  DGVLRSWQAQ ALVKEDKVVV EAIERRRAYV EANGIRPAML SCDEAAVRVS
401  REIEKLEQLE AA
```

Figure 2. Deduced Amino Acid Sequence of the CTP4 Targeting Sequence and the DMO Protein

The amino acid sequence of the MON 87419 DMO precursor protein was deduced from the full-length coding nucleotide sequence present in PV-ZMHT507801 (See Table 1 for more detail). The first 72 amino acids of the precursor protein (underlined) are the CTP from *Petunia hybrida* EPSPS (*CTP4*). CTP targets MON 87419 DMO protein to the chloroplast. CTP is partially cleaved in the chloroplast producing the mature 352 amino acid MON 87419 DMO protein that begins with the serine at position 60. The double underline shows the twelve amino acids from *CTP4* that are at the N-terminus of the mature MON 87419 DMO protein, referred to as MON 87419 DMO+12. MON 87419 DMO+7 does not contain the first five amino acids of MON 87419 DMO+12.

The *pat* Coding Sequence and the PAT Protein

The *pat* expression cassette encodes for 183 amino acids. MON 87419 expresses a ~25 kDa PAT protein consisting of a single polypeptide of 182 amino acids, except for the lead methionine which is cleaved during a co-translational process in MON 87419 (Wehrmann *et al.*, 1996; Wohlleben *et al.*, 1988) (Figure 3). The *pat* open reading frame in the expression cassette includes sequence from *S. viridochromogenes* that encodes the PAT protein (Wehrmann *et al.*, 1996; Wohlleben *et al.*, 1988). The expression of PAT protein confers glufosinate tolerance.

```
  1  MSPERRPVEI RPATAADMAA VCDIVNHYIE TSTVNFRTEP QTPQEWIDDL
 51  ERLQDRYPWL VAEVEGVVAG IAYAGPWKAR NAYDWTVEST VYVSHRHQRL
101  GLGSTLYTHL LKSMEAQGFK SVVAVIGLPN DPSVRLHEAL GYTARGTLRA
151  AGYKHGGWHD VGFWQRDFEL PAPPRPVRPV TQI
```

Figure 3. Deduced Amino Acid Sequence of the PAT (*pat*) Protein

The amino acid sequence of the MON 87419 produced PAT (*pat*) protein was deduced from the full-length coding nucleotide sequence present in PV-ZMHT507801 (See Table 1 for more detail). The lead methionine of the PAT protein produced in MON 87419 is cleaved during a co-translational process in MON 87419.

Regulatory Sequences

The *dmo* coding sequence in MON 87419 is under the regulation of the *PClSV* promoter, the chlorophyll a/b binding protein (CAB) leader, the *Ract1* intron, the *CTP4* transit peptide, and the heat shock protein 17 (*Hsp17*) 3′ untranslated region. The *PClSV* promoter is the promoter for the Full-Length Transcript (FLt) of peanut chlorotic streak caulimovirus (Maiti and Shepherd, 1998) that directs transcription in plant cells. The *Cab* leader sequence is the 5' untranslated region from the chlorophyll a/b binding (CAB) protein of *Triticum aestivum* and is involved in regulating gene expression (Lamppa *et al.*, 1985). The *Ract1* intron is the intron from the *act1* gene from *Oryza sativa* (McElroy *et al.*, 1990). The CTP directs transport of the DMO protein to the chloroplast in MON 87419 and is derived from the chloroplast targeting sequence of the *Petunia hybrid ShkG* gene (Gasser *et al.*, 1988; Herrmann, 1995). The *Hsp17* 3′ non-translated region is the 3′ untranslated region from the heat shock protein, Hsp17, of *Triticum aestivum* (McElwain and Spiker, 1989) that directs polyadenylation of the mRNA.

The *pat* coding sequence in MON 87419 is under the regulation of the *Ubq* promoter, the *Ubq* leader, the *Ubq* intron and the *Ara5* 3′ untranslated region. The *Ubq* promoter is the promoter for an ubiquitin gene (*Ubq*) from *Andropogon gerardii* (Joung and Kamo, 2006) that directs transcription in plant cells. The *Ubq* leader is the 5′ untranslated region from an ubiquitin gene (*Ubq)* from *Andropogon gerardii* (Joung and Kamo, 2006) and is involved in regulating gene expression. The *Ubq* intron is the intron from an ubiquitin gene (*Ubq*) from *Andropogon gerardii* (Joung and Kamo, 2006). The *Ara5* 3′ untranslated region is the 3′ untranslated region from the alpha-amylase/trypsin inhibitor gene (*Ara5*) gene of *Oryza sativa* encoding the *RA5B* precursor gene and directs polyadenylation of the mRNA (Hunt, 1994).

The *cp4 epsps* coding sequence in PV-ZMHT507801 is under the regulation of the *Ract1* promoter, the *Ract1* leader, the *Ract1* intron, the *CTP2* targeting sequence, and the *nos* 3′ untranslated region. The *Ract1* promoter is the promoter for the *act1* gene from *Oryza sativa* (McElroy *et al.*, 1990) that directs transcription in plant cells. The *Ract1* leader is the leader sequence of the *act1* gene from *Oryza sativa* (McElroy *et al.*, 1990) that is involved in regulating gene expression. The *Ract1* intron is the intron and flanking untranslated sequence of the *act1* gene from *Oryza sativa* (McElroy *et al.*, 1990) that is involved in regulating gene expression. The chloroplast transit peptide CTP2 is the targeting sequence of the *ShkG* gene from *Arabidopsis thaliana* encoding the EPSPS transit peptide region that directs transport of the protein to the chloroplast (Herrmann, 1995; Klee *et al.*, 1987). The *nos* 3′ untranslated region is the 3′ untranslated region of the nopaline synthase (*nos*) gene from *Agrobacterium tumefaciens* pTi encoding NOS that directs polyadenylation (Bevan *et al.*, 1983; Fraley *et al.*, 1983).

T-DNA Borders

PV-ZMHT507801 contains Left and Right Border regions (

Figure **4** and Table 1) that were derived from *Agrobacterium tumefaciens* plasmids. The border regions each contain a nick site that is the site of DNA exchange during transformation (Barker *et al.*, 1983; Depicker *et al.*, 1982; Zambryski *et al.*, 1982). The border regions separate the T-DNA from the plasmid backbone region and are involved in the efficient transfer of T-DNA into the maize genome.

Genetic Elements Outside of the T-DNA Borders

Genetic elements that exist outside of the T-DNA border regions are those that are essential for the maintenance or selection of PV-ZMHT507801 in bacteria and are referred to as plasmid backbone. The origin of replication, *ori-V*, is required for the maintenance of the plasmid in *Agrobacterium* and is derived from the broad host plasmid RK2 (Stalker *et al.*, 1981). The origin of replication *ori-pBR322* is required for the maintenance of the plasmid in *E. coli* and is derived from the plasmid vector pBR322 (Sutcliffe, 1979). Coding sequence *rop* encodes the repressor of primer (ROP) protein which is necessary for the maintenance of plasmid vector copy number in *E. coli* (Giza and Huang, 1989). The selectable marker *aadA* is a bacterial promoter, coding sequence and 3′ untranslated region for an enzyme from transposon Tn7 that confers spectinomycin and streptomycin resistance (Fling *et al.*, 1985) in *E. coli* and *Agrobacterium* during molecular cloning. Because these elements are outside the border regions, they are not expected to be transferred into the maize genome. The absence of the backbone and other unintended plasmid vector sequence in MON 87419 was confirmed by sequencing and bioinformatic analyses (see Section A3(d)(ii)).

Table 1. Summary of Genetic Elements in PV-ZMHT507801

Genetic Element	Location in Plasmid Vector	Function (Reference)
T-DNA I		
B[1]-Right Border Region	1-285	DNA region from *Agrobacterium tumefaciens* containing the right border sequence used for transfer of the T-DNA (Depicker *et al.*, 1982; Zambryski *et al.*, 1982)
Intervening Sequence	286-410	Sequence used in DNA cloning
P[2]-*Ubq*	411-2054	Promoter for a ubiquitin gene (*Ubq*) from *Andropogon gerardii* (big bluestem grass) that initiates and directs transcription (Joung and Kamo, 2006)
L[3]-*Ubq*	2055-2153	5' UTR leader sequence for the ubiquitin gene (*Ubq*) from *Andropogon gerardii* (big bluestem grass) that is involved in regulating gene expression (Joung and Kamo, 2006)
I[4]-*Ubq*	2154-3195	Intron sequence of the ubiquitin gene (*Ubq*) from *Andropogon gerardii* (big bluestem grass) that is involved in regulating gene expression (Joung and Kamo, 2006)
Intervening Sequence	3196-3200	Sequence used in DNA cloning
CS[5]-*pat*	3201-3752	Coding sequence for the phosphinothricin N-acetyltransferase (PAT) protein of *Streptomyces viridochromogenes* that confers tolerance to glufosinate (Wehrmann *et al.*, 1996; Wohlleben *et al.*, 1988)
Intervening Sequence	3753-3760	Sequence used in DNA cloning
T[6]-*Ara5*	3761-3973	3'UTR sequence of the RA5B precursor gene from *Oryza sativa* (rice), encoding an alpha-amylase/trypsin inhibitor (*Ara5*) that directs polyadenylation of mRNA (Hunt, 1994)
Intervening Sequence	3974-4120	Sequence used in DNA cloning
P-*PClSV*	4121-4553	Promoter for the full length transcript (FLt) of peanut chlorotic streak caulimovirus (PClSV) that directs transcription in plant cells (Maiti and Shepherd, 1998)
Intervening Sequence	4554-4558	Sequence used in DNA cloning

Table 1 (continued). Summary of Genetic Elements in PV-ZMHT507801

Genetic Element	Location in Plasmid Vector	Function (Reference)
L-*Cab*	4559-4619	5' UTR leader sequence from chlorophyll a/b-binding (CAB) protein of *Triticum aestivum* (wheat) that is involved in regulating gene expression (Lamppa *et al.*, 1985)
Intervening Sequence	4620-4635	Sequence used in DNA cloning
I-*Ract1*	4636-5115	Intron and flanking UTR sequence of the *act1* gene from *Oryza sativa* (rice) encoding rice Actin 1 protein (McElroy *et al.*, 1990) that is involved in regulating gene expression
Intervening Sequence	5116-5124	Sequence used in DNA cloning
TS[7]-*CTP4*	5125-5340	Targeting and 5' UTR leader sequence of the *ShkG* gene from *Petunia hybrida* encoding the EPSPS transit peptide region that directs the protein to the chloroplast (Gasser *et al.*, 1988; Herrmann, 1995)
CS-*dmo*	5341-6363	Codon optimized coding sequence for the dicamba mono-oxygenase (DMO) protein of *Stenotrophomonas maltophilia* that confers dicamba resistance (Herman *et al.*, 2005; Wang *et al.*, 1997)
Intervening Sequence	6364-6393	Sequence used in DNA cloning
T-*Hsp17*	6394-6603	3' UTR sequence from a heat shock protein, Hsp17, of *Triticum aestivum* (wheat) (McElwain and Spiker, 1989) that directs polyadenylation of the mRNA
Intervening Sequence	6604-6765	Sequence used in DNA cloning
B-Left Border Region	6766-7207	DNA region from *Agrobacterium tumefaciens* containing the left border sequence used for transfer of the T-DNA (Barker *et al.*, 1983)
		Backbone
Intervening Sequence	7208-7293	Sequence used in DNA cloning
OR[8]-*ori V*	7294-7690	Origin of replication from the broad host range plasmid RK2 for maintenance of plasmid in *Agrobacterium* (Stalker *et al.*, 1981)
Intervening Sequence	7691-7696	Sequence used in DNA cloning

Table 1 (continued). Summary of Genetic Elements in PV-ZMHT507801

Genetic Element	Location in Plasmid Vector	Function (Reference)
T-DNA II		
B-Left Border Region	7697-8015	DNA region from *Agrobacterium tumefaciens* containing the left border sequence used for transfer of the T-DNA (Barker *et al.*, 1983)
Intervening Sequence	8016-8045	Sequence used in DNA cloning
T-*nos*	8046-8298	3' UTR sequence of the *nopaline synthase* (*nos*) gene from *Agrobacterium tumefaciens* pTi encoding NOS that directs polyadenylation (Bevan *et al.*, 1983; Fraley *et al.*, 1983)
Intervening Sequence	8299-8313	Sequence used in DNA cloning
CS-*cp4 epsps*	8314-9681	Coding sequence of the *aroA* gene from *Agrobacterium* sp. strain CP4 encoding the CP4 EPSPS protein that provides herbicide tolerance (Barry *et al.*, 2001; Padgette *et al.*, 1996)
TS-*CTP2*	9682-9909	Targeting sequence of the *ShkG* gene from *Arabidopsis thaliana* encoding the EPSPS transit peptide region that directs transport of the protein to the chloroplast (Herrmann, 1995; Klee *et al.*, 1987)
Intervening Sequence	9910-9918	Sequence used in DNA cloning
I-*Ract1*	9919-10396	Intron and flanking UTR sequence of the *act1* gene from *Oryza sativa* (rice) encoding rice Actin 1 protein (McElroy *et al.*, 1990) that is involved in regulating gene expression
L-*Ract1*	10397-10476	Leader sequence of the *act1* gene from *Oryza sativa* (rice) encoding the rice Actin 1 protein (McElroy *et al.*, 1990) that is involved in regulating gene expression
P-*Ract1*	10477-11317	Promoter of the *act1* gene from *Oryza sativa* (rice) encoding the rice Actin 1 protein (McElroy *et al.*, 1990) that directs transcription in plant cells
Intervening Sequence	11318-11343	Sequence used in DNA cloning
B-Right Border Region	11344-11700	DNA region from *Agrobacterium tumefaciens* containing the right border sequence used for transfer of the T-DNA (Depicker *et al.*, 1982; Zambryski *et al.*, 1982)

Table 1 (continued). Summary of Genetic Elements in PV-ZMHT507801

Genetic Element	Location in Plasmid Vector	Function (Reference)
Backbone		
Intervening Sequence	11701-11926	Sequence used in DNA cloning
CS-*rop*	11927-12118	Coding sequence for repressor of primer protein from the ColE1 plasmid for maintenance of plasmid copy number in *E. coli* (Giza and Huang, 1989)
Intervening Sequence	12119-12545	Sequence used in DNA cloning
OR-*ori-pBR322*	12546-13134	Origin of replication from plasmid pBR322 for maintenance of plasmid in *E. coli* (Sutcliffe, 1979)
Intervening Sequence	13135-13664	Sequence used in DNA cloning
aadA	13665-14553	Bacterial promoter, coding sequence, and 3' UTR for an aminoglycoside-modifying enzyme, 3''(9)-*O*-nucleotidyltransferase from the transposon Tn*7* (Fling *et al.*, 1985) that confers spectinomycin and streptomycin resistance
Intervening Sequence	14554-14569	Sequence used in DNA cloning

[1] B, Border
[2] P, Promoter
[3] L, Leader
[4] I, Intron
[5] CS, Coding Sequence
[6] T, Transcription Termination Sequence
[7] TS, Targeting Sequence
[8] OR, Origin of Replication

A3(c)(ii) Detailed map of the location and orientation of all genetic elements

Figure 4. Circular Map of PV-ZMHT507801

A circular map of the plasmid vector PV-ZMHT507801 used to develop MON 87419 is shown. PV-ZMHT507801 contains two T-DNAs, designated as T-DNA I and T-DNA II. Genetic elements are shown on the exterior of the map.

A3(d) Full characterisation of the genetic modification

A3(d)(i) Identification of GM elements

This section contains a comprehensive molecular characterisation of the genetic modification present in MON 87419. It provides information on the DNA insertion(s) into the plant genome of MON 87419, and additional information relative to the arrangement and stability of the introduced genetic material. The information provided in this section addresses the relevant factors in Codex Plant Guidelines, Section 4, paragraphs 30, 31, 32, and 33 (Codex Alimentarius, 2009).

Characterisation of the genetic modification in MON 87419 was conducted using a combination of sequencing, PCR, and bioinformatics. The results of this characterisation demonstrate that MON 87419 contains one copy of the intended transfer DNA (T-DNA I) containing the *dmo* and *pat* expression cassettes that is stably integrated at a single locus and is inherited according to Mendelian principles over multiple generations. These conclusions are based on several lines of evidence:

- Molecular characterisation of MON 87419 by Next Generation Sequencing and Junction Sequence Analysis (NGS/JSA) demonstrated that MON 87419 contains a single DNA insert. These whole-genome sequence analyses provided a comprehensive assessment of MON 87419 to determine the presence of sequences derived from PV-ZMHT507801 (DuBose *et al.*, 2013; Kovalic *et al.*, 2012) and demonstrated that MON 87419 contained a single T-DNA I insert with no detectable backbone or T-DNA II sequences.
- Directed sequencing (locus-specific PCR, DNA sequencing and analyses) performed on MON 87419 was used to determine the complete sequence of the single DNA insert from PV-ZMHT507801, the adjacent flanking DNA, and the 5' and 3' insert-to-flank junctions. This analysis confirmed that the sequence and organization of the DNA is identical to the corresponding region in the PV-ZMHT507801 T-DNA I. Furthermore, the genomic organization at the insertion site was assessed by comparing the sequences flanking the T-DNA I insert in MON 87419 to the sequence of the insertion site in conventional maize. This analysis determined that no major DNA rearrangement occurred at the insertion site in MON 87419 upon DNA integration.
- Generational stability analysis by NGS/JSA demonstrated that the single PV-ZMHT507801 T-DNA I insert in MON 87419 has been maintained through five breeding generations, thereby confirming the stability of the T-DNA I insert in MON 87419.
- Segregation analysis corroborates the insert stability demonstrated by NGS/JSA and independently establishes the nature of the T-DNA I insert at a single chromosomal locus.

Taken together, the characterisation of the genetic modification in MON 87419 demonstrates that a single copy of the intended T-DNA I was stably integrated at a single locus of the maize genome and that no plasmid backbone or T-DNA II sequences are present in MON 87419.

A schematic representation of the NGS/JSA methodology and the basis of the characterisation using NGS/JSA and PCR sequencing are illustrated in Figure 5 below.

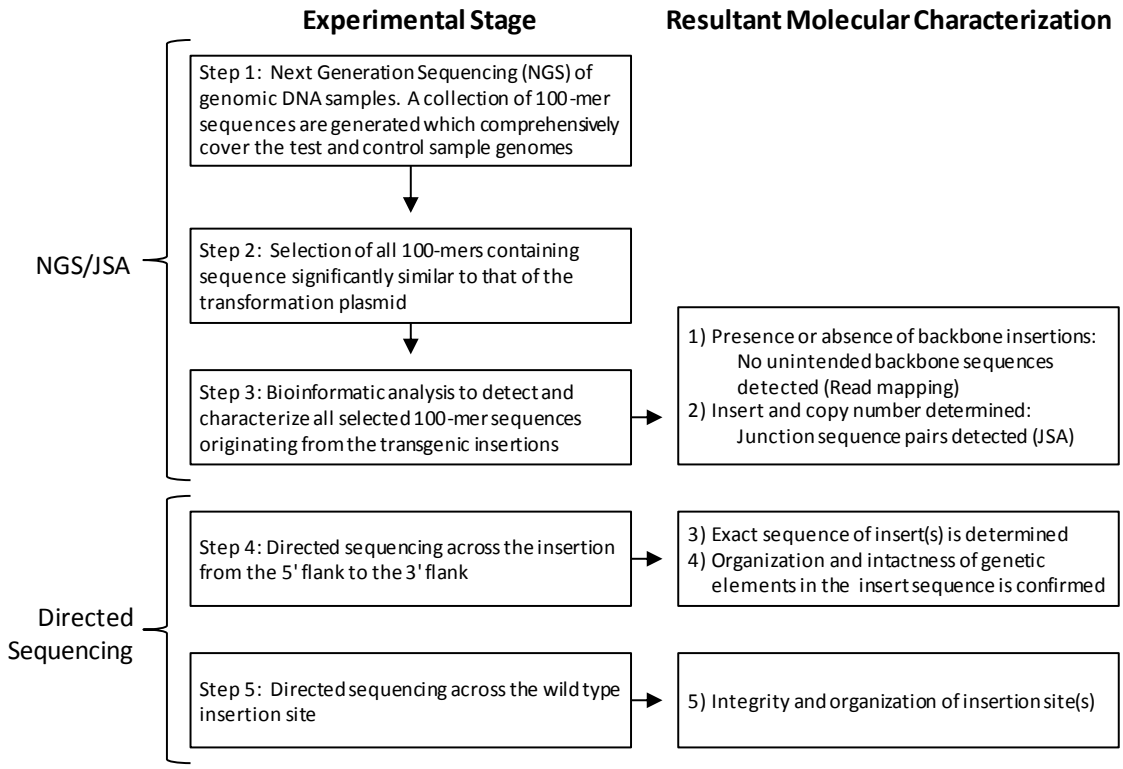

Figure 5. Molecular Characterisation using Sequencing and Bioinformatics

Genomic DNA from MON 87419 and the conventional control was sequenced using Next Generation Sequencing (NGS), which can be used to reach the same conclusions that can be determined using traditional Southern blotting (Kovalic *et al.*, 2012). NGS technology produces a set of short, randomly distributed sequence reads (each approximately 100 bp long) that comprehensively covers both MON 87419 and control genomes (Step 1). Utilizing these genomic sequences, bioinformatics search tools were used to select all sequence reads that were significantly similar to PV-ZMHT507801 (Step 2) for use in read mapping to determine the presence/absence of backbone sequences and T-DNA II and Junction Sequence Analysis (JSA) bioinformatics to determine the insert and copy number (Step 3). Overlapping PCR products are also produced which span any inserts and their wild type loci (Step 4 and Step 5, respectively); these overlapping PCR products are sequenced to allow for detailed characterization of the inserted DNA and insertion site(s).

The NGS/JSA method characterized the genomic DNA from MON 87419 and the conventional control using short (~100 bp) randomly distributed sequence fragments (sequencing reads) generated in sufficient number to ensure comprehensive coverage of the sample genomes. It has been previously demonstrated that 75× coverage of the soybean genome is adequate to provide comprehensive coverage and ensure detection of inserted DNA (Kovalic *et al.*, 2012). Similarly, it is expected that 75× will provide comprehensive coverage of the maize genome. To confirm sufficient sequence coverage of the genome, the 100-mer sequence reads are analyzed to determine the coverage of a known single-copy endogenous gene, this demonstrates the depth of coverage (the median number of times each base of the genome is independently sequenced). The level of sensitivity achieved in this characterization was sufficient to detect ≥ 99% of the plasmid vector sequence when present at 1/10th the mean coverage of the conventional control genome. Analysis of the sampling data thus confirmed the method's ability to detect any sequences derived from PV-ZMHT507801. Bioinformatics analysis was then used to select sequencing reads that contained sequences similar to PV-ZMHT507801, and these were analysed in depth to determine the number and the identity of sequence in the DNA insert(s). NGS/JSA was run on all five generations of MON 87419 samples and the conventional controls. NGS/JSA methodology utilizes sequencing and bioinformatics to produce characterizations equivalent to those achieved previously by traditional Southern blotting (Kovalic *et al.*, 2012). Results of NGS/JSA are shown in Sections A3(d) and A3(f).

Directed sequencing (locus-specific PCR and DNA sequencing analyses, Figure 5, Step 4) complements the NGS/JSA. Sequencing of the insert and flanking genomic DNA determined the complete sequence of the insert and flanks by evaluating if the sequence of the insert was identical to the corresponding sequence from the T-DNA I in PV-ZMHT507801, and if each genetic element in the insert was intact. It also characterizes the flank sequence beyond the insert corresponding to the genomic DNA of the transformed maize. Results are described in Sections A3(d)(i) and A3(d)(ii).

The stability of the T-DNA I present in MON 87419 across multiple breeding generations was evaluated by NGS/JSA as described above. This information was used to determine the number and identity of the DNA inserts in each generation. For a single copy T-DNA I insert, two junction sequence classes are expected. In the case of an event where a single locus is stably inherited over multiple breeding generations, two identical junction sequence classes would be detected in all the breeding generations tested. Results are described in Section A3(f)(i).

Segregation analysis of the T-DNA I was conducted to determine the inheritance and stability of the insert in MON 87419. Segregation analysis corroborates the insert stability demonstrated by NGS/JSA and independently establishes the genetic behavior of the T-DNA I. Results are described in Section A3(f)(i).

A3(d)(ii) Determination of number and identity of DNA inserts in MON 87419

The number of insertion sites of PV-ZMHT507801 DNA in MON 87419 was assessed by performing NGS/JSA on MON 87419 genomic DNA. A plasmid map of PV-Z MHT507801 is shown in Figure 4. Table 2 provides descriptions of the genetic elements present in MON 87419. A schematic representation of the insert and flanking sequences in MON 87419 is shown in Figure 6.

Next Generation Sequencing of MON 87419 and Conventional Control Genomic DNA

Genomic DNA from five breeding generations of MON 87419 (Figure 7) and the conventional control was isolated from seed and prepared for sequencing using the Illumina TruSeq DNA Sample Preparation Kit (Illumina). These genomic DNA libraries were used to generate short (~100 bp) randomly distributed sequence fragments (sequencing reads) of the maize genome (see Figure 6).

To demonstrate sufficient sequence coverage the 100-mer sequence reads were analyzed by mapping all reads to a known single copy endogenous gene (*Zea mays* pyruvate decarboxylase (*pdc3*), GenBank accession version: AF370006.2) in each of the five breeding generations. The analysis of sequence coverage plots showed that the depth of coverage (*i.e.,* the median number of times any base of the genome is expected to be independently sequenced) was 75× or greater for the five generations of MON 87419 (R_3, R_4, R_5, R_3F_1 and R_4F_1) and the conventional control. It has been previously demonstrated that 75× coverage of the soybean genome is adequate to provide comprehensive coverage and ensure detection of inserted DNA (Kovalic *et al.*, 2012). Similarly, it is expected that 75× will provide comprehensive coverage of the maize genome.

To demonstrate the method's ability to detect any sequences derived from the PV-ZMHT507801 transformation plasmid, a sample of conventional control genomic DNA spiked with PV-ZMHT507801 DNA was analyzed by NGS and bioinformatics. The level of sensitivity of this method was demonstrated to a level of one genome equivalent, 100% nucleotide identity was observed over 100% of PV-ZMHT507801. This result demonstrates that all nucleotides of PV-ZMHT507801 are observed by the sequencing and bioinformatic assessments performed. Also, observed coverage was adequate at a level 1/10th genomic equivalent (99.43% coverage at 100% identity) and, hence, a detection level of at most 1/10th genome equivalent was achieved for the plasmid DNA sequence assessment.

Characterisation of Insert Number in MON 87419 using Bioinformatic Analysis

The number of insertion sites of DNA from PV-ZMHT507801 in MON 87419 was assessed by performing NGS/JSA on MON 87419 genomic DNA using the R_3 generation (Figure 7).

Table 2. Summary of Genetic Elements in MON 87419

Genetic Element[1]	Location in Sequence[2]	Function (Reference)
Flanking DNA	1-1246	Flanking DNA
B[3]-Right Border Region r1	1247-1317	DNA region from *Agrobacterium tumefaciens* containing the right border sequence used for transfer of the T-DNA (Depicker *et al.*, 1982; Zambryski *et al.*, 1982)
Intervening Sequence	1318-1442	Sequence used in DNA cloning
P[4]-*Ubq*	1443-3086	Promoter for a ubiquitin gene (*Ubq*) from *Andropogon gerardii* (big bluestem grass) that initiates and directs transcription (Joung and Kamo, 2006)
L[5]-*Ubq*	3087-3185	5' UTR leader sequence for the ubiquitin gene (*Ubq*) from *Andropogon gerardii* (big bluestem grass) that is involved in regulating gene expression (Joung and Kamo, 2006)
I[6]-*Ubq*	3186-4227	Intron sequence of the ubiquitin gene (*Ubq*) from *Andropogon gerardii* (big bluestem grass) that is involved in regulating gene expression (Joung and Kamo, 2006)
Intervening Sequence	4228-4232	Sequence used in DNA cloning
CS[7]-*pat*	4233-4784	Coding sequence for the phosphinothricin N-acetyltransferase (PAT) protein of *Streptomyces viridochromogenes* that confers tolerance to glufosinate (Wehrmann *et al.*, 1996; Wohlleben *et al.*, 1988)
Intervening Sequence	4785-4792	Sequence used in DNA cloning
T[8]-*Ara5*	4793-5005	3'UTR sequence of the RA5B precursor gene from *Oryza sativa* (rice), encoding an alpha-amylase/trypsin inhibitor (*Ara5*) that directs polyadenylation of mRNA (Hunt, 1994)
Intervening Sequence	5006-5152	Sequence used in DNA cloning
P-*PClSV*	5153-5585	Promoter for the full-length transcript (FLt) of peanut chlorotic streak caulimovirus (PClSV) that directs transcription in plant cells (Maiti and Shepherd, 1998)
Intervening Sequence	5586-5590	Sequence used in DNA cloning

Table 2 (continued). Summary of Genetic Elements in MON 87419

Genetic Element[1]	Location in Sequence[2]	Function (Reference)
L-*Cab*	5591-5651	5' UTR leader sequence from chlorophyll a/b-binding (CAB) protein of *Triticum aestivum* (wheat) that is involved in regulating gene expression (Lamppa *et al.*, 1985)
Intervening Sequence	5652-5667	Sequence used in DNA cloning
I-*Ract1*	5668-6147	Intron and flanking UTR sequence of the *act1* gene from *Oryza sativa* (rice) encoding rice Actin 1 protein (McElroy *et al.*, 1990) that is involved in regulating gene expression
Intervening Sequence	6148-6156	Sequence used in DNA cloning
TS[9]-*CTP4*	6157-6372	Targeting and 5' UTR leader sequence of the *ShkG* gene from *Petunia hybrida* encoding the EPSPS transit peptide region that directs the protein to the chloroplast (Gasser *et al.*, 1988; Herrmann, 1995)
CS-*dmo*	6373-7395	Codon optimized coding sequence for the dicamba mono-oxygenase (DMO) protein of *Stenotrophomonas maltophilia* that confers dicamba resistance (Herman *et al.*, 2005; Wang *et al.*, 1997)
Intervening Sequence	7396-7425	Sequence used in DNA cloning
T-*Hsp17*	7426-7635	3' UTR sequence from a heat shock protein, Hsp17, of *Triticum aestivum* (wheat) (McElwain and Spiker, 1989) that directs polyadenylation of the mRNA
Intervening Sequence	7636-7797	Sequence used in DNA cloning
B-Left Border Region [r1]	7798-8008	DNA region from *Agrobacterium tumefaciens* containing the left border sequence used for transfer of the T-DNA (Barker *et al.*, 1983)
Flanking DNA	8009-9259	Flanking DNA

[1] Although flanking sequences and intervening sequence are not functional genetic elements, they comprise a portion of the sequence.
[2] Numbering refers to the sequence of the insert in MON 87419 and adjacent DNA.
[3] B, Border
[4] P, Promoter
[5] L, Leader
[6] I, Intron
[7] CS, Coding Sequence
[8] T, Transcription Termination Sequence
[9] TS, Targeting Sequence
[r1] Superscript in Left and Right Border Regions indicate that the sequence in MON 87419 was truncated compared to the sequences in PV-ZMHT507801.

Figure 6. Schematic Representation of the Insert and Flanking Sequences in MON 87419

DNA derived from T-DNA I of PV-ZMHT507801 integrated in MON 87419. Right-angled arrows indicate the ends of the integrated T-DNA and the beginning of the flanking sequence. Identified on the map are genetic elements within the insert. This schematic diagram is drawn to scale. The exact coordinates of every element are shown in Table 2.

[r1] Superscript in Left and Right Border Regions indicate that the sequence in MON 87419 was truncated compared to the sequences in PV-ZMHT507801.

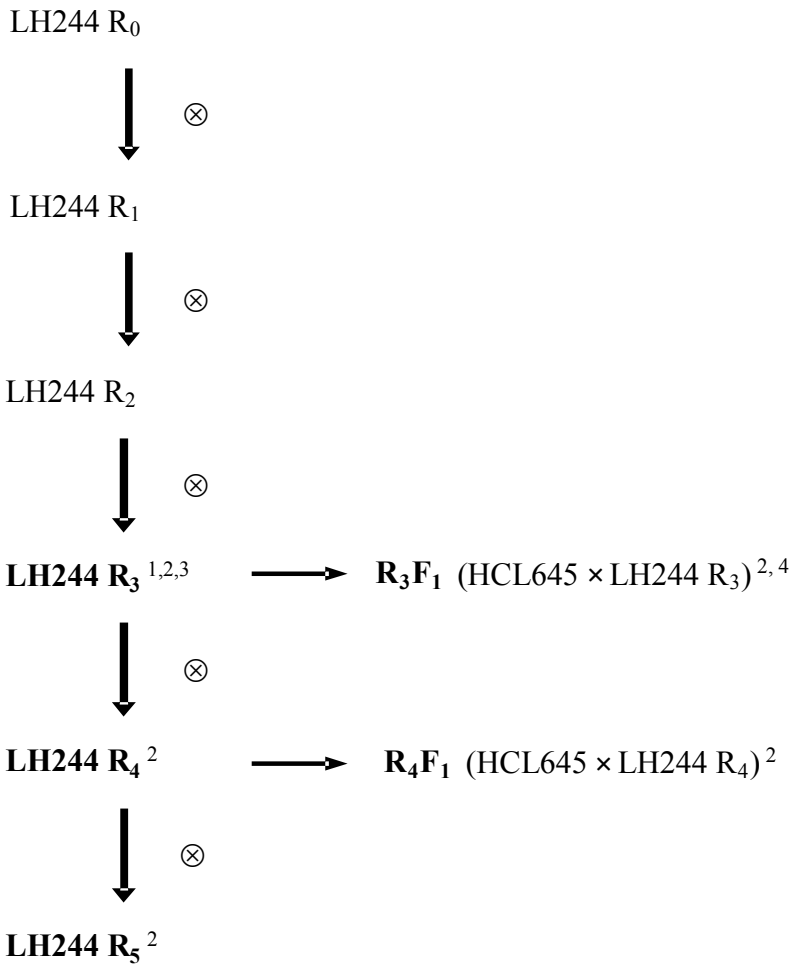

Figure 7. Breeding History of MON Number

R_0 corresponds to the transformed plant, F# is the filial generation, ⊗ designates self pollination.

[1] Generation used for molecular characterization

[2] Generations used to confirm insert stability

[3] Generation used for commercial development of MON 87419

[4] Generation used for agronomic/phenotypic and compositional analysis studies

Selection of Sequence Reads Containing Sequence of the PV-ZMHT507801

PV-ZMHT507801 was transformed into the parental variety LH244 to produce MON 87419. Consequently, any DNA inserted into MON 87419 will consist of sequences that are similar to the PV-ZMHT507801 DNA sequence. Therefore, to fully characterize the DNA from PV-ZMHT507801 inserted in MON 87419, it is sufficient to completely analyze only the sequence reads that have similarity to PV-ZMHT507801 (Figure 5, Step 2).

Using established criteria , sequence reads similar to PV-ZMHT507801 were selected from MON 87419 sequence datasets and were then used as input data for bioinformatic junction sequence analysis. PV-ZMHT507801 sequences were also compared against the conventional control sequence dataset.

Determination of the Insert Number and Copy Number

The NGS/JSA method described above used the entire plasmid vector sequence as a query to determine the DNA insertion site number. Any inserted transformation plasmid vector sequence, regardless of origin, either T-DNA I, T-DNA II, or backbone, can be identified by aligning reads to the transformation plasmid vector sequence while the number of inserted DNA molecules can be determined using JSA.

Therefore unlike the traditional Southern blot analysis that separately hybridizes T-DNA or backbone probes, NGS/JSA determines the T-DNA I insert number and the absence of backbone, T-DNA II, or unintended sequences by the identification of sequence reads that match PV-ZMHT507801, the determination of the overall insert number in the genome. This alternative method can be used to reach the same conclusions regarding the number of inserts and presence or absence of backbone or T-DNA II that can be determined using traditional Southern blots (Kovalic *et al.*, 2012).

By evaluating the number of unique junction classes, the number of DNA insertion sites can be determined (Figure 5, Step 3). If MON 87419 contains a single T-DNA I insert, two junction sequence classes (JSCs), each containing portions of T-DNA I sequence and flanking sequence, will be detected.

To determine the insert number in MON 87419, the selected sequence reads described above were analyzed using JSA (Kovalic *et al.*, 2012). JSA uses bioinformatic analysis to find and classify partially matched reads characteristic of the ends of insertions. The number of resultant unique JSCs were determined by this analysis and are shown in Table 3.

Table 3. Unique Junction Sequence Class Results

Sample	Junction Sequence Classes Detected
MON 87419	2
LH244	0

The location and orientation of the junction sequences relative to the T-DNA I insert determined for MON 87419 are illustrated in **Figure 8**. As shown in the figure, there are two junction sequence classes identified in MON 87419. Junction Sequence Class A and Class B (JSC-A and JSC-B) both contain the T-DNA I border sequence joined to genomic flanking sequence, indicating that they represent the sequences at the junctions of the intended T-DNA I insert and genomic flanking sequence.

Complete alignment of the JSCs to the full flank/insert sequence confirms that both of these JSCs originate from the same locus of the MON 87419 genome and are linked by contiguous, known and expected DNA that makes up the single insert.

Figure 8. Junction Sequences Detected by NGS/JSA

Linear map of MON 87419 illustrating the relationship of the detected junction sequences to the event locus. The individual junction sequences detected by JSA are illustrated as stacked bars.

[r1]Superscript in Left and Right Border Regions indicate that the sequence in MON 87419 was truncated compared to the sequences in PV-ZMHT507801.

A3(d)(iii) Full DNA sequence, including junction regions

Organisation and Sequence of the Insert and Adjacent DNA in MON 87419

The organization of the elements within the DNA insert and the adjacent genomic DNA was assessed using directed DNA sequence analysis (refer to Figure 5, Step 4). PCR primers were designed to amplify six overlapping regions of the MON 87419 genomic DNA that span the entire length of the insert (Figure 9). The amplified PCR products were subjected to DNA sequencing analyses. The results of this analysis confirm that the MON 87419 insert is 6,762 bp and that each genetic element within the T-DNA I is intact compared to PV-ZMHT507801, with the exception of the border regions. The border regions both contain small terminal deletions with the remainder of the inserted border regions being identical to the sequence in PV-ZMHT507801. The sequence and organization of the insert was also shown to be identical to the corresponding T-DNA I of PV-ZMHT507801 as intended. This analysis also shows that only T-DNA I elements (described in Table 2) were present. Moreover, the result, together with the conclusion of single DNA insert detected by NGS/JSA, demonstrated that no PV-ZMHT507801 backbone or T-DNA II elements are present in MON 87419.

Figure 9. Overlapping PCR Analysis across the Insert in MON 87419

PCR was performed on both conventional control genomic DNA and MON 87419 genomic DNA using six pairs of primers to generate overlapping PCR fragments from MON 87419 for sequencing analysis. To verify the PCR products, a portion of each PCR was loaded on the gel. The expected product size for each amplicon is provided in the illustration. Lane designations are as follows:

Lane		Lane	
1	1 Kb Plus DNA Ladder	14	1 Kb Plus DNA Ladder
2	MON 87419	15	MON 87419
3	Conventional Control LH244	16	PV-ZMHT507801
4	No template control	17	Conventional Control LH244
5	MON 87419	18	No template control
6	PV ZMHT507801	19	MON 87419
7	Conventional Control LH244	20	PV-ZMHT507801
8	No template control	21	Conventional Control LH244
9	MON 87419	22	No template control
10	PV ZMHT507801	23	MON 87419
11	Conventional Control LH244	24	Conventional Control LH244
12	No template control	25	No template control
13	1 Kb Plus DNA Ladder	26	1 Kb Plus DNA Ladder

Arrows next to the agarose gel photograph denote the size of the DNA, in kilobase pairs, obtained from the 1 Kb DNA Plus Ladder (Invitrogen) on the ethidium bromide stained gel.

[r1]Superscript in Left and Right Border Regions indicate that the sequence in MON 87419 was truncated compared to the sequences in PV-ZMHT507801.

Sequencing of the MON 87419 Insertion Site

PCR and sequence analysis were performed on genomic DNA extracted from the conventional control to examine the insertion site in conventional maize (see Figure 5, Step 5). The PCR was performed with one primer specific to the genomic DNA sequence flanking the 5' end of the MON 87419 insert paired with a second primer specific to the genomic DNA sequence flanking the 3' end of the insert (Figure 10). A sequence comparison between the PCR product generated from the conventional control and the sequence generated from the 5' and 3' flanking sequences of MON 87419 indicates that 602 bases of maize genomic DNA were deleted during integration of the T-DNA I. The remainder of the flanks in MON 87419 are identical to the conventional control. Such changes are common during plant transformation and these changes presumably resulted from double stranded break repair mechanisms in the plant during *Agrobacterium*-mediated transformation process (Salomon and Puchta, 1998).

Figure 10. PCR Amplification of the MON 87419 Insertion Site
PCR analysis was performed to evaluate the insertion site. PCR was performed on conventional control DNA using Primer A, specific to the 5′ flanking sequence, and Primer B, specific to the 3′ flanking sequence of the insert in MON 87419. The amplicon generated from the conventional control PCR was used for sequencing analysis. This illustration depicts the MON 87419 insertion site in the conventional control (upper panel) and the MON 87419 insert (lower panel). To verify the PCR products, a portion of each PCR was loaded on the gel. Lane designations are as follows:

Lane	
1	1 Kb Plus DNA Ladder
2	Conventional Control
3	No template DNA control
4	1 Kb Plus DNA Ladder

Arrows next to the agarose gel photograph denote the size of the DNA, in kilobase pairs, obtained from the 1 Kb DNA Plus Ladder (Invitrogen) on the ethidium bromide stained gel.

[r1]Superscript in Left and Right Border Regions indicate that the sequence in MON 87419 was truncated compared to the sequences in PV-ZMHT507801.

For details, please also refer to [redacted]., 2014 (MSL0025902).

A3(d)(iv) Map of the organisation of the inserted DNA (each site)

PCR and DNA sequence analyses performed on MON 87419 and the conventional control determined the organisation of the genetic elements within the insert as given in Figure 9.

A3(d)(v) Identification and characterisation of unexpected ORFs

Unlike the previous section where prior safety assessments can be applied due to identical coding regions, each unique transformation (MON 87419) must be assessed with bioinformatic analyses to confirm a lack of allergenic or toxic effects due to the specific location in which the transformation occurred.

The 2009 Codex Alimentarius Commission guidelines for the safety assessment of food derived from biotechnology crops (Codex Alimentarius, 2009) includes an assessment element on the identification and evaluation of *"open reading frames within the inserted DNA or created by the insertion with contiguous plant genomic DNA."* These assessments examine the potential homology of any putative polypeptides or proteins that could be produced from open reading frames (ORFs) in the insert or at the plant-insert junction to known toxins or allergens. These analyses are conducted even if there is no evidence that such ORFs at the plant-insert junction or alternative reading frames in the insert are capable of being transcribed or translated into a protein. Results from these bioinformatics analyses demonstrate that any putative polypeptides in MON 87419 are unlikely to exhibit allergenic, toxic or otherwise biologically adverse properties.

In addition to the bioinformatic analyses conducted on MON 87419 DMO and PAT protein sequences (Sections B4(a) and B5(b)), bioinformatic analyses were also performed on the MON 87419 insert to assess the potential for allergenicity, toxicity, or biological activity of putative polypeptides encoded by all six reading frames present in the MON 87419 insert DNA, as well as ORFs present in the 5' and 3' flanking sequence junctions. These various bioinformatic evaluations are depicted in Figure 11. ORFs spanning the 5' and 3' maize genomic DNA-inserted DNA junctions were translated from stop codon to stop codon in all six reading frames (three forward reading frames and three reading frames in reverse orientation)[3]. Polypeptides of eight amino acids or greater from each reading frame were then compared to toxin, allergen and all proteins databases using bioinformatic tools. Similarly, the entire T-DNA I sequence was translated in all six reading frames and the resulting deduced amino acid sequence was subjected to bioinformatic analyses. The data generated from these analyses confirm that even in the highly unlikely occurrence that a translation product other than MON 87419 DMO and PAT proteins were derived from frames one to six of the insert DNA or the ORFs spanning the insert junctions, they would not share a sufficient degree of sequence similarity with other proteins to indicate they would

[3] An evaluation of sequence translated from stop codon to stop codon represents the most conservative approach possible for flank junction analysis as it does not take into consideration that a start codon is necessary for the production of a protein sequence.

be potentially allergenic, toxic, or have other safety implications. Therefore, there is no evidence for concern regarding the relatedness of the putative polypeptides for MON 87419 to known toxins, allergens, or biologically active putative peptides.

Bioinformatics Assessment of Insert DNA Reading Frames

Bioinformatic analyses were performed to assess the potential of toxicity, allergenicity or biological activity of any putative peptides encoded by translation of reading frames 1 through 6 of the inserted DNA in MON 87419 (Figure 11).

The FASTA sequence alignment tool was used to assess structural relatedness between the query sequences and any protein sequences in the AD_2014, TOX_2014, and PRT_2014 databases. Structural similarities shared between each putative polypeptide with each sequence in the database were examined. The extent of structural relatedness was evaluated by detailed visual inspection of the alignment, the calculated percent identity and alignment length to ascertain if alignments exceeded Codex (Codex Alimentarius, 2009) thresholds for FASTA searches of the AD_2014 database, and the *E*-score. Alignments having an *E*-score less than 1×10^{-5} are deemed significant because they may reflect shared structure and function among sequences. In addition to structural similarity, each putative polypeptide was screened for short polypeptide matches using a pair-wise comparison algorithm. In these analyses, eight contiguous and identical amino acids were defined as immunologically relevant, where eight represents the typical minimum sequence length likely to represent an immunological epitope (Silvanovich *et al.*, 2006) and evaluated against the AD_2014 database.

The results of the search comparisons showed that no relevant structural similarity to known allergens or toxins were observed for any of the putative polypeptides when compared to proteins in the allergen (AD_2014) or toxin (TOX_2014) databases. Furthermore, no short (eight amino acid) polypeptide matches were shared between any of the putative polypeptides and proteins in the allergen database.

When used to query the PRT_2014 database, translations of frames 2-4 and 6 yielded alignments with *E*-scores less than or equal to 1e-5. One of the top alignments from frame 2 translation positively identified phosphinothricin-N-acetyltransferase (GI-393008205) with a significant *E*-score of 3.3 e-71 and 100% identity over a 183 amino acid region, and is consistent with the known insert structure in MON 87419. Alignment of frame 2 with the coding sequence for the phosphinothricin N-acetyltransferase (PAT) protein of *S. viridochromogenes* is expected as it confers tolerance to glufosinate (Wehrmann *et al.*, 1996; Wohlleben *et al.*, 1988) and is one of the key components in MON 87419. The frame 3 translation yielded several alignments with significant *E*-scores (~1960 alignments). Two distinct groups of alignments were observed with the frame 3 query sequence. The first group of alignments was observed from 290 to 490 amino acids of the query sequence while the second group of alignment was in the ~1560 to ~2170 amino acids region of the query sequence. Four alignments (GI-375890316, GI-314752046, GI-375893503 and GI-314755233) were observed in the regions of 290 to 490 amino acids and were punctuated with numerous stop codons in the query sequence and needed gaps to optimize the alignments. The second group of alignments between regions of ~1560 to ~2170 amino

acids positively identified an entry whose description is: *"chloroplast CP4-EPSPS fusion protein precursor"* (GI-48995007) and a second *"CTP for efficient targeting of the DMO protein"* (GI-507614803). Further investigation of the frame 3 alignment with GI-48995007 revealed that the alignment was limited to the Chloroplast Transit Peptide region, which is upstream of CP4 EPSPS sequence in GI-48995007. These alignments of frame 3 with transit peptides is consistent with the known insert structure of MON 87419 which includes the coding sequence for a chloroplast targeting peptide. Inspection of frame 4 and 6 translation revealed that the alignments were punctuated with numerous stop codons in the query sequence and required numerous gaps to optimize the alignment.

Taken together, these data demonstrate the lack of relevant similarities between known allergens or toxins for putative peptides derived from all six reading frames from the inserted DNA sequence of MON 87419. As a result, it is unlikely these alignments reflect a conserved structure. In the unlikely event that a translation product other than the MON 87419 DMO or PAT protein sequences were derived from reading frames 1 to 6, these putative polypeptides are not expected to be cross-reactive allergens, toxins, or display adverse biological activity.

Insert Junction Open Reading Frame Bioinformatics Analysis

Analyses of putative polypeptides encoded by DNA spanning the 5' and 3' genomic junctions of the MON 87419 inserted DNA were performed using a bioinformatic comparison strategy (Figure 11). The purpose of the assessment was to evaluate the potential for novel ORFs that may have homology to known allergens, toxins, or proteins that display adverse biological activity. Sequences spanning the 5' and 3' maize genomic DNA-inserted DNA junctions (Figure 11) were translated from stop codon (TGA, TAG, TAA) to stop codon in all six reading frames. Putative polypeptides from each reading frame of eight amino acids or greater in length, were compared to AD_2014, TOX_2014, and PRT_2014 databases using FASTA and to the AD_2014 database using an eight amino acid sliding window search.

The FASTA sequence alignment tool was used to assess structural relatedness between the query sequences and protein sequences in the AD_2014, TOX_2014, and PRT_2014 databases. Structural similarities shared between 11 putative polypeptides with each sequence in the database were examined. The extent of structural relatedness was evaluated by detailed visual inspection of the alignment, the calculated percent identity and the alignment length to ascertain if alignments exceeded Codex (Codex Alimentarius, 2009) thresholds for FASTA searches of the AD_2014 database, and the *E*-score. In addition to structural similarity, each putative polypeptide was screened for short polypeptide matches using a pair-wise comparison algorithm. In these analyses, eight contiguous and identical amino acids were defined as immunologically relevant, where eight represents the typical minimum sequence length likely to represent an immunological epitope, and evaluated against the AD_2014 database (Silvanovich *et al.*, 2006).

When used to search the AD_2014 and TOX_2014, no biologically relevant structural similarity to known allergens or toxins, respectively, were observed for any of the putative polypeptides. Furthermore, when used to search the PRT_2014 database, query sequence 5_4 generated one alignment with hypothetical protein from *Zea mays* (GI-413918917) with

an *E*-score of 1e-12 displaying 95.6% identity. Inspection of the alignment revealed that the aligning region was from 50-95 amino acids of the query sequence which is located 66 nucleotides upstream of the T-DNA I insertion site in the genomic DNA. Although less than the *E*-score limit of 1e-5, considering there is no function related to this hypothetical protein, the alignment did not provide any indication of adverse biological activity. Additionally, no short (eight amino acid) polypeptide matches were shared between any of the putative polypeptides and proteins in the AD_2014 database. As a result, in the unlikely event that a translation product was derived from DNA spanning the maize genomic DNA-insert junctions of MON 87419, these putative polypeptides are not expected to be allergens, toxins, or display adverse biological activity.

Bioinformatic Asessment of Allergenicity, Toxicity, and Adverse Biological Activity Potential of MON 87419 Polypeptides Putatively Encoded by the Insert and Flanking Sequences Summary and Conclusions

A conservative bioinformatic assessment of allergenicity, toxicity and adverse biological activity for putative polypeptides that are encoded on all reading frames and spanning the 5' and 3' junctions of MON 87419 was conducted. The data generated from these analyses confirm that even in the highly unlikely occurrence that a translation product other than MON 87419 DMO or PAT protein sequences were derived from frames 1 to 6 for the insert DNA, or the insert junctions, they would not share a sufficient degree of sequence similarity with other proteins to indicate they would be potentially allergenic, toxic, or have other safety implications. Furthermore, no short (eight amino acid) polypeptide matches were shared between any of the putative polypeptides and proteins in the allergen database. Therefore, there is no evidence for concern regarding the putative polypeptides for MON 87419 relatedness to known toxins, allergens or biologically active proteins.

For details, please also refer to [redacted], 2014 (MSL0025907), [redacted], 2014 (MSL0025920) and [redacted], 2014 (MSL0026123).

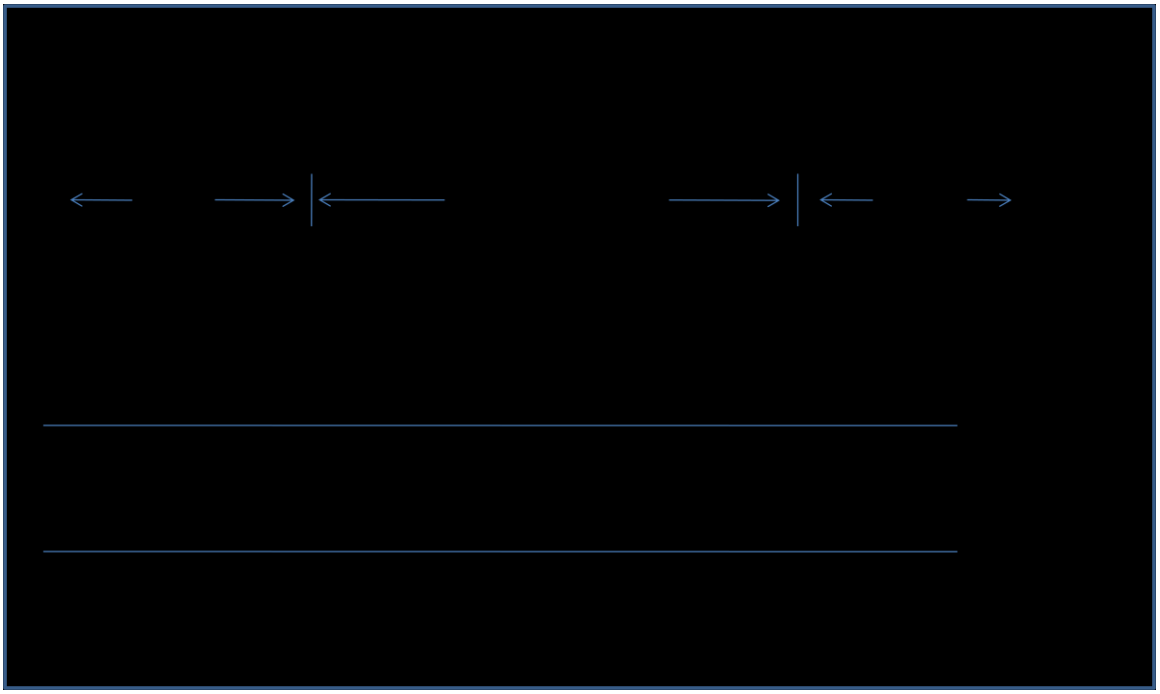

AD= AD_2014; TOX= TOX_2014 and PRT= PRT_2014 (GenBank release #199): 8-mer = the eight amino acid sliding window search.

Figure 11. Schematic Summary of MON 87419 Bioinformatic Analyses

A3(e) Family tree or breeding process

The MON 87419 transformation was conducted with inbred maize line LH244, a patented maize line assigned to Holden's Foundation Seeds LLC in 2001 (U.S. Patent #6,252,148). LH244 is a medium season yellow dent maize line with a Stiff Stalk background that is best adapted to the central regions of the U.S. corn belt. LH244 was initiated from a single cross of LH197 × LH199 followed by a backcross to LH197. The F_2 combination ((LH197 × LH199) × LH197) was then selfed and used in the development of LH244.

Following transformation of immature LH244 embryos, a single transformed plant was selected and self-crossed to increase seed supplies. A homozygous inbred line was developed though further self-crossing and selection and was then used to produce other MON 87419 lines that were used for product testing, safety assessment studies, and commercial hybrid development. The non-transformed LH244 was used as a conventional maize comparator (hereafter referred to as the conventional control) in the safety assessment of MON 87419. For more details, see MON 87419 breeding history, Figure 7.

Please also refer to Section A3(f)(i).

A3(f) Evidence of the stability of the genetic changes

A3(f)(i) Pattern of inheritance of insert and number of generations monitored

Determination of Insert Stability over Multiple Generations of MON 87419

In order to demonstrate the stability of the T-DNA I present in MON 87419 through multiple breeding generations, NGS/JSA was performed using DNA obtained from five breeding generations of MON 87419. The breeding history of MON 87419 is presented in Figure 7, and the specific generations tested are indicated in the figure legend. The MON 87419 R_3 generation was used for the molecular characterization analyses discussed in Sections A3(d)(i) and A3(d)(ii) and shown in Figure 7. To assess stability, four additional generations were evaluated by NGS/JSA as previously described in Section A3(d)(i), and compared to the fully characterized R_3 generation. The conventional controls used for the generational stability analysis included LH244, with similar background genetics to the R_3, R_4 and the R_5 generations and represents the original transformation line; and HCL645 × LH244, a hybrid with similar background genetics to the R_3F_1 hybrid and to the R_4F_1 hybrid. Genomic DNA isolated from each of the selected generations of MON 87419 and conventional control was used for NGS/JSA.

To determine the insert number in the MON 87419 generations, the sequences selected as described in Section A3(d)(ii) were analyzed using JSA (Kovalic *et al.*, 2012).

Table 4 shows the number of resultant JSCs containing PV-ZMHT507801 DNA sequence determined by this analysis.

Table 4. Junction Sequence Classes Detected

Sample	Junction Sequence Classes Detected
MON 87419 (R_3)	2
MON 87419 (R_3F_1)	2
MON 87419 (R_4)	2
MON 87419 (R_4F_1)	2
MON 87419 (R_5)	2
LH244	0
HCL645 × LH244	0

Alignment of the JSCs from each of the assessed MON 87419 generations (R_4, R_5, R_3F_1, and R_4F_1) to the full flank/insert sequence and JSCs determined for the MON 87419 R_3 generation, confirms that the pair of JSCs originates from the same region of the MON 87419 genome and is linked by contiguous, known and expected DNA sequence. This single identical pair of JSCs is observed as a result of the insertion of PV-ZMHT507801 T-DNA I at a single locus in the genome of MON 87419. The consistency of these JSC data across all generations tested demonstrates that this single locus was stably maintained throughout the MON 87419 breeding process, thereby confirming the stability of the insert. Based on this comprehensive sequence data and bioinformatic analysis (NGS/JSA), it is concluded that MON 87419 contains a single and stable T-DNA I insertion.

For details, please also refer to [redacted]., 2014 (MSL0025902).

Inheritance of the Genetic Insert in MON 87419

The MON 87419 T-DNA I resides at a single locus within the maize genome and therefore should be inherited according to Mendelian principles of inheritance. During development of lines containing MON 87419, phenotypic and genotypic segregation data were recorded to assess the inheritance and stability of the MON 87419 T-DNA I using Chi square (χ^2) analysis over several generations. The χ^2 analysis is based on comparing the observed segregation ratio to the expected segregation ratio according to Mendelian principles.

The MON 87419 breeding path for generating segregation data is described in Figure 12. The transformed R_0 plant was self-pollinated to generate R_1 seed. An individual plant

homozygous for the MON 87419 T-DNA I was identified in the R_1 segregating population via a Real-Time TaqMan® PCR assay.

The homozygous positive R_1 plant was self-pollinated to give rise to R_2 seed. The R_2 plants were self-pollinated to produce R_3 seed. R_3 plants homozygous for the MON 87419 T-DNA I were crossed via traditional breeding techniques to a Monsanto proprietary recurrent parent that does not contain the *dmo* or *pat* coding sequences to produce hemizygous R_3F_1 seed. The R_3F_1 plants were crossed with the recurrent parent to produce BC_1F_1 seed. The BC_1F_1 generation was tested for the presence of the T-DNA I by End-Point TaqMan PCR to select for hemizygous MON 87419 plants. BC_1F_1 plants hemizygous for MON 87419 T-DNA I were crossed with the recurrent parent to produce the BC_2F_1 plants. The BC_2F_1 plants were assessed using a glufosinate spray treatment to select for plants containing the MON 87419 T-DNA I. The surviving BC_2F_1 plants were self-pollinated to produce the BC_2F_2 plants.

The inheritance of the MON 87419 T-DNA I was assessed in the BC_1F_1, BC_2F_1, and BC_2F_2 generations. At the BC_1F_1 and BC_2F_1 generations, the MON 87419 T-DNA I was predicted to segregate at a 1:1 ratio (hemizygous positive: homozygous negative) according to Mendelian inheritance principles. At the BC_2F_2 generation, the MON 87419 T-DNA I was predicted to segregate at a 1:2:1 ratio (homozygous positive: hemizygous positive: homozygous negative) according to Mendelian inheritance principles.

A Pearson's chi square (χ^2) analysis was used to compare the observed segregation ratios of the MON 87419 T-DNA I coding sequence to the expected ratios.

The Chi square was calculated as:

$$\chi^2 = \sum [(| o - e |)^2 / e]$$

where o = observed frequency of the genotype or phenotype and e = expected frequency of the genotype or phenotype. The level of statistical significance was predetermined to be 5% ($\alpha = 0.05$).

The results of the χ^2 analysis of the segregating progeny of MON 87419 are presented in Table 5. The χ^2 value in the BC_1F_1 and BC_2F_1 generations indicated no statistically significant difference between the observed and expected 1:1 segregation ratio (hemizygous positive: homozygous negative) of MON 87419 T-DNA I. The χ^2 value in the BC_2F_2 generation indicated no statistically significant difference between the observed and expected 1:2:1 ratio (homozygous positive: hemizygous positive: homozygous negative) of MON 87419 T-DNA I. These results support the conclusion that the MON 87419 T-DNA I resides at a single locus within the maize genome and is inherited according to Mendelian principles of inheritance. These results are also consistent with the molecular

® TaqMan is a registered trademark of Roche Molecular Systems, Inc.

characterization data indicating that MON 87419 contains a single intact copy of the *dmo* and *pat* expression cassettes inserted at a single locus in the maize genome.

For details, please also refer to [redacted] 2014 (MSL0025519).

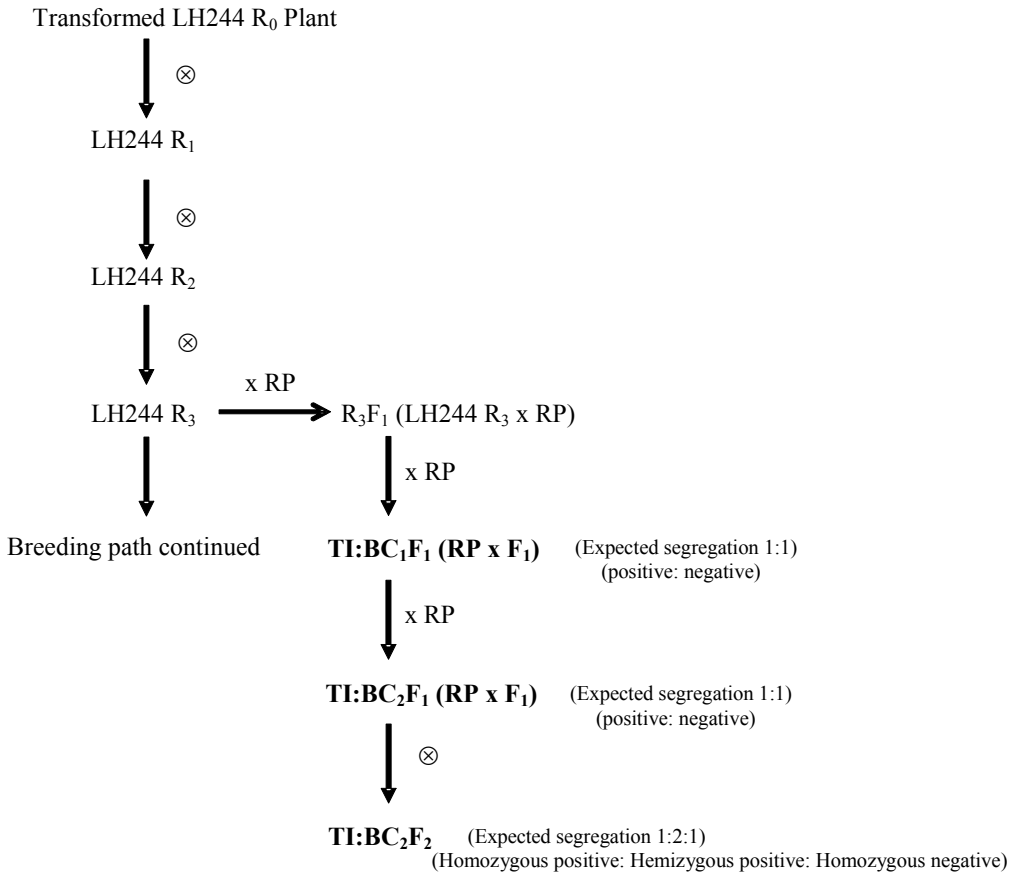

Figure 12. Breeding Path for Generating Segregation Data for MON 87419

Chi-square analysis was conducted on segregation data from BC_1F_1, BC_2F_1, and BC_2F_2 generations (bolded text).

TI: Trait Integration: Replacement of genetic background of MON 87419 by recurrent background except inserted gene.

RP: Recurring parent.

BC: Back-Cross.

⊗: Self-Pollinated.

Table 5. Segregation of the Expression Cassette During the Development of MON 87419

				1:1 Segregation			
Generation	**Number of Plants**	**Observed Positives**	**Observed Negatives**	**Expected Positives**	**Expected Negatives**	**χ^2**	**Probability**
BC_1F_1	126	64	62	63	63	0.03	0.859
BC_2F_1	381	192	189	190.5	190.5	0.02	0.878

					1:2:1 Segregation				
Generation	**Number of Plants**	**Observed Homozygous Positives**	**Observed Hemizygous Positives**	**Observed Homozygous Negatives**	**Expected Homozygous Positives**	**Expected Hemizygous Positives**	**Expected Homozygous Negatives**	**χ^2**	**Probability**
BC_2F_2	164	48	83	33	41	82	41	2.77	0.251

Characterization of the Genetic Modification Summary and Conclusion

Molecular characterization of MON 87419 by NGS/JSA and directed sequencing demonstrated that a single copy of the intended transfer DNA I (T-DNA I) containing the *dmo* and the *pat* expression cassettes from PV-ZMHT507801 was integrated into the maize genome at a single locus. These analyses also showed no PV-ZMHT507801 backbone elements or T-DNA II sequences were present in MON 87419.

Directed sequence analyses performed on MON 87419 confirmed the organization and intactness of the full T-DNA I and all expected elements within the insert, with the exception of incomplete Right and Left Border sequences that do not affect the functionality of the *dmo* and *pat* expression cassettes. Analysis of the T-DNA I insertion site in maize showed that the 5′ and 3′ genomic DNA flanking the T-DNA I insert in MON 87419 are identical to the conventional control, except for a 602 base pair deletion of genomic DNA at the insertion site in MON 87419. Such changes are common during plant transformation and these changes presumably resulted from double stranded break repair mechanisms in the plant during *Agrobacterium*-mediated transformation process (Salomon and Puchta, 1998). This deletion is not expected to affect food or feed safety.

Generational stability analysis by NGS/JSA demonstrated that the T-DNA I in MON 87419 was maintained through five breeding generations, thereby confirming the stability of the insert. Results from segregation analyses show heritability and stability of the insert occurred as expected across multiple breeding generations, which corroborates the molecular insert stability analysis and establishes the genetic behavior of the T-DNA I in MON 87419 at a single chromosomal locus

A3(f)(ii) Pattern of expression of phenotype over several generations

In order to assess the presence of the DMO and PAT (*pat*) protein in MON 87419 across multiple breeding generations, western blot analysis of MON 87419 was conducted on seed tissue collected from generations R_3, R_3F_1, R_4, R_4F_1, and R_5 of MON 87419, using seed tissue of the conventional control (LH244) as negative control.

The presence of the MON 87419 DMO protein was demonstrated in five breeding generations of MON 87419 using western blot analyses (Figure 13). The *E. coli*-produced DMO protein reference standard (1.5 ng) was used as a reference for the positive identification of the DMO protein (Figure 13, lane 4). The presence of the DMO protein in MON 87419 seed tissue samples was determined by visual comparison of the bands detected in five breeding generations (Figure 13, lanes 7-11) to the *E. coli*-produced DMO protein reference standard (Figure 13, lane 4). The MON 87419-produced DMO protein was observed in all five generations and migrated indistinguishably from that of the *E. coli*-produced protein standard analyzed on the same western blot. As expected, the DMO protein was not detected in the conventional control seed extract used as the negative control (Figure 13, lane 6). Additional faint bands

corresponding to proteins other than the expected DMO protein were detected in both MON 87419 and conventional seed samples. The presence in both samples is likely the result of cross-reactivity between the primary or secondary antibodies to proteins endogenous to maize seed. The non-specific binding of the antibodies resulted in the appearance of bands approximately 40 kDa and 80 kDa (Figure 13, lanes 6-11), in both MON 87419 and conventional control samples. The presence of these non-specific bands does not affect the conclusions of the present study which establishes the generational stability of the DMO protein in MON 87419.

The presence of the PAT (*pat*) protein was demonstrated in five breeding generations of MON 87419 using western blot analyses (Figure 14). The *E. coli*-produced PAT (*pat*) protein reference standard (1.0 ng) was used as a reference for the positive identification of the PAT (*pat*) protein (Figure 14, lane 4). The presence of the PAT (*pat*) protein in MON 87419 seed tissue samples was determined by visual comparison of the bands detected in five breeding generations (Figure 14, lanes 7-11) to the *E. coli*-produced PAT (*pat*) protein reference standard (Figure 14, lane 4). The MON 87419-produced PAT (*pat*) protein was observed in all five generations and migrated indistinguishably from that of the *E. coli*-produced protein standard analyzed on the same western blot. As expected, the PAT (*pat*) protein was not detected in the conventional control seed extract used as the negative control (Figure 14, lane 6).

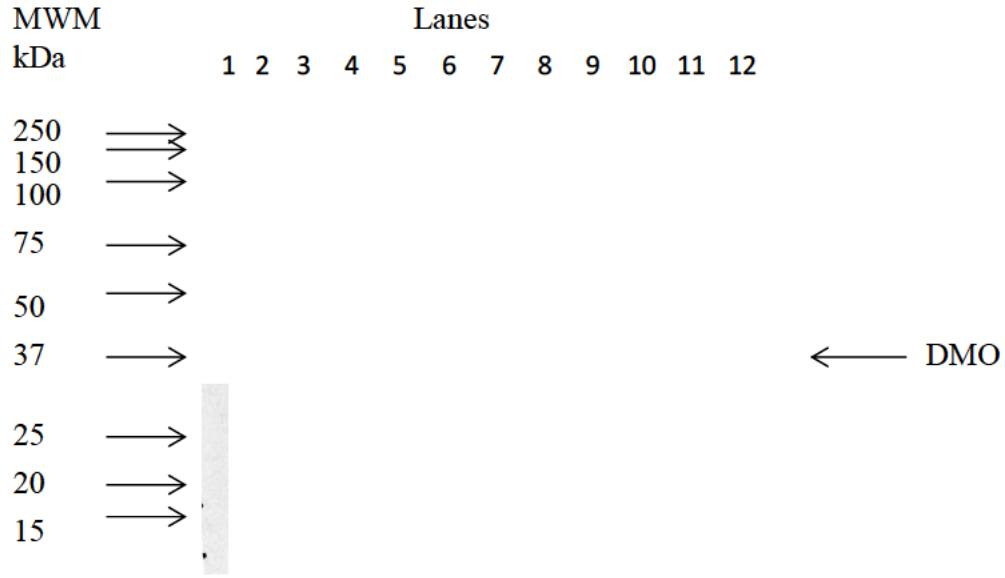

Figure 13. Presence of DMO Protein in Multiple Generations of MON 87419

Extracts from five generations of MON 87419 seed tissue, conventional control seed tissue, *E. coli*-produced DMO protein standard, and molecular weight markers were subjected to SDS-PAGE and electrotransferred to a nitrocellulose membrane. The membrane was incubated with goat anti-DMO antibody and immunoreactive bands visualized through the use of chemiluminescent reagents. Exposure time was six minutes. The molecular weights (in kDa) of the standards are shown on the left. Lane designations are as follows:

Lane	Sample	Amount Loaded on Gel
1	Blank	-
2	Precision Plus Protein Dual Color Molecular Weight Marker	5 µl
3	Blank	-
4	*E. coli*-produced DMO protein (1.5 ng)	15 µl
5	Blank	-
6	Conventional Control	10 µl
7	MON 87419 R_3 Generation	10 µl
8	MON 87419 R_3F_1 Generation	10 µl
9	MON 87419 R_4 Generation	10 µl
10	MON 87419 R_4F_1 Generation	10 µl
11	MON 87419 R_5 Generation	10 µl
12	Blank	-

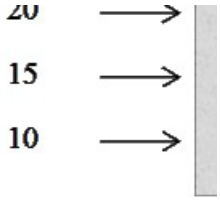

Figure 14. Presence of PAT (*pat*) Protein in Multiple Generations of MON 87419

Extracts from five generations of MON 87419 seed tissue, conventional control seed tissue, *E. coli*-produced PAT (*pat*) protein standard, and molecular weight markers were subjected to SDS-PAGE and electrotransferred to a nitrocellulose membrane. The membrane was incubated with goat anti-PAT (*bar*) antibody and immunoreactive bands visualized through the use of chemiluminescent reagents. Exposure time was seven minutes. The molecular weights (in kDa) of the standards are shown on the left. Lane designations are as follows:

Lane	Description	Amount Loaded on Gel
1	Blank	-
2	Precision Plus Protein Dual Color Molecular Weight Marker	5 µl
3	Blank	-
4	*E. coli*-produced PAT (*pat*) protein (1.0 ng)	10 µl
5	Blank	-
6	Conventional Control	10 µl
7	MON 87419 R_3 Generation	10 µl
8	MON 87419 R_3F_1 Generation	10 µl
9	MON 87419 R_4 Generation	10 µl
10	MON 87419 R_4F_1 Generation	10 µl
11	MON 87419 R_5 Generation	10 µl
12	Blank	-

A4 Analytical Method for Detection

The event-specific DNA-based detection methods such as PCR can be used as the monitoring tool to determine the presence of MON 87419 in a collected sample.

B. INFORMATION RELATED TO THE SAFETY OF THE GM FOOD

B1 Equivalence Studies

B1(a) Characterisation and equivalence of MON 87419 DMO protein from MON 87419

Identity and Function of the DMO Protein

DMO proteins have been isolated from the bacterium *S. maltophilia* strain DI-6 (Herman *et al.*, 2005; Krueger *et al.*, 1989; Palleroni and Bradbury, 1993). MON 87419 expresses the DMO protein to confer tolerance to dicamba herbicide. DMO is an enzyme that catalyzes the demethylation of dicamba to the non-herbicidal compounds 3,6 dichlorosalicylic acid (DCSA) and formaldehyde (Chakraborty *et al.*, 2005). DCSA is a known metabolite of dicamba in cotton, soybean, soil, and livestock, whose safety has been evaluated by the FAO-WHO and EPA (FAO-WHO, 2011b; U.S. EPA, 2009b). The other reaction product, formaldehyde, is found naturally in many plants at levels up to several hundred ppm (Adrian-Romero *et al.*, 1999).

MON 87419 DMO is targeted to chloroplasts by CTP to allow co-localization with the endogenous reductase and ferredoxin enzymes that supply electrons for the DMO demethylation reaction as described by Behrens et al. (2007). In the construction of the plasmid vector used in the development of MON 87419, PV-ZMHT507801, a CTP chloroplast transit peptide coding sequence from *Petunia hybrida* EPSPS (*CTP4*, Table 2) was joined to the *dmo* coding sequence; this coding sequence results in the production of a precursor protein consisting of the DMO protein and a N-terminal 72 amino acid CTP, which is utilized to target the precursor protein to the chloroplast (Herrmann, 1995; Klee *et al.*, 1987). Typically, transit peptides are precisely removed from the precursor protein following delivery to the targeted plastid (della-Cioppa *et al.*, 1986) resulting in the full length protein. However, there are examples in the literature of alternatively processed forms of a protein targeted to a plant's chloroplast (Behrens *et al.*, 2007; Clark and Lamppa, 1992). Such alternative processing is observed with the DMO precursor protein produced in MON 87419. Two forms of DMO proteins expressed in MON 87419 have been identified by the N-terminal sequencing analysis, resulting from an alternative processing of the CTP. One form, referred to as MON 87419 DMO+12 and the other, MON 87419 DMO+7. MON 87419 DMO+7 does not contain the first five amino acids of MON 87419 DMO+12. The amino acid differences between these two forms of DMO proteins occur at the N-termini, which are derived from *CTP*. Because the amino acid residues present in MON 87419 DMO+7 are also present in MON 87419 DMO+12 and both forms of DMO are indistinguishableby Coomassie stain and western blot analyses of SDS-PAGE with the apparent molecular weight of ~39.5 kDa, MON 87419 DMO protein will be used to refer to both forms of the protein collectively and distinctions will only be made where necessary.

Except for the amino acids derived from the *CTP4* (7 or 12) and an additional leucine at position two, the MON 87419 DMO protein has an identical sequence to the wild-type DMO protein from the DI-6 strain of *S. maltophilia* (Herman *et al.*, 2005) (Figure 15). The

differences in the amino acid sequence between the wild-type DMO proteins and MON 87419 DMO protein are not anticipated to have an effect on structure of the catalytic site, functional activity, immunoreactivity or specificity because the N-terminus and position two are sterically distant from the catalytic site (D'Ordine *et al.*, 2009; Dumitru *et al.*, 2009).

The MON 87419 DMO+12 and MON 87419 DMO+7 proteins are identical to MON 88701 DMO, except for the amino acids derived from CTP at the N-terminus, which are 12 or 7 amino acids encoded by the CTP4 gene for MON 87419 DMO+12 and MON 87419 DMO+7, respectively, and 9 amino acids encoded by the CTP2 gene for MON 88701 DMO (Figure 15). The MON 87419 DMO+12 and MON 87419 DMO+7 proteins are also identical to MON 87708 DMO (fully processed), except for an addition of 12 or 7 amino acids, respectively, from CTP4, a methionine that remained at the N-terminus from the *dmo* gene, and two single amino acid changes at positions 2 and 112 (Figure 15). These amino acids in MON 87419 DMO+12 or MON 87419 DMO+7 differed from the DMO proteins expressed in MON 88701 or MON 87708 are not involved in the catalytic site (D'Ordine *et al.*, 2009; Dumitru *et al.*, 2009). Therefore, MON 87419 DMO protein is identical in structure of the catalytic site, function, immunoreactivity and specificity to DMO proteins previously assessed and deregulated by USDA-APHIS (MON 87708, USDA-APHIS # 10-180-01p and MON 88701, USDA-APHIS # 10-188-01p). DMO proteins in both MON 87708 and MON 88701 also completed U.S. FDA consultation (BNF 000125 and BNF 000135), which determined that food and feed products derived from MON 87708 and MON 88701 and its progeny are as safe and nutritious as food and feed derived from conventional soybean and cotton. Furthermore, MON 87708 and MON 87701 (A1063 and A1080) have been approved by FSANZ. Therefore, all appropriate acute toxicology, digestibility and heat susceptibility studies reported on DMO proteins in A1063 and A1080 apply.

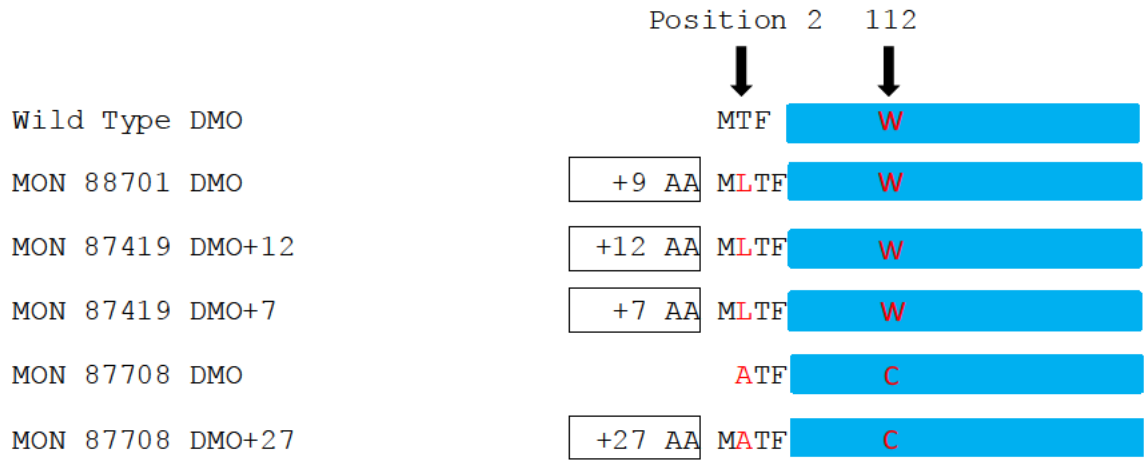

Figure 15. Forms of DMO Protein and Their Relation to the Wild-Type DMO Protein

The diagram represents the various DMO forms discussed in this section. The blue regions indicate regions of 100% amino acid identity. The wild-type DMO form isolated from *S. maltophilia* was the first form sequenced (Herman *et al.*, 2005). The MON 88701 DMO protein is identical to wild type DMO, except for an insertion of a leucine at position 2, and an addition of 9 amino acids from CTP2 at the N-terminus. The MON 87419 DMO+12 and +7 proteins are also identical to wild type DMO, except for an insertion of a leucine at position 2 and an addition of 12 or 7 amino acids, respectively, from CTP4 at the N-terminus. The MON 87419 DMO+12 and MON 87419 DMO+7 proteins are identical to MON 88701 DMO, except for the amino acids derived from CTP at the N-terminus, which are 12 or 7 amino acids encoded by the CTP4 gene for MON 87419 DMO+12 and MON 87419 DMO+7, respectively, and 9 amino acids encoded by the CTP2 gene for MON 88701 DMO. The MON 87419 DMO+12 and MON 87419 DMO+7 proteins are also identical to MON 87708 DMO (fully processed), except for an addition of 12 or 7 amino acids, respectively, from CTP4, a methionine that remained at the N-terminus from the *dmo* gene, and two single amino acid changes at positions 2 and 112. Position refers to amino acid residues as wild type DMO and boxed regions correspond to CTP, except for MON 87708 DMO+27 that is encoded by the *RbcS* coding region.

Equivalence Studies of the DMO Protein

The safety assessment of crops derived through biotechnology includes characterization of the physicochemical and functional properties of and confirmation of the safety of the introduced protein(s). Because the minor differences in the amino acid sequences between MON 87419 DMO+12 and MON 87419 DMO+7 occur at the N-terminus, which derived from CTP4, they are not expected to have an effect on structure of the catalytic site, functional activity, immunoreactivity or specificity because "the catalytic domain of DMO is distinct in that it contains no contribution from an N-terminal extension" (D'Ordine *et al.*, 2009). Importantly, the DMO functional activity assay demonstrated that the functional activity of *E. coli*-produced MON 87419 DMO+12 is equivalent to MON 87419 DMO, which are 240.1 and 232.5 nmol × $minute^{-1}$ × mg^{-1}, respectively (Table 10). Furthermore, the amino acid residues present in MON 87419 DMO+7 are also present in MON 87419 DMO+12. Therefore, an assessment of *E. coli*-produced MON 87419 DMO+12 is considered comprehensive and applies to *E. coli*-produced MON 87419 DMO+7 because physiochemical and functional equivalence between MON 87419 DMO+12 and the MON 87419-produced DMO protein was established.

Hence, *E.coli*-produced MON 87419 DMO+12 proteins were purified and used as test substance for the safety assessments. For the safety data generated using *E. coli*-produced MON 87419 DMO+12, herein referred to as *E. coli*-produced MON 87419 DMO, to be applied to MON 87419 DMO protein produced in MON 87419, the equivalence of the plant- and *E. coli*-produced proteins must be assessed. To assess the equivalence between MON 87419-produced DMO and *E. coli*-produced MON 87419 DMO proteins, a small quantity of the MON 87419 DMO protein was purified from grain of MON 87419 maize. The MON 87419-produced DMO protein was characterized and the equivalence of the physicochemical characteristics and functional activity between the MON 87419-produced DMO and the *E. coli*-produced MON 87419 DMO proteins was assessed using a panel of six analytical tests as shown in Table 6. Taken together, these data provide a detailed characterization of the MON 87419-produced DMO protein and establish the equivalence of MON 87419-produced DMO and *E. coli*-produced MON 87419 DMO proteins.

For details please refer to [redacted] 2014 (MSL0026361).

Table 6. Summary of MON 87419 DMO Protein Identity and Equivalence

Analytical Test Assessment	Section Cross Reference	Analytical Test Outcome
1. N-terminal sequence analysis of the MON 87419-produced DMO protein to assess the N-terminal sequence	B1(a)(i)	The N-terminal sequences of two forms of DMO proteins were identified, referred to as MON 87419 DMO+12 and MON 87419 DMO+7
2. MALDI-TOF MS1 analysis of peptides derived from tryptic digested MON 87419-produced DMO protein to assess identity	B1(a)(ii)	MALDI-TOF MS1 analysis yielded peptide masses consistent with the peptide masses from the theoretical trypsin digest of the MON 87419-produced DMO sequence
3. Western blot analysis using anti-DMO polyclonal antibodies to assess identity and immunoreactive equivalence between MON 87419-produced DMO and the *E. coli*-produced MON 87419 DMO proteins	B1(a)(iii)	MON 87419-produced DMO protein identity was confirmed using a western blot probed with an antibody specific for DMO proteins Immunoreactive properties of the MON 87419-produced DMO and the *E. coli*-produced MON 87419 DMO proteins were shown to be equivalent
4. SDS-PAGE2 to assess equivalence of the apparent molecular weight between MON 87419-produced DMO and the *E. coli*-produced MON 87419 DMO proteins	B1(a)(iv)	Electrophoretic mobility and apparent molecular weight of the MON 87419-produced DMO and the *E. coli*-produced MON 87419 DMO proteins were shown to be equivalent
5. Glycosylation analysis of the MON 87419 DMO protein to assess equivalence between the MON 87419-produced DMO and the *E. coli*-produced MON 87419 DMO proteins	B1(a)(v)	MON 87419-produced DMO and the *E. coli*-produced MON 87419 DMO proteins were both shown to not be glycosylated
6. DMO enzymatic activity analysis to assess functional equivalence between the MON 87419-produced DMO and the *E. coli*-produced MON 87419 DMO proteins	B1(a)(vi)	Functional activity of the MON 87419-produced DMO and the *E. coli*-produced MON 87419 DMO proteins were shown to be equivalent

[1] MALDI-TOF MS = Matrix Assisted Laser Desorption Ionization Time-of-Flight Mass Spectrometry
[2] SDS-PAGE = sodium dodecyl sulfate-polyacrylamide gel electrophoresis

A summary of the data obtained to support the characterization of the MON 87419-produced DMO and a conclusion of protein equivalence is below.

B1(a)(i) Results of the N-terminal sequencing analysis

Fifteen cycles of N-terminal sequencing was performed on MON 87419-produced DMO protein. The observed amino acid sequence for the DMO protein was consistent with the sequence deduced from the *dmo* expression cassette present in maize of MON 87419 was observed. The experimentally determined sequence corresponds to the deduced DMO protein beginning at the initial serine (MON 87419 DMO+12, Figure 16 Top). In addition, a shorter form of the DMO protein that does not contain the first five amino acids of MON 87419 DMO+12, MON 87419 DMO+7, was observed (Figure 16 Bottom). Hence, the sequence information identified the N-terminal sequences of the DMO proteins isolated from the grain of MON 87419.

Amino Acids Residue # from the N-terminus	→	1	2	3	4	5	6	7	8	9	10	11	12	13	14	15
Deduced Sequence	→	S	F	R	I	S	A	S	V	A	T	A	C	M	L	T
Experimental Sequence (+12)	→	| S	| F	| R	| I	| S	| A	| S	| V	| A	| T	| A	X	X	X	X
Amino Acids Residue # from the N-terminus	→	1	2	3	4	5	6	7	8	9	10	11	12	13	14	15
Deduced Sequence (+7)	→	A	S	V	A	T	A	C	M	L	T	F	V	R	N	A
Experimental Sequence (+7)	→	| A	| S	| V	| A	| T	| A	X	X	X	X	X	X	X	X	X

Figure 16. N-Terminal Sequence of the MON 87419-produced DMO Protein

The experimental sequences obtained from the MON 87419-produced DMO were compared to the sequence deduced from the *dmo* gene present in MON 87419 (Top: MON 87419 DMO+12; Bottom: MON 87419 DMO+7). The N-terminal sequences of two forms of DMO proteins identified correspond to the CTP. The amino acid at position S of the deduced sequence is shown as position 1 of the observed protein for MON 87419 DMO+12 (Top) as well as that at position A of the deduced sequence is shown as position 1 of the observed protein for MON 87419 DMO+7 (Bottom). The single letter International Union of Pure and Applied Chemistry - International Union of Biochemistry (IUPAC-IUB) amino acid code is A, alanine; C, cysteine; F, phenylalanine; I, isoleucine; L, leucine; M, methionine; N, asparagines; R, arginine; S, serine; T, threonine; V, valine. "X" indicates that the residue was not identifiable.

B1(a)(ii) Results of MALDI-TOF Tryptic Mass Map analysis

The identity of the MON 87419-produced DMO protein was confirmed by MALDI-TOF MS analysis of peptide fragments produced by the trypsin digestion of the MON 87419-produced DMO protein. The ability to identify a protein using this method is dependent upon matching a sufficient number of observed tryptic peptide fragment masses with predicted tryptic peptide fragment masses. In general, protein identification made by peptide mapping is considered to be reliable if ≥ 40% of the protein sequence was identified by matching experimental masses observed for the tryptic peptide fragments to the expected masses for the fragments (Biron *et al.*, 2006; Krause *et al.*, 1999).

There were 37 unique peptides identified that corresponded to the calculated masses (

Table 7). The identified masses were used to assemble a peptide map of the MON 87419 DMO protein. The experimentally determined coverage of the MON 87419 DMO protein was 77% (Figure 17, 272 out of 352 amino acids). This analysis confirms the identity of MON 87419-produced DMO protein.

Table 7. Summary of the Tryptic Masses Identified for the MON 87419-produced DMO Using MALDI-TOF MS

Experimental Mass	Calculated Mass[2]	Difference[3]	Fragment[4]	Sequence[5]
1626.7737	1626.8109	-0.0372	4-18	ISAS.....TFVR
2142.0752	2142.1109	-0.0357	19-37	NAWY.....PLGR
1274.6915	1274.7234	-0.0320	38-48	TILD.....ALYR
3017.5625	3017.6008	-0.0383	38-64	TILD.....CPHR
1760.8528	1760.8880	-0.0351	49-64	QPDG.....CPHR
832.4121	832.4443	-0.0322	111-117	SFPVVER
1469.6354	1469.6245	0.0109	149-161	TVGG.....CNYK
3444.5726	3444.6343	-0.0618	149-178	TVGG.....YVHR
1992.9860	1993.0204	-0.0343	162-178	LLVD.....YVHR
3480.7068	3480.7320	-0.0252	162-191	LLVD.....RLER
1107.4616	1107.4945	-0.0329	179-188	ANAQ.....AFDR
1505.6868	1505.7222	-0.0354	179-191	ANAQ.....RLER
2988.4524	2988.4975	-0.0450	179-205	ANAQ.....ALMK
1898.9833	1899.0135	-0.0302	189-205	LERE.....ALMK
1500.7408	1500.7858	-0.0450	192-205	EVIV.....ALMK
1169.6055	1169.6478	-0.0423	206-217	IPGG.....LMAK
1585.8609	1585.9014	-0.0405	206-220	IPGG.....KFLR
1427.6513	1427.6793	-0.0280	221-233	GANT.....NDIR
1855.8617	1855.8965	-0.0348	221-236	GANT.....RWNK
3581.7244	3581.8089	-0.0845	221-253	GANT.....GTPK
3009.5040	3009.5494	-0.0455	234-260	WNKV.....IHSR
1743.8305	1743.9229	-0.0924	237-253	VSAM.....GTPK
2581.2884	2581.3322	-0.0439	237-260	VSAM.....IHSR
855.3948	855.4199	-0.0250	254-260	EQSIHSR
2397.0259	2397.0696	-0.0436	261-281	GTHI.....GSSR
1576.6827	1576.7192	-0.0365	282-295	NFGI.....GVLR
1029.5247	1029.5607	-0.0360	296-304	SWQAQALVK
1401.6680	1401.7252	-0.0572	296-307	SWQA.....KEDK
2297.1993	2297.2379	-0.0387	296-315	SWQA.....AIER
1285.6536	1285.6878	-0.0341	305-315	EDKV.....AIER
1441.7338	1441.7889	-0.0551	305-316	EDKV.....IERR
913.4900	913.5233	-0.0333	308-315	VVVEAIER
1069.5792	1069.6244	-0.0452	308-316	VVVEAIERR
2449.1089	2449.1842	-0.0752	317-338	RAYV.....AAVR
2293.0455	2293.0831	-0.0376	318-338	AYVE.....AAVR
1613.8257	1613.8624	-0.0367	339-352	VSRE.....LEAA
1271.6128	1271.6608	-0.0480	342-352	EIEK.....LEAA

[1] Only experimental masses that matched calculated masses are listed in the table.
[2] The calculated mass is the relative molecular mass calculated from the matched peptide sequence.
[3] The calculated difference between the experimental mass and the calculated mass.
[4] Position refers to amino acid residues within the predicted MON 87419-produced DMO sequence as depicted in Figure 17.
[5] For peptide matches greater than nine amino acids in length the first 4 residues and last 4 residues are show separated by dots (**.....**).

```
  1 SFRISASVAT ACMLTFVRNA WYVAALPEEL SEKPLGRTIL DTPLALYRQP
 51 DGVVAALLDI CPHRFAPLSD GILVNGHLQC PYHGLEFDGG GQCVHNPHGN
101 GARPASLNVR SFPVVERDAL IWIWPGDPAL ADPGAIPDFG CRVDPAYRTV
151 GGYGHVDCNY KLLVDNLMDL GHAQYVHRAN AQTDAFDRLE REVIVGDGEI
201 QALMKIPGGT PSVLMAKFLR GANTPVDAWN DIRWNKVSAM LNFIAVAPEG
251 TPKEQSIHSR GTHILTPETE ASCHYFFGSS RNFGIDDPEM DGVLRSWQAQ
301 ALVKEDKVVV EAIERRRAYV EANGIRPAML SCDEAAVRVS REIEKLEQLE
351 AA
```

Figure 17. MALDI-TOF MS Coverage Map of the MON 87419-produced DMO

The amino acid sequence of the MON 87419-produced DMO protein was deduced from the *dmo* expression cassette present in MON 87419. Boxed regions correspond to peptides that were identified from the MON 87419-produced DMO protein sample using MALDI-TOF MS. In total, 77% coverage (272 out of 352 amino acids) of the expected protein sequence was identified.

B1(a)(iii) Results of western blot analysis of the MON 87419 DMO protein isolated from the grain of MON 87419 and immunoreactivity comparison to *E. coli*-produced MON 87419 DMO

Western blot analysis was conducted using goat anti-DMO polyclonal antibody as additional means to confirm the identity of the MON 87419 DMO protein isolated from the grain of MON 87419 and to assess the equivalence of the immunoreactivity of the MON 87419-produced and *E. coli*-produced MON 87419 DMO proteins.

The results showed that immunoreactive bands with the same electrophoretic mobility were present in all lanes loaded with the MON 87419-produced and *E. coli*-produced MON 87419 DMO proteins (Figure 18). For each amount loaded, comparable signal intensity was observed between the MON 87419-produced and *E. coli*-produced MON 87419 DMO protein bands. As expected, the signal intensity increased with increasing load amounts of the MON 87419-produced DMO and *E. coli*-produced MON 87419 DMO proteins, thus, supporting identification of MON 87419-produced DMO protein. There was a higher molecular weight immunoreactive band (~70 kDa) observed in the lanes loaded with MON 87419-produced DMO, but not observed in the lanes loaded with *E. coli*-produced MON 87419 DMO, which is likely the result of aggregation of MON 87419 DMO protein.

To compare the immunoreactivity of the MON 87419-produced and the *E. coli*-produced MON 87419 DMO proteins, densitometric analysis was conducted on the bands that migrated at the expected apparent MW for DMO proteins (~ 39.5 kDa). The signal intensity (reported in OD × mm^2) of the band of interest in lanes loaded with MON 87419-produced and the *E. coli*-produced MON 87419 DMO proteins was measured (

Table 8). Because the mean signal intensity of the MON 87419-produced DMO protein band was within ± 35% of the mean signal of the *E. coli*-produced MON 87419 DMO protein, the MON 87419-produced DMO and *E. coli*-produced MON 87419 DMO proteins were determined to have equivalent immunoreactivity.

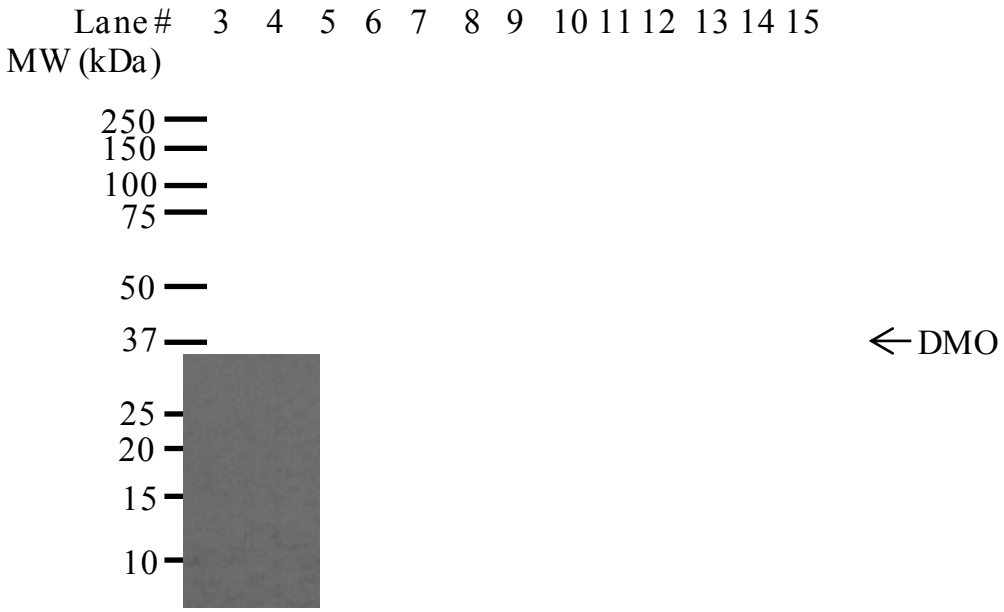

Figure 18. Western Blot Analysis of MON 87419-produced and *E. coli*-produced MON 87419 DMO Proteins

Aliquots of the MON 87419-produced DMO protein and the *E. coli*-produced MON 87419 DMO protein were subjected to SDS-PAGE and electrotransferred to a PVDF membrane. Proteins were detected using anti-DMO antibodies as the primary antibodies. Immunoreactive bands were visualized using HRP-conjugated secondary antibodies and an ECL system. The approximate MW (kDa) of the standards are shown on the left. Lanes 1 and 2 were cropped from the image. Lane designations are as follows:

Lane	Sample	Amount (ng)
1	Precision Plus Protein™ Standards	-
2	Blank	-
3	MON 87419-produced DMO	1
4	MON 87419-produced DMO	1
5	MON 87419-produced DMO	2
6	MON 87419-produced DMO	2
7	MON 87419-produced DMO	3
8	MON 87419-produced DMO	3
9	Blank	-
10	*E. coli*-produced MON 87419 DMO	1
11	*E. coli*-produced MON 87419 DMO	1
12	*E. coli*-produced MON 87419 DMO	2
13	*E. coli*-produced MON 87419 DMO	2
14	*E. coli*-produced MON 87419 DMO	3
15	*E. coli*-produced MON 87419 DMO	3

Table 8. Comparison of Immunoreactive Signal Between MON 87419-produced and *E. coli*-produced MON 87419 DMO Proteins

Mean Signal Intensity from MON 87419-Produced DMO [1] (OD x mm^2)	Mean Signal Intensity from *E. coli*-Produced MON 87419 DMO [1] (OD x mm^2)	Acceptance Limits[2] (OD x mm^2)
2.51	2.23	1.45-3.01

[1] Value refers to mean calculated based on n = 6. Values are rounded to two decimal places.

[2] The acceptance limits are for the MON 87419-produced DMO protein and are based on the interval between -35% (2.23 x 0.65 = 1.45) and +35 % (2.23 x 1.35 = 3.01) of overall mean of the *E. coli*-produced MON 87419 DMO signal intensity at all loads.

B1(a)(iv) Results of MON 87419 DMO protein molecular weight analysis

For apparent MW determination, the MON 87419-produced DMO and the *E. coli*-produced MON 87419 DMO proteins were subjected to SDS-PAGE. Following electrophoresis, the gel was stained with Brilliant Blue G-Colloidal stain and analyzed by densitometry. The intact MON 87419-produced DMO protein migrated to the same position on the gel as the *E. coli*-produced MON 87419 DMO protein and the apparent MW was calculated to be 39.8 kDa (Figure 19, Table 9). Because the experimentally determined apparent MW of the MON 87419-produced DMO protein was within the acceptance limits that were calculated based on 95% prediction interval derived from apparent MW determinations for *E. coli*-produced MON 87419 DMO protein for equivalence assessment (Table 9), the MON 87419-produced DMO and *E. coli*-produced MON 87419 DMO proteins were determined to have equivalent apparent molecular weights.

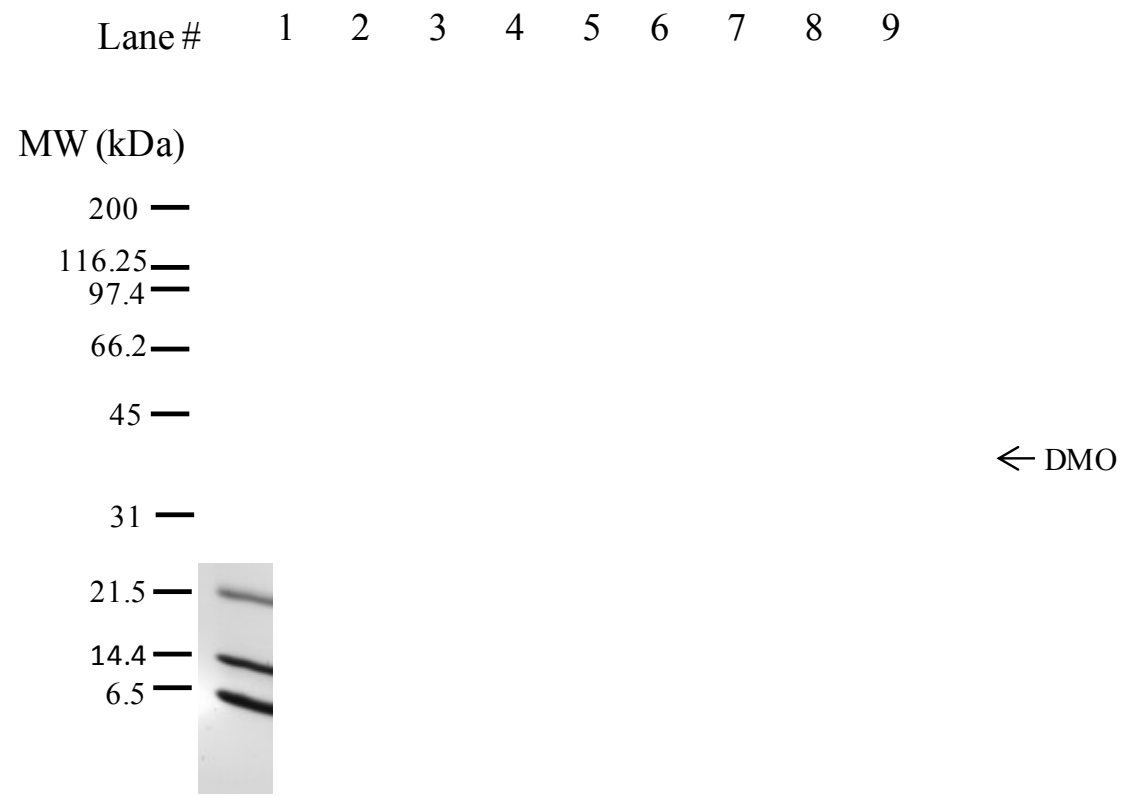

Figure 19. Molecular Weight Analysis of the MON 87419-produced DMO Protein

Aliquots of the MON 87419-produced DMO and the *E. coli*-produced MON 87419 DMO proteins were subjected to SDS-PAGE and the gel was stained with Brilliant Blue G-Colloidal stain. The MWs (kDa) are shown on the left and correspond to the standards loaded in lanes 1 and 9. Lane 10 was cropped from the image. Lane designations are as follows:

Lane	Sample	Amount (µg)
1	Broad Range MW Standards	4.5
2	*E. coli*-produced MON 87419 DMO	1.0
3	MON 87419-produced DMO	0.5
4	MON 87419-produced DMO	0.5
5	MON 87419-produced DMO	1.0
6	MON 87419-produced DMO	1.0
7	MON 87419-produced DMO	1.5
8	MON 87419-produced DMO	1.5
9	Broad Range MW Standards	4.5
10	Blank	-

Table 9. Molecular Weight Comparison Between the MON 87419-produced and *E. coli*-produced MON 87419 DMO Proteins Based on SDS-PAGE

Apparent MW of MON 87419-Produced DMO Protein (kDa)	Apparent MW of *E. coli*-Produced MON 87419 DMO Protein[1] (kDa)	Acceptance Limits[2] (kDa)
39.8	39.5	38.6 - 40.4

[1] Value refers to mean calculated based on n = 6.
[2] As reported on the Certificate of Analysis for *E. coli*-produced MON 87419 DMO protein (lot 11383588).
[3] Calculated lower and upper bounds for equivalent assessment based on 95% prediction interval derived from apparent MW determinations for *E. coli*-produced MON 87419 DMO protein .

B1(a)(v) MON 87419 DMO glycosylation analysis

Eukaryotic proteins can be post-translationally modified with carbohydrate moieties (Rademacher *et al.*, 1988). To test whether the MON 87419 DMO protein was glycosylated when expressed in the grain of MON 87419, the MON 87419-produced DMO protein was analyzed using an ECL™ glycoprotein detection method. To assess equivalence of the MON 87419-produced to *E. coli*-produced MON 87419 DMO proteins, both the MON 87419- and *E. coli*-produced DMO proteins were analyzed.

In the lanes containing the positive control (transferrin) a clear glycosylation signal was observed at the expected molecular weight (~ 80 kDa) and the band intensity increased with increasing concentration (Figure 20 Panel A, Lanes 2-4). In contrast, no glycosylation signal was observed in the lanes containing the *E. coli*-produced MON 87419 DMO protein (Figure 20 Panel A, Lanes 6 and 7) or MON 87419-produced DMO protein (Figure 20 Panel A, Lanes 9 and 10).

To confirm that MON 87419-produced DMO and *E. coli*-produced MON 87419 DMO proteins were appropriately loaded for glycosylation analysis, a second membrane with identical loadings and transfer time was stained with Coomassie Blue R-250 for protein detection. Both the MON 87419-produced and *E. coli*-produced MON 87419 DMO proteins were detected (Figure 20 Panel B, Lanes 9-10 and 6-7, respectively). These data indicate that MON 87419-produced DMO protein is not glycosylated and, therefore, equivalent to the *E. coli*-produced MON 87419 DMO protein, which was also shown to be non-glycosylated.

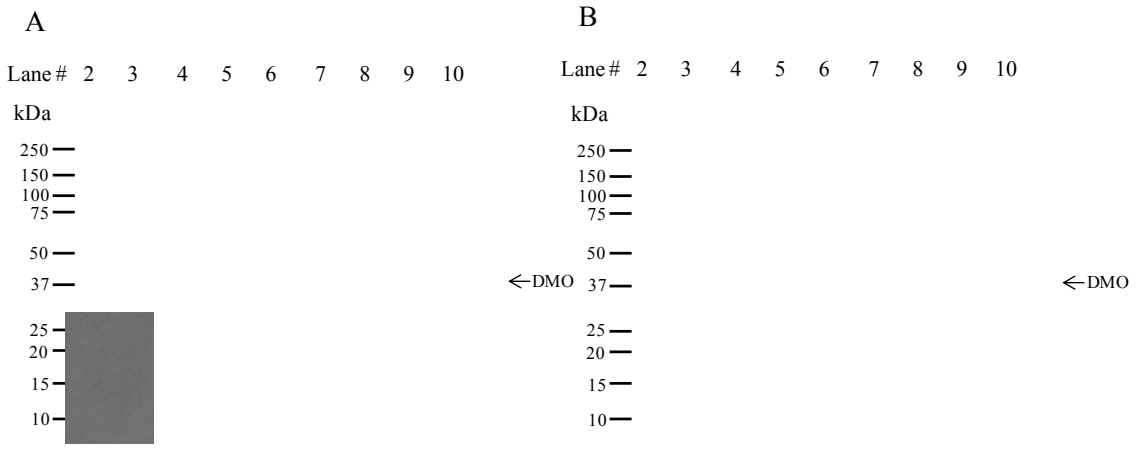

Figure 20. Glycosylation Analysis of the MON 87419-produced DMO Protein

Aliquots of the transferrin (positive control), *E. coli*-produced MON 87419 DMO and MON 87419-produced DMO were subjected to SDS-PAGE and electrotransferred to a PVDF membrane. The MWs (kDa) correspond to the Precision Plus Protein™ Standards. Lanes loaded with MW standards are cropped. The arrows show the expected migration of the MON 87419-produced and *E. coli*-produced MON 87419 DMO proteins. (A) Where present, the labeled carbohydrate moieties were detected by addition of streptavidin conjugated to HRP followed by a luminol-based the detection using ECL reagents and exposure to Hyperfilm®. The 15-minute exposure is shown. (B) An equivalent blot was stained with Coomassie Blue R-250 to confirm the presence of proteins. Lane designations are as follows:

Lane	Sample	Amount of Purity-corrected Protein (ng)
1	Precision Plus Protein™ Standards	-
2	Transferrin (positive control)	50
3	Transferrin (positive control)	100
4	Transferrin (positive control)	200
5	Blank	-
6	*E. coli*-produced MON 87419 DMO (negative control)	100
7	*E. coli*-produced MON 87419 DMO (negative control)	200
8	Blank	-
9	MON 87419-produced DMO	100
10	MON 87419-produced DMO	200

B1(a)(vi) MON 87419 DMO functional activity

The active form of these proteins, necessary to confer dicamba tolerance, is a trimer comprised of three DMO monomers. The functional activities of the MON 87419-produced and *E. coli*-produced MON 87419 DMO proteins were determined by measuring the amount of dicamba that was converted to DCSA via High Performance Liquid Chromatography (HPLC) separation and fluorescence detection. In this assay, *E. coli*-produced MON 87419 DMO protein was used as a positive control and activity is expressed as specific activity of DMO protein (nmol × minute^{-1} × mg^{-1}). The MON 87419-produced and *E. coli*-produced MON 87419 DMO proteins were considered functionally equivalent if the specific activity of both were within acceptance limits of 99.3 to 251.5 nmol × minute^{-1} × mg^{-1} of DMO protein.

The specific activities of the MON 87419-produced and *E. coli*-produced MON 87419 DMO proteins were determined to be 232.5 and 240.1 nmol × minute^{-1} × mg^{-1}, respectively (Table 10). Because the specific activities of MON 87419-produced and *E. coli*-produced MON 87419 DMO proteins were within the acceptance limits (Table 10), the MON 87419-produced and *E. coli*-produced MON 87419 DMO proteins were determined to have equivalent functional activity.

Table 10. MON 87419 DMO Functional Assay

MON 87419-Produced DMO [1] (nmol × minute^{-1} × mg^{-1})	*E. coli*-Produced MON 87419 DMO [1] (nmol × minute^{-1} × mg^{-1})	Acceptance Limits[2] (nmol × minute^{-1} × mg^{-1})
232.5	240.1	99.3 – 251.5

[1] Value refers to mean calculated based on n = 3. Values are rounded to one decimal place.

[2] Calculated lower and upper bounds for equivalent assessment based on 95% prediction interval derived from functional activity assays for *E. coli*-produced MON 87419 DMO.

B1(a)(vii) MON 87419 DMO protein identity and equivalence - Conclusion

The MON 87419 DMO protein purified from grain of MON 87419 was characterized and the equivalence of the physicochemical and functional properties between the plant-produced MON 87419 DMO and the *E. coli*-produced MON 87419 DMO proteins was established using a panel of analytical tests: 1) the N-terminal sequence of the MON 87419-produced DMO protein was confirmed by N-terminal sequence analysis; 2) MALDI-TOF MS analysis yielded peptide masses consistent with the expected peptide masses from the theoretical trypsin digest of the MON 87419-produced DMO sequence; 3) MON 87419-produced DMO protein was detected on a western blot probed with an antibody specific for DMO proteins and the immunoreactive and physicochemical properties of the MON 87419-produced DMO and *E. coli*-produced MON 87419 DMO proteins were shown to be equivalent; 4) the electrophoretic mobility and apparent molecular weight of the MON 87419-produced DMO and *E. coli*-produced MON 87419 DMO proteins were shown to be equivalent; 5) MON 87419-produced DMO and *E. coli*-produced MON 87419 DMO proteins were

determined to not be glycosylated; and 6) functional activities of the MON 87419-produced DMO and the *E. coli*-produced MON 87419 DMO proteins were demonstrated to be equivalent.

Taken together, these data provide a detailed characterization of the MON 87419-produced DMO protein and establish the equivalence of the MON 87419-produced DMO and the *E. coli*-produced MON 87419 DMO proteins. This equivalence justifies the use of the *E. coli*-produced DMO protein in studies to establish the safety of the DMO protein expressed in MON 87419.

B1(b) Characterisation and equivalence of MON 87419-produced PAT (*pat*) protein

Identity and Function of the PAT Protein

PAT proteins have been isolated from two separate species of *Streptomyces*, *S. hygroscopicus* (Thompson *et al.*, 1987) and *S. viridochromogenes* (Wohlleben *et al.*, 1988). The PAT protein isolated from *S. hygroscopicus* is encoded by the *bar* gene, and the PAT protein isolated from *S. viridochromogenes* is encoded by the *pat* gene. These PAT proteins are made up of 183 amino acids with 85% identity at the amino acid level (Wohlleben *et al.*, 1988). Based on previous studies (Wehrmann *et al.*, 1996) that have extensively characterized PAT proteins produced from *bar* and *pat* genes, OECD recognizes both proteins to be equivalent with regard to function and safety (OECD, 1999). The PAT protein produced in MON 87419 is encoded by the *pat* gene and is identical to the wild type PAT protein encoded by *S. viridochromogenes* except for the first methionine, which is removed due to co-translational processing in MON 87419, which results in a single polypeptide of 182 amino acids that has an apparent molecular weight of ~25.2 kDa. N-terminal methionine cleavage is common and naturally occurs in the vast majority of proteins (Meinnel and Giglione, 2008). The PAT protein in MON 87419 is also identical to PAT protein expressed in several commercially available glufosinate tolerant maize products including T25, TC1507 and DAS-59122-7, except for the first methionine that is removed in MON 87419, and therefore has an extensive history of safe use (Hérouet *et al.*, 2005; ILSI-CERA, 2011).

The mode-of-action for PAT protein has been extensively assessed, as numerous glufosinate-tolerant products including oilseed rape, corn, canola, sugar beet, soybean, rice, and cotton have been reviewed by the FDA (U.S. FDA, 1995a; 1995b; 1996; 1997; 1998b; 1998a; 2000; 2003) and many other regulatory agencies (ILSI-CERA, 2011; OECD, 1999; 2002a). PAT is an enzyme classified as an acetyltransferase which acetylates glufosinate to produce non-herbicidal N-acetyl glufosinate. The PAT proteins are highly specific for glufosinate.

The PAT protein expressed in MON 87419 is identical to the wild type PAT protein encoded by *S. viridochromogenes* and PAT protein expressed in several commercially available glufosinate tolerant maize products including T25, TC1507 and DAS-59122-7, except for the first methionine, which is removed due to co-translational processing in MON 87419. Thus, these prior safety assessments for the PAT protein are directly applicable to the PAT protein expressed in MON 87419.

Identity and Equivalence Studies of the PAT (*pat*) Protein

As previously described, the safety assessment of crops derived through biotechnology includes characterization of the physicochemical and functional properties of and confirmation of the safety of the introduced protein(s). For the safety data generated using *E. coli*-produced PAT (*pat*) to be applied to PAT (*pat*) protein produced in MON 87419, the equivalence of the plant- and *E. coli*-produced proteins must be estabilished. To assess the equivalence between MON 87419-produced and *E. coli*-produced PAT (*pat*) proteins, a small quantity of the PAT (*pat*) protein was purified from grain of MON 87419 maize. The MON 87419-produced PAT (*pat*) protein was characterized and the equivalence of the physicochemical characteristics and functional activity between the MON 87419-produced and the *E. coli*-produced PAT (*pat*) proteins was assessed using a panel of six analytical tests as shown in Table 11. Taken together, these data provide a detailed characterization of the MON 87419-produced PAT (*pat*) protein and establish the equivalence of MON 87419-produced PAT (*pat*) and *E. coli*-produced MON 87419 PAT (*pat*) proteins.

For details, please refer to [redacted], 2014 (MSL0026031).

Table 11. Summary of MON 87419 PAT (*pat*) Protein Identity and Equivalence

Analytical Test Assessment	Section Cross Reference	Analytical Test Outcome
1. N-terminal sequence analysis of the MON 87419-produced PAT (*pat*) protein to assess the N-terminal sequence	B1(b)(i)	The expected N-terminal sequence was confirmed
2. MALDI-TOF MS1 analysis of peptides derived from tryptic digested MON 87419-produced PAT (*pat*) protein to assess identity	B1(b)(ii)	MALDI-TOF MS1 analysis yielded peptide masses consistent with the expected peptide masses from the theoretical trypsin digest of the MON 87419-produced PAT (*pat*) sequence
3. Western blot analysis using anti-PAT (*bar*) polyclonal antibodies to assess identity and immunoreactive equivalence between MON 87419-produced PAT (*pat*) and the *E. coli*-produced MON 87419 PAT (*pat*) proteins	B1(b)(iii)	MON 87419-produced PAT (*pat*) protein identity was confirmed using a western blot probed with an antibody specific for PAT (*pat*) proteins Immunoreactive properties of the MON 87419-produced PAT and the *E. coli*-produced MON 87419 PAT (*pat*) proteins were shown to be equivalent
4. SDS-PAGE2 to assess equivalence of the apparent molecular weight between MON 87419-produced PAT (*pat*) and the *E. coli*-produced MON 87419 PAT (*pat*) proteins	B1(b)(iv)	Electrophoretic mobility and apparent molecular weight of the MON 87419-produced PAT (*pat*) and the *E. coli*-produced MON 87419 PAT (*pat*) proteins were shown to be equivalent
5. Glycosylation analysis of the MON 87419 PAT *(pat*) protein to assess equivalence between the MON 87419-produced PAT (*pat*) and *E. coli*-produced MON 87419 PAT (*pat*) proteins	B1(b)(v)	MON 87419-produced PAT (*pat*) and the *E. coli*-produced MON 87419 PAT (*pat*) proteins were each shown to not be glycosylated
6. PAT enzymatic activity analysis to assess functional equivalence between the MON 87419-produced PAT (*pat*) and the *E. coli*-produced MON 87419 PAT (*pat*) proteins	B1(b)(vi)	Functional activity of the MON 87419-produced PAT (*pat*) and the *E. coli*-produced MON 87419 PAT (*pat*) proteins were shown to be equivalent

[1] MALDI-TOF MS = Matrix Assisted Laser Desorption Ionization Time-of-Flight Mass Spectrometry
[2] SDS-PAGE = sodium dodecyl sulfate-polyacrylamide gel electrophoresis

A summary of the data obtained to support a conclusion of protein equivalence is below.

B1(b)(i) Results of the N-terminal sequencing analysis

Fifteen cycles of N-terminal sequencing was performed on MON 87419-produced PAT (*pat*) protein. The expected sequence for the PAT (*pat*) protein deduced from the *pat* gene present in maize of MON 87419 was observed. The experimentally determined sequence corresponds to the deduced PAT (*pat*) protein beginning at amino acid position 2 (Figure 21). Note that removal of the N-terminal methionine by methionine aminopeptidase is common (Meinnel and Giglione, 2008). Hence, the sequence information confirms the expected N-terminal sequence of the PAT (*pat*) protein isolated from the grain of MON 87419.

Amino acid residue # from the N-terminus	→	1	2	3	4	5	6	7	8	9	10	11	12	13	14	15	16
Expected Sequence	→	M	S	P	E	R	R	P	V	E	I	R	P	A	T	A	A
			|	|	|	|	|	|	|	|	|	|	|	|	|	|	|	|
Experimental Sequence	→	X	S	P	E	R	R	P	V	E	I	R	P	A	T	A	A

Figure 21. N-Terminal Sequence of the MON 87419-produced PAT (*pat*) Protein

The experimental sequence obtained from the MON 87419-produced PAT (*pat*) was compared to the expected sequence deduced from the *pat* gene present in MON 87419. The experimentally determined sequence corresponds to the deduced PAT (*pat*) protein beginning at amino acid position 2. The single letter International Union of Pure and Applied Chemistry - International Union of Biochemistry (IUPAC-IUB) amino acid code is; M, methionine; S, serine; P, proline; E, glutamic acid; R, arginine; V, valine; I, isoleucine; A, alanine; T, threonine. "X" indicates that the residue was not identifiable.

B1(b)(ii) Results of MALDI-TOF Tryptic Mass Map analysis

The identity of the MON 87419-produced PAT (*pat*) protein was confirmed by MALDI-TOF MS analysis of peptide fragments produced by the trypsin digestion of the MON 87419-produced PAT (*pat*) protein. The ability to identify a protein using this method is dependent upon matching a sufficient number of observed tryptic peptide fragment masses with predicted tryptic peptide fragment masses. In general, protein identification made by peptide mapping is considered to be reliable if ≥ 40% of the protein sequence was identified by matching experimental masses observed for the tryptic peptide fragments to the expected masses for the fragments (Biron *et al.*, 2006; Krause *et al.*, 1999).

There were 9 unique peptides identified that corresponded to the expected masses (Table 12). The identified masses were used to assemble a peptide map of the PAT (*pat*) protein. The

experimentally determined coverage of the PAT (*pat*) protein was 68% (Figure 22, 124 out of 182 amino acids, except for the lead methionine which is cleaved during a co-translational process in MON 87419). This analysis further confirms the identity of MON 87419-produced PAT (*pat*) protein.

Table 12. Summary of the Tryptic Masses Identified for the MON 87419-produced PAT (*pat*) Protein Using MALDI-TOF MS

Experimental Mass[1]	Calculated Mass[2]	Difference[3]	Fragment[4]	Sequence[5]
1855.7840	1855.8588	-0.0748	38 - 52	TEPQ…DLER
2886.3733	2886.5068	-0.1335	53 - 78	LQDR…GPWK
2374.1114	2374.2361	-0.1248	57 - 78	YPWL…GPWK
1925.8105	1925.8908	-0.0803	81 - 96	NAYD…VSHR
1414.7530	1414.8184	-0.0654	100 - 112	LGLG…HLLK
1521.7924	1521.8515	-0.0591	121 - 135	SVVA…PSVR
1129.5478	1129.5880	-0.0402	136 - 145	LHEA…YTAR
1480.6202	1480.6749	-0.0547	155 - 166	HGGW…FWQR
1930.9843	1931.0629	-0.0786	167 - 183	DFEL…VTQI

[1] Only experimental masses that matched calculated masses are listed in the table.
[2] The calculated mass is the relative molecular mass calculated from the matched peptide sequence.
[3] The calculated difference between the experimental mass and the calculated mass.
[4] Position refers to amino acid residues within the predicted MON 87419-produced PAT (*pat*) sequence as depicted in Figure 22.
[5] For peptide matches greater than nine amino acids in length the first 4 residues and last 4 residues are shown separated by dots (…).

```
  1 MSPERRPVEI RPATAADMAA VCDIVNHYIE TSTVNFRTEP QTPQEWIDDL
 51 ERLQDRYPWL VAEVEGVVAG IAYAGPWKAR NAYDWTVEST VYVSHRHQRL
101 GLGSTLYTHL LKSMEAQGFK SVVAVIGLPN DPSVRLHEAL GYTARGTLRA
151 AGYKHGGWHD VGFWQRDFEL PAPPRPVRPV TQI
```

Figure 22. MALDI-TOF MS Coverage Map of the MON 87419-produced PAT (*pat*) Protein

The amino acid sequence of the MON 87419-produced PAT (*pat*) protein was deduced from the *pat* gene present in MON 87419. Boxed regions correspond to peptides that were identified from the MON 87419-produced PAT (*pat*) protein sample using MALDI-TOF MS. In total, 68% (124 out of 182 amino acids, except for the lead methionine which is cleaved during a co-translational process in MON 87419) of the expected protein sequence was identified

B1(b)(iii) Results of western blot analysis of the PAT (*pat*) protein isolated from the grain of MON 87419 and immunoreactivity comparison to *E. coli*-produced MON 87419 PAT (*pat*) protein

Western blot analysis was conducted using goat anti-PAT (*bar*) polyclonal antibody as additional means to confirm the identity of the PAT (*pat*) protein isolated from the grain of

MON 87419 and to assess the equivalence of the immunoreactivity of the MON 87419-produced and *E. coli*-produced PAT (*pat*) proteins. The goat anti-PAT (*bar*) polyclonal antibody was raised against *E. coli*-produced PAT (*bar*) protein, but it recognized both PAT (*pat*) and PAT (*bar*) protein specifically.

The results showed that immunoreactive bands migrating with the same electrophoretic mobility were present in all lanes loaded with the MON 87419-produced or *E. coli*-produced PAT (*pat*) proteins (Figure 23). For each amount loaded, comparable signal intensity was observed between the MON 87419-produced and *E. coli*-produced PAT (*pat*) protein bands (Figure 23). As expected, the signal intensity increased with increasing load amounts of the MON 87419-produced and *E. coli*-produced PAT (*pat*) proteins, thus, supporting identification of MON 87419-produced PAT (*pat*) protein.

To compare the immunoreactivity of the MON 87419-produced and the *E. coli*-produced PAT (*pat*) proteins, densitometric analysis was conducted on bands that migrated to the expected apparent MW for PAT (*pat*) proteins (~ 25 kDa). The signal intensity (reported in OD × mm^2) of the band(s) of interest in lanes loaded with MON 87419-produced and the *E. coli*-produced PAT (*pat*) protein was measured. Because the mean signal intensity of the MON 87419-produced PAT (*pat*) protein band was within ± 35% of the mean signal of the *E. coli*-produced PAT (*pat*) protein (Table 13), the MON 87419-produced and *E. coli*-produced PAT (*pat*) proteins were determined to have equivalent immunoreactivity.

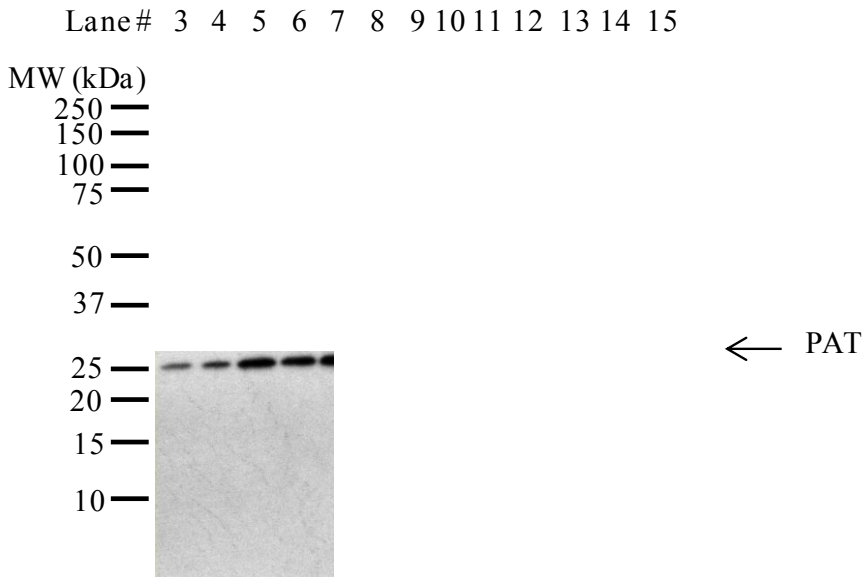

Figure 23. Western Blot Analysis of the MON 87419-produced and *E. coli*-produced MON 87419 PAT (*pat*) Protein

Aliquots of the MON 87419-produced PAT (*pat*) protein and the *E. coli*-produced PAT (*pat*) protein were subjected to SDS-PAGE and electrotransferred to a PVDF membrane. Proteins were detected using anti-PAT (*bar*) antibodies as the primary antibodies. Immunoreactive bands were visualized using HRP-conjugated secondary antibodies and an ECL system. The approximate MW (kDa) of the standards are shown on the left. The Precision Plus Protein Standards lane (lane 1) and blank lane (lane 2) were cropped from the image. Lane designations are as follows:

Lane	Sample	Amount of PAT (*pat*) Protein (ng)
1	Precision Plus Protein™ Standards	-
2	Blank	-
3	*E. coli*-produced PAT (*pat*)	1
4	*E. coli*-produced PAT (*pat*)	1
5	*E. coli*-produced PAT (*pat*)	2
6	*E. coli*-produced PAT (*pat*)	2
7	*E. coli*-produced PAT (*pat*)	3
8	*E. coli*-produced PAT (*pat*)	3
9	Blank	
10	MON 87419-produced PAT (*pat*)	1
11	MON 87419-produced PAT (*pat*)	1
12	MON 87419-produced PAT (*pat*)	2
13	MON 87419-produced PAT (*pat*)	2
14	MON 87419-produced PAT (*pat*)	3
15	MON 87419-produced PAT (*pat*)	3

Table 13. Comparison of Immunoreactive Signals between MON 87419-produced and *E. coli*-produced MON 87419 PAT (*pat*) Proteins

Mean Signal intensity from MON 87419-produced PAT (*pat*) [1] (OD × mm^2)	Mean Signal intensity from *E. coli*-produced PAT (*pat*) [1] (OD × mm^2)	Acceptance limits[2] (OD × mm^2)
3.93	3.26	2.12-4.40

[1]Value refers to mean calculated based on n = 6. Values are rounded to two decimal places.
[2]The acceptance limits are for the MON 87419-produced PAT (*pat*) protein and are based on the interval between -35% (3.26 × 0.65 = 2.12) and +35 % (3.26 × 1.35 = 4.40) of overall mean of the *E. coli*-produced MON 87419 PAT (*pat*) signal intensity at all loads.

B1(b)(iv) Results of the MON 87419-produced PAT (*pat*) protein molecular weight analysis

For apparent MW determination, the MON 87419-produced and the *E. coli*-produced PAT (*pat*) proteins were subjected to SDS-PAGE. Following electrophoresis, the gel was stained with Brilliant Blue G-Colloidal stain and analyzed by densitometry. The MON 87419-produced PAT (*pat*) protein migrated to the same position on the gel as the *E. coli*-produced PAT (*pat*) protein (Figure 24) and the apparent MW was calculated to be 25.2 kDa (Table 14). Because the experimentally determined apparent MW of the MON 87419-produced PAT (*pat*) protein was within the acceptance limits for equivalence (Table 14), the MON 87419-produced and *E. coli*-produced PAT (*pat*) proteins were determined to have equivalent apparent molecular weights.

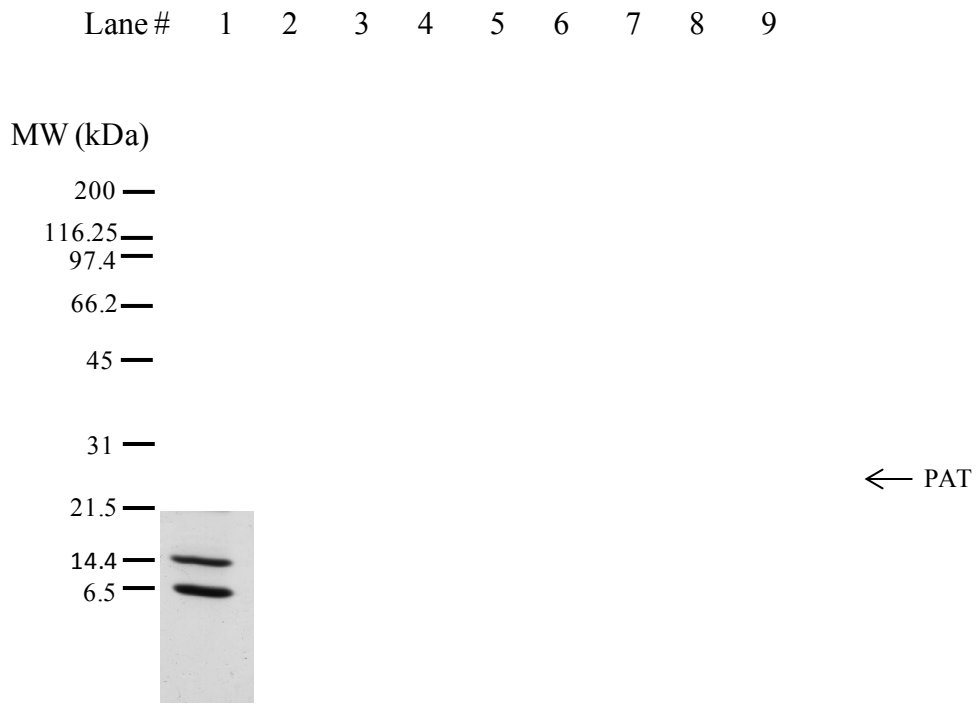

Figure 24. Molecular Weight Analysis of the MON 87419-produced PAT (*pat*) Protein

Aliquots of the MON 87419-produced and the *E. coli*-produced PAT (*pat*) proteins were subjected to SDS-PAGE and the gel was stained with Brilliant Blue G-Colloidal stain. The MWs (kDa) are shown on the left and correspond to the standards loaded in lanes 1 and 9. Blank lane (lane 10) was cropped from the image. Lane designations are as follows:

Lane	Sample	Amount of Total Protein (µg)
1	Broad Range Standards	~ 4.5
2	*E. coli*-produced PAT (*pat*)	1
3	MON 87419-produced PAT (*pat*)	1
4	MON 87419-produced PAT (*pat*)	1
5	MON 87419-produced PAT (*pat*)	2
6	MON 87419-produced PAT (*pat*)	2
7	MON 87419-produced PAT (*pat*)	3
8	MON 87419-produced PAT (*pat*)	3
9	Broad Range Standards	~ 4.5
10	Blank	-

Table 14. Molecular Weight Comparison Between the MON 87419-produced and *E. coli*-produced MON 87419 PAT (*pat*) Proteins Based on SDS-PAGE

Apparent MW of MON 87419-produced PAT (*pat*) Protein[1] (kDa)	Apparent MW of *E. coli*-produced PAT (*pat*) Protein[2] (kDa)	Acceptance Limits[3] (kDa)
25.2	24.8	23.8 - 25.8

[1] Value refers to mean calculated based on n = 6.
[2] As reported on the Certificate of Analysis *for E. coli*-produced PAT (*pat*) protein (lot 11378701).
[3] Calculated lower and upper bounds for one future assay based on 95% prediction interval derived from apparent MW determinations for *E. coli*-produced PAT (*pat*) protein.

B1(b)(v) MON 87419 PAT (*pat*) glycosylation analysis

Eukaryotic proteins can be post-translationally modified with carbohydrate moieties (Rademacher *et al.*, 1988). To test whether PAT (*pat*) protein was glycosylated when expressed in the grain of MON 87419, the MON 87419-produced PAT (*pat*) protein was analyzed using an ECL™ Glycoprotein Detection Method (GE Healthcare). To assess equivalence of the MON 87419-produced to *E. coli*-produced MON 87419 PAT (*pat*) proteins, both the MON 87419- and *E. coli*-produced PAT (*pat*) proteins were analyzed.

In the lanes containing the positive control (transferrin) a clear glycosylation signal was observed at the expected molecular weight (~ 80 kDa) and the band intensity increased with increasing concentration (Figure 25 Panel A, Lanes 3 and 4). In contrast, no glycosylation signal was observed in the lanes containing the MON 87419-produced PAT (*pat*) protein or *E. coli*-produced PAT (*pat*) protein (Figure 25 Panel A, Lanes 8-9 and 6-7, respectively).

To confirm that MON 87419-produced and *E. coli*-produced PAT (*pat*) proteins were appropriately loaded for glycosylation analysis, a second membrane with identical loadings and transfer time was stained with Coomassie Blue R-250 for protein detection. Both the MON 87419-produced PAT (*pat*) and *E. coli*-produced PAT (*pat*) proteins were detected (Figure 25 Panel B, Lanes 8-9 and 6-7, respectively). These data indicate that MON 87419-produced PAT (*pat*) protein is not glycosylated and, therefore, equivalent to the *E. coli*-produced PAT (*pat*) protein, which was also shown to be non-glycosylated.

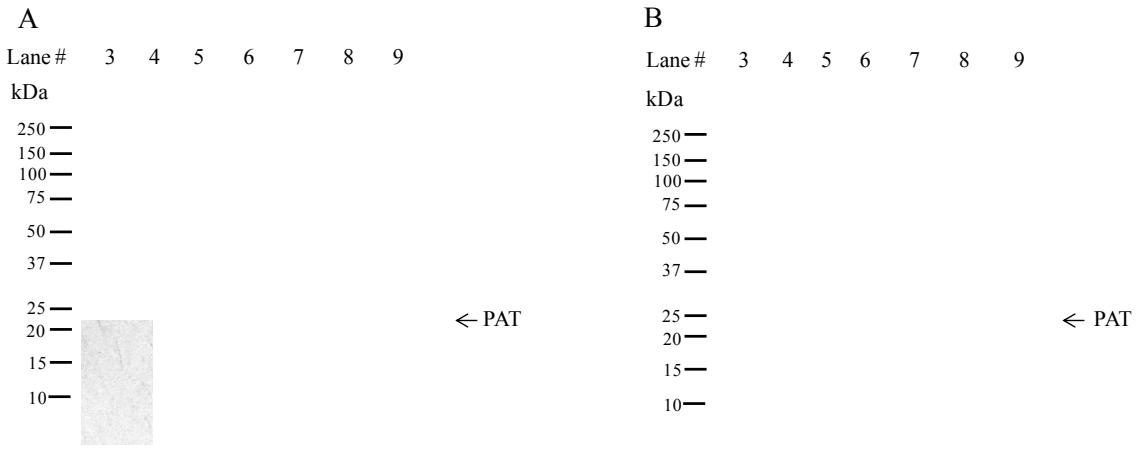

Figure 25. Glycosylation Analysis of the MON 87419-produced PAT (*pat*) Protein

Aliquots of the transferrin (positive control), *E. coli*-produced PAT (*pat*) and MON 87419-produced PAT (*pat*) were subjected to SDS-PAGE and electrotransferred to a PVDF membrane. The MWs (kDa) correspond to the Precision Plus Protein™ Standards. The arrows show the expected migration of the MON 87419-produced and *E. coli*-produced PAT (*pat*) proteins. (A) Where present, the labeled carbohydrate moieties were detected by addition of streptavidin conjugated to HRP followed by a luminol-based the detection using ECL reagents and exposure to Hyperfilm®. The 5-minute exposure is shown. (B) An equivalent blot was stained with Coomassie Blue R-250 to confirm the presence of proteins. Blank lanes (lanes 2 and 10) and the Precision Plus protein standards lane (lane 1) were cropped from both images. Lane designations are as follows:

Lane	Sample	Amount of Purity-corrected Protein (ng)
1	Precision Plus Protein™ Standards	-
2	Blank	-
3	Transferrin (positive control)	50
4	Transferrin (positive control)	100
5	Blank	-
6	*E. coli*-produced PAT (*pat*) (negative control)	50
7	*E. coli*-produced PAT (*pat*) (negative control)	100
8	MON 87419-produced PAT (*pat*)	50
9	MON 87419-produced PAT (*pat*)	100
10	Blank	-

B1(b)(vi) PAT (*pat*) functional activity

The functional activities of the MON 87419-produced and *E. coli*-produced PAT (*pat*) proteins were determined using a coenzyme A (CoA) release assay. In this assay, activity is expressed as specific activity of PAT (*pat*) protein (µmol × minute^{-1} × mg^{-1}). The MON 87419-produced and *E. coli*-produced PAT (*pat*) proteins were considered functionally equivalent if the specific activity of both were within acceptance limits of 18.5 to 65.9 µmol × minute^{-1} × mg^{-1} of PAT (*pat*) protein.

The specific activities of the MON 87419-produced and *E. coli*-produced PAT (*pat*) proteins were determined to be 36.6 and 39.2 µmol × minute^{-1} × mg^{-1} of PAT (*pat*) protein, respectively (Table 15). Because the specific activities of MON 87419-produced and *E. coli*-produced PAT (*pat*) proteins were within the acceptance limits, the MON 87419-produced and *E. coli*-produced PAT (*pat*) proteins were determined to have equivalent functional activity.

Table 15. PAT Functional Assay

MON 87419-produced PAT (*pat*)[1] (µmol × minute^{-1} × mg^{-1})	*E. coli*-produced PAT (*pat*)[1] (µmol × minute^{-1} × mg^{-1})	Acceptance Limits[2] (µmol × minute^{-1} × mg^{-1})
36.6	39.2	18.5 – 65.9

[1] Value refers to mean calculated based on n = 5. Values are rounded to one decimal place.
[2] Calculated lower and upper bounds for one future assay based on 95% prediction interval derived from functional activity assays for *E. coli*-produced MON 87419 PAT (*pat*) .

B1(b)(vii) MON 87419 PAT (*pat*) protein identity and equivalence – Conclusion

The PAT (*pat*) protein purified from grain of MON 87419 maize was characterized and the equivalence of the immunoreactive and physicochemical characteristics and functional activity between the MON 87419-produced and the *E. coli*-produced PAT (*pat*) proteins was established using a panel of analytical tests: 1) the N-terminal sequence of the MON 87419-produced PAT (*pat*) protein was confirmed by N-terminal sequence analysis; 2) MALDI-TOF MS analysis yielded peptide masses consistent with the expected peptide masses from the theoretical trypsin digest of the MON 87419-produced PAT (*pat*) sequence; 3) MON 87419-produced PAT (*pat*) protein was detected on a western blot probed with antibodies specific for PAT protein and the immunoreactive properties of the MON 87419-produced and *E. coli*-produced PAT (*pat*) proteins were shown to be equivalent; 4) the electrophoretic mobility and apparent molecular weight of the MON 87419-produced and *E. coli*-produced PAT (*pat*) proteins were shown to be equivalent; 5) MON 87419-produced and *E. coli*-produced PAT (*pat*) proteins were determined to not be glycosylated; and 6) functional activities of the MON 87419-produced and *E. coli*-produced PAT (*pat*) proteins were demonstrated to be equivalent.

Taken together, these data provide a detailed characterization of the MON 87419-produced PAT (*pat*) protein and establish the equivalence of the MON 87419-produced and the *E. coli*-produced PAT (*pat*) proteins. This equivalence justifies the use of the *E. coli*-produced PAT (*pat*) protein in studies to establish the safety of the PAT (*pat*) protein expressed in MON 87419.

B2 Antibiotic Resistance Marker Genes

MON 87419 does not contain genes that encode resistance to antibiotic markers. Molecular characterisation data presented in Section A demonstrate the absence of antibiotic resistance marker gene in MON 87419.

B2(a) Clinical importance of antibiotic that GM is resistant to (if any)

Not applicable.

B2(b) Presence in food of antibiotic resistance protein (if any)

Not applicable.

B2(c) Safety of antibiotic protein

Not applicable.

B2(d) If GM organism is micro-organism, is it viable in final food?

Not applicable.

B3 Characterisation of Novel Proteins or Other Novel Substances

B3(a) Biochemical function and phenotypic effects of novel substances

B3(a)(i) Description, mode-of-action, and specificity of DMO protein expressed in MON 87419

Description of DMO Protein Expressed in MON 87419

Wild type DMO was initially purified from *Stenotrophomonas maltophilia* (*S. maltophilia*) strain DI-6 (Herman *et al.*, 2005; Palleroni and Bradbury, 1993), isolated from soil at a dicamba manufacturing plant (Krueger *et al.*, 1989). DMO is targeted to the chloroplast by chloroplast transit peptide (CTP) to allow co-localization with the endogenous reductase and ferredoxin enzymes that supply electrons for the DMO demethylation reaction as described by Behrens et al. (2007). In the construction of the plasmid vector used in the development of MON 87419, PV-ZMHT507801, a CTP coding sequence from *Petunia hybrida* EPSPS (*CTP4*) was joined to the *dmo* coding sequence; this coding sequence results in the production of a precursor protein consisting of the DMO protein and a N-terminal 72 amino acid CTP that is utilized to target the precursor protein to the chloroplast (Herrmann, 1995; Klee *et al.*, 1987). Typically, transit peptides are precisely removed from the precursor protein following delivery to the targeted plastid (della-Cioppa *et al.*, 1986) resulting in the full length mature protein. However, there are examples in the literature of alternatively processed forms of a protein targeted to a plant's chloroplast (Behrens *et al.*, 2007; Clark and Lamppa, 1992). Such alternative processing is observed with the DMO precursor protein produced in MON 87419.

MON 87419 contains a *dmo* expression cassette that encodes for a single MON 87419 DMO precursor protein that is post-translationally processed into two forms of DMO. Two forms of MON 87419 DMO have been identified by the N-terminal sequencing analysis. One form, referred to as MON 87419 DMO+12 and the other, MON 87419 DMO+7. MON 87419 DMO+7 does not contain the first five amino acids of MON 87419 DMO+12. Because the difference in molecular weight between these two forms is beyond the resolution of the SDS-PAGE used, only one single band was observable by Coomassie stain of SDS-PAGE and western blot analyses with the apparent molecular weight of ~39.5 kDa. Therefore, MON 87419 DMO protein will be used to refer to both forms of the protein collectively and distinctions will only be made where necessary. Since the minor differences in the amino acid sequences between MON 87419 DMO+12 and MON 87419 DMO+7 occur at the N-terminus, which are derived from CTP4, they are not expected to have an effect on structure of the catalytic site, functional activity, immunoreactivity or specificity because the N-terminus is sterically distant from the catalytic site (D'Ordine *et al.*, 2009; Dumitru *et al.*, 2009). Importantly, the DMO functional activity assay demonstrated that the functional activity of *E. coli*-produced MON 87419 DMO+12 is equivalent to MON 87419 DMO, which are 240.1 and 232.5 nmol × minute^{-1} × mg^{-1}, respectively (Table 10). Furthermore, the amino acid residues present in MON 87419 DMO+7 are also present in MON 87419 DMO+12. Therefore, an assessment of *E. coli*-produced MON 87419 DMO+12 is considered comprehensive and applies to *E. coli*-produced MON 87419 DMO+7 because the

physiochemical and functional equivalence between MON 87419 DMO +12 and the MON 87419-produced DMO protein was established. Therefore, *E.coli*-produced MON 87419 DMO+12 proteins were purified and used as test substance for the safety assessments. Except for the amino acids derived from the *CTP4* (7 or 12) and an additional leucine at position two, the MON 87419 DMO protein has an identical sequence to the wild-type DMO protein from the DI-6 strain of *S. maltophilia* (Herman *et al.*, 2005) (Figure 15). The differences in the amino acid sequence between the wild-type DMO protein and MON 87419 DMO protein are not anticipated to have an effect on structure of the catalytic site, functional activity, immunoreactivity or specificity because the N-terminus and position two are sterically distant from the catalytic site (D'Ordine *et al.*, 2009; Dumitru *et al.*, 2009).

With the exception of minor differences in amino acid sequence, the DMO proteins produced in MON 87419 are identical in structure of the catalytic site, function, immunoreactivity, and specificity to DMO proteins previously assessed and deregulated by USDA-APHIS (MON 87708, USDA-APHIS # 10-188-01p and MON 88701, USDA-APHIS # 12-185-01p). DMO proteins in both MON 87708 and MON 88701 also completed consultation with U.S. FDA (BNF 000125 and BNF 000135, respectively), which determined that food and feed products from MON 87708 and MON 88701 are as safe as food and feed from soybean and cotton, respectively, currently available on the market.

Mode-of-Action of DMO Expressed in MON 87419

MON 87419 contains a demethylase gene from *S. maltophilia* that expresses a DMO protein to confer tolerance to dicamba herbicide. DMO is an enzyme that catalyzes the demethylation of dicamba to the non-herbicidal compound 3,6 dichlorosalicylic acid (DCSA) and formaldehyde (Chakraborty *et al.*, 2005). DMO is a Rieske-type non-heme iron oxygenase and is part of a three component system comprised of a reductase, a ferredoxin, and a terminal oxygenase, which in this case is the DMO protein. These three proteins work together in a redox system similar to many other oxygenases to transport electrons from nicotinamide adenine dinucleotide (NADH) to oxygen and catalyze the demethylation of an electron acceptor substrate, in this case dicamba (Chakraborty *et al.*, 2005). This three-component redox system is presented in Figure 26.

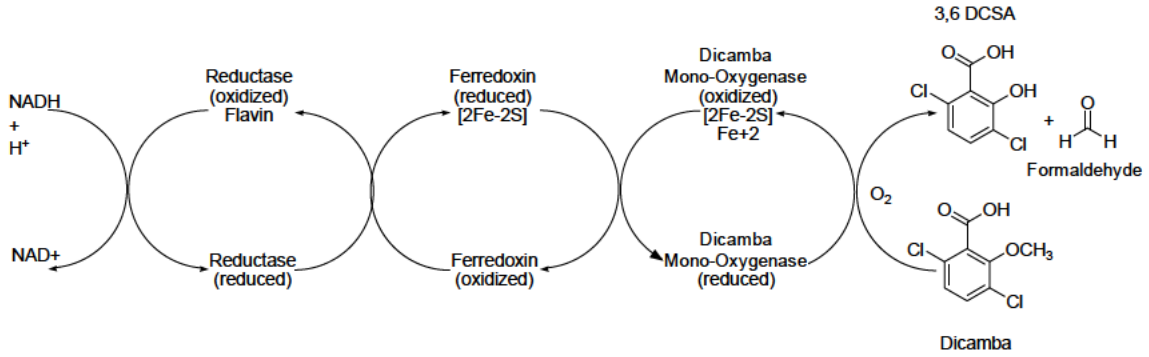

Figure 26. Three Components of the DMO Oxygenase System

Depicted is the electron transport chain that starts with NADH and ends with DMO resulting in the demethylation of dicamba to form DCSA.

The crystal structure of a C-terminal histidine tagged DMO protein, which is identical to wild-type DMO except for an additional alanine at position two and the C-terminal histidine tag (Figure 15), has been solved (D'Ordine *et al.*, 2009; Dumitru *et al.*, 2009). The addition of a polyhistidine tag fused to the N- or C-terminus of a protein of interest is a common tool used to aid in protein purification (Hochuli *et al.*, 1988). The crystal structure of DMO was determined to be a trimer comprised of three identical DMO (D'Ordine *et al.*, 2009; Dumitru *et al.*, 2009). Each DMO monomer contains a Rieske [2Fe-2S] cluster domain and a non-heme iron center domain (D'Ordine *et al.*, 2009; Dumitru *et al.*, 2009) that are typical of all Rieske-type mono-oxygenases (Ferraro *et al.*, 2005). To catalyze the demethylation of dicamba, electrons transferred from NADH are shuttled through an endogenous reductase and ferredoxin to the terminal DMO protein. The electrons are received by the Rieske [2Fe-2S] cluster of one DMO protein molecule in the trimer and transferred to the non-heme iron center at the catalytic site of an adjacent DMO protein molecule in the trimer (D'Ordine *et al.*, 2009; Dumitru *et al.*, 2009), where it reductively activates oxygen to catalyze the final demethylation of dicamba. Electron transport from the Rieske [2Fe-2S] cluster domain to the non-heme iron center domain cannot occur within a monomer since the distance is too vast (D'Ordine *et al.*, 2009; Dumitru *et al.*, 2009). As a result of the demethylation reaction, the non-herbicidal compound DCSA and formaldehyde are formed from dicamba. DCSA is a known cotton, soybean, soil, and livestock metabolite whose safety has been evaluated by the FAO-WHO and EPA (FAO-WHO, 2011a; 2011b; U.S. EPA, 2009b). Formaldehyde is found naturally in many plants at levels up to several hundred ppm (Adrian-Romero *et al.*, 1999). Thus, neither DCSA nor formaldehyde generated by the action of DMO on dicamba pose a significant food or feed safety risk.

As described previously the active form of DMO is a trimer (Chakraborty *et al.*, 2005; Dumitru *et al.*, 2009). For MON 87419-produced DMO to be functionally active and confer dicamba tolerance to MON 87419, a trimeric structure is required. The activity of MON 87419-produced DMO was confirmed during characterization (Section B1(a)).

Specificity of DMO Expressed in MON 87419

The substrate specificity of DMO expressed in MON 87419 was evaluated to understand potential interactions DMO may have with endogenous compounds structurally similar to dicamba that are found in plant. The literature indicates the specificity of DMO for dicamba is due to the specific interactions that occur at the catalytic site between the substrate and the protein (D'Ordine *et al.*, 2009; Dumitru *et al.*, 2009). Dicamba interacts with amino acids in the catalytic site of DMO through both the carboxylate moiety and the chlorine atoms of dicamba, which are primarily involved in orienting the substrate in the catalytic site. These chlorine atoms are required for catalysis to occur (D'Ordine *et al.*, 2009; Dumitru *et al.*, 2009). 2-methoxy benzoic acid (O-anisic acid) as a substrate, which is identical in structure to dicamba except for the absence of chlorines was tested by two independent laboratories (D'Ordine *et al.*, 2009; Dumitru *et al.*, 2009). No significant turnover was detected under standard assay conditions using HPLC or through liquid chromatography/mass spectrometry methods where picomole levels of products can be observed. 4-Hydroxy-3-methoxybenzoic acid (vanillic acid) was also tested with similar results. Given the limited existence of chlorinated compounds with structures similar to dicamba in plants and other eukaryotes (Wishart, 2010; Wishart *et al.*, 2009), it is unlikely that DMO produced in MON 87419 will catalyze the conversion of other endogenous substrates.

The potential for DMO to metabolize endogenous plant compounds was evaluated previously through *in vitro* experiments using a purified N-terminal histidine tagged DMO in support of MON 87708 and MON 88701 (BNF 000125 and BNF 000135, respectively). N-terminal histidine tagged DMO was identical to wild-type DMO, except for a histidine tag at the N-terminus added to aid in protein purification. A comparison of amino acid sequence of wild-type DMO, histidine tagged DMO, MON 87708 DMO, MON 88701 DMO, and MON 87419 DMO is shown in Section B1. Importantly, these DMO proteins all have identical amino acid sequence at the catalytic site of the enzyme (D'Ordine *et al.*, 2009). D'Ordine et al. (2009) and Dumitru et al. (2009) demonstrated that the substrate specificity of DMO for dicamba is due to the specific interactions that occur at the catalytic site (D'Ordine *et al.*, 2009; Dumitru *et al.*, 2009). Therefore, DMO expressed in MON 87419 is unlikely to change its substrate specificity for dicamba because the catalytic site of the DMO expressed in MON 87419 is identical to the wild-type DMO and others listed in Figure 15. Our data present below further confirmed this conclusion. A set of potential endogenous substrates was selected for evaluation based on structural similarity of the compounds to dicamba and their presence in cotton, corn, or soybean (Buchanan *et al.*, 2000; Janas *et al.*, 2000; Lege *et al.*, 1995; Schmelz *et al.*, 2003). The potential substrates tested were *o*-anisic acid (2-methoxybenzoic acid), vanillic acid (4-hydroxy-3-methoxybenzoic acid), syringic acid (3,5-dimethoxy-4-hydroxybenzoic acid), ferulic acid [3-(4-hydroxy-3-methoxy-phenyl) prop-2-enoic acid] and sinapic acid [3-(4-hydroxy-3,5-dimethoxyphenyl)prop-2-enoic acid] (Figure 27). The assay mixture included NADH, reductase, ferredoxin and DMO. Dicamba was first used as a positive control to demonstrate that the assay system was functional. The disappearance of potential substrates and the formation of potential oxidation products were monitored using liquid chromatography-ultraviolet (LC-UV) and

liquid chromatography-mass spectrometry (LC-MS). None of the tested substrates, except dicamba, were metabolized by the histidine tagged DMO in these *in vitro* experiments. To assess whether DMO expressed in MON 87419 has the same specificity as the histidine tagged DMO used in the *in vitro* experiments, the *E. coli*-produced MON 87419 DMO+12 protein, shown to be equivalent to the plant-produced MON 87419 DMO protein (Section B1(a)), was incubated with *o*-anisic acid, the endogenous compound that has the greatest structural similarity to dicamba. Again dicamba was used as a positive control to demonstrate the assay system was functional. This analysis demonstrated that *o*-anisic acid was not metabolized by the *E. coli*-produced MON 87419 DMO+12 protein, but dicamba was. These results indicate that DMO proteins, including the MON 87419 DMO protein, are specific for dicamba as a substrate.

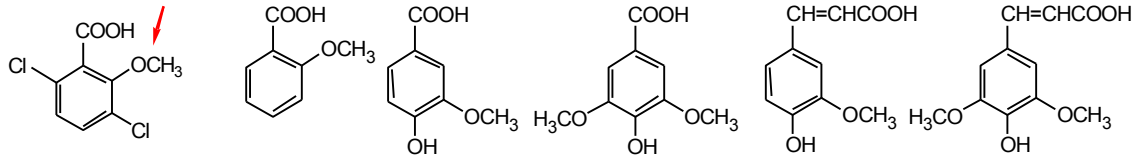

Dicamba o-Anisic Acid Vanillic Acid Syringic Acid Ferulic Acid Sinapic Acid

Figure 27. Dicamba and Potential Endogenous Substrates Tested through *In Vitro* Experiments with DMO

The arrow indicates methyl group removed by DMO.

B3(a)(ii) Description, mode-of-action, and specificity of PAT (*pat*) proteins expressed in MON 87419

Description of PAT (*pat*) Protein

PAT proteins conferring tolerance to glufosinate herbicide (2-amino-4-(hydroxymethylphosphinyl) butanoic acid) have been isolated from two separate species of *Streptomyces*, *S. hygroscopicus* (Thompson *et al.*, 1987) and *S. viridochromogenes* (Wohlleben *et al.*, 1988). The PAT protein isolated from *S. hygroscopicus* is encoded by the *bar* gene, and the PAT protein isolated from *S. viridochromogenes* is encoded by the *pat* gene. For clarity, the PAT protein encoded by the *bar* gene will be referred to as PAT (*bar*) as well as the PAT protein encoded by the *pat* gene will be referred to as PAT (*pat*). Both PAT (*bar*) and PAT (*pat*) proteins are comprised of 183 amino acids which share 85% identity at the amino acid level (Wehrmann *et al.*, 1996). Based on previous studies (Wehrmann *et al.*, 1996) that have extensively characterized PAT proteins produced from both the *bar* and *pat* genes, OECD recognizes both the proteins to be equivalent with regard to function and safety (OECD, 1999). In addition, the EPA has issued a tolerance exemption for the PAT protein regardless of the encoding gene or crop (U.S. EPA, 1997). The safety of PAT proteins present in biotechnology-derived crops has been extensively assessed (Hérouet *et al.*, 2005; ILSI-CERA, 2011), leading to a conclusion that there is a reasonable certainty of no harm resulting from the consumption of PAT proteins in human food or animal feed (Hérouet *et al.*, 2005).

The PAT protein produced in MON 87419 is from the *pat* gene , referred to as PAT (*pat*), and is identical to the wild type PAT protein encoded by *S. viridochromogenes*, except for the first methionine that is removed due to co-translational processing in MON 87419. N-terminal methionine cleavage is common and naturally occurs in the vast majority of proteins (Meinnel and Giglione, 2008). The resulting MON 87419-produced PAT (*pat*) protein is a single polypeptide of 182 amino acids that has an apparent molecular weight of ~25.2 kDa. The PAT (*pat*) protein in MON 87419 is also identical to the PAT (*pat*) protein expressed in several commercially available glufosinate tolerant maize products including T25, TC1507 and DAS-59122-7, except for the first methionine that is removed in MON 87419 and therefore has an extensive history of safe use (Hérouet *et al.*, 2005; ILSI-CERA, 2011).

PAT (*pat*) Mode-of-Action

The mode-of-action of the PAT protein has been extensively assessed, as numerous glufosinate-tolerant products including those in cotton, corn, soy, canola, sugar beet and rice have been reviewed by the FDA (U.S. FDA, 1995a; 1995b; 1996; 1997; 1998b; 1998a; 2000; 2003) and many other regulatory agencies (ILSI-CERA, 2011; OECD, 1999; 2002a). PAT, including the PAT (*pat*) protein produced in MON 87419, is an enzyme classified as an acetyltransferase that acetylates glufosinate to produce non-herbicidal N-acetyl glufosinate. Glufosinate is a racemic mixture of the D- and L-forms of phosphinothricin. The herbicidal activity of glufosinate results from the binding of L-phosphinothricin to glutamine synthetase (OECD, 1999; 2002a). Glutamine synthetase is responsible for the assimilation of ammonia generated during photorespiration. The binding of L-phosphinothricin to glutamine synthetase results in the inactivation of glutamine synthetase and a subsequent toxic build-up of ammonia within the plant, resulting in death of the plant (Manderscheid and Wild, 1986; OECD, 1999; 2002a; Wild and Manderscheid, 1984).

The PAT (*pat*) protein produced in MON 87419 acetylates the free amine group of L-phosphinothricin form of glufosinate to produce non-herbicidal N-acetyl glufosinate. The acetylated glufosinate is unable to bind to glutamine synthetase and therefore does not disrupt photorespiration and does not result in the build up of ammonia. Therefore, the production of the PAT (*pat*) protein in MON 87419 confers glufosinate herbicide tolerance through this mechanism.

PAT (*pat*) Specificity

The PAT proteins, including PAT (*pat*), are highly specific for glufosinate in the presence of acetyl-CoA (Thompson *et al.*, 1987; Wehrmann *et al.*, 1996). Glufosinate is a racemic mixture of the D- and L-forms of phosphinothricin. The herbicidal activity of glufosinate results from the binding of L-phosphinothricin to glutamine synthetase (OECD, 1999; 2002a). Other L-amino acids that are structurally similar to L-phosphinothricin are unable to be acetylated by the PAT protein and substrate competition assays containing glufosinate, high concentrations of structurally similar amino acids and PAT showed no inhibition of glufosinate acetylation (Wehrmann *et al.*, 1996). Furthermore, the presence of L-glutamate, an analogue of glufosinate, also showed no inhibition of glufosinate acetylation in competition assays (Wehrmann *et al.*, 1996). Thus, the PAT protein has high substrate

specificity for L-phosphinothricin, the herbicidal component of glufosinate, and it has been shown in other PAT (*pat*)-expressing maize products (e.g., T25, TC1507, and DAS-59122-7) that PAT does not affect maize metabolism.

B3(b) Identification of novel substances (e.g. metabolites), levels and site

Herbicide metabolites are discussed in greater details in Section B6.

The protein expression levels determined in MON 87419 are used to assess exposure to the introduced proteins via food or feed ingestion and potential environmental exposure. The most appropriate tissues to evaluate DMO and PAT protein levels are leaf, root, forage, and grain tissue samples. Levels of the introduced proteins were determined in forage and grain tissue to evaluate food and feed exposure in humans and animals, where the levels are utilized to also calculate margins of exposure for each protein. Leaf and root tissues are distinct above and below ground plant tissues that are important to estimate environmental exposure.

MON 87419 DMO and PAT protein levels in various tissues of MON 87419 relevant to the characterisation and risk assessment were determined by a validated immunoassay. Tissues of MON 87419 were collected from four replicate plots planted in a randomized complete block field design during the 2013 growing season from the following five field sites in the U.S.: Boone County, Iowa (IAPY), Clinton County, Indiana (INKI), Pawnee County, Kansas (KSLA), York County, Nebraska (NEYO), and Lehigh County, Pennsylvania (PAGR). The field sites were representative of maize-producing regions suitable for commercial production. Leaf, root, forage, and grain tissue samples were collected from each replicated plot at all field sites treated with dicamba and glufosinate.

For details, please refer to [redacted] 2014 (MSL0025758).

B3(b)(i) Expression levels of MON 87419 DMO protein

MON 87419 DMO protein levels were determined in all four tissue types. The results obtained from immunoassay are summarized in Table 16. The mean DMO protein levels were determined across five sites treated with dicamba and glufosinate. Samples with values determined to be less than the LOD or LOQ were not included in mean determinations. The individual DMO protein levels in MON 87419 across all samples analyzed from all sites ranged from 0.14 to 37 µg/g dw. The mean DMO protein level among all tissue types was highest in leaf at 26 µg/g dw and lowest in grain at 0.19 µg/g dw.

Table 16. Summary of MON 87419 DMO Protein Levels in Tissues from MON 87419 Grown in 2013 U.S. Field Trials (Treated with Dicamba and Glufosinate)

Tissue Type	Development Stage[1]	Mean (SD) Range (µg/g fw)[2]	Mean (SD) Range (µg/g dw)[3]	LOQ/LOD (µg/g fw)[4]
Leaf	V3	3.7 (0.77) 1.9-5.1	26 (6.6) 13-37	0.157/0.027
Root	V3	0.81 (0.16) 0.58-1.1	7.4 (1.4) 5.0-11	0.125/0.038
Forage	R5	1.8 (0.62) 1.0-3.7	6.0 (2.7) 3.1-14	0.157/0.024
Grain	R6	0.17 (0.044) 0.13-0.29	0.19 (0.048) 0.14-0.31	0.125/0.022

[1] The crop development stage each tissue was collected.
[2] DMO protein levels are expressed as the arithmetic mean and standard deviation (SD) as microgram (µg) of protein per gram (g) of tissue on a fresh weight basis (fw). The means, SD, and ranges (minimum and maximum values) were calculated for each tissue across all sites (number of sites (n)=20 except grain where n=11 due to nine samples having levels <LOQ).
[3] DMO protein levels are expressed as the arithmetic mean and standard deviation (SD) as microgram (µg) of protein per gram (g) of tissue on a dry weight basis (dw). The dry weight values were calculated by dividing the µg/g fw by the dry weight conversion factor obtained from moisture analysis data.
[4] LOQ=limit of quantitation; LOD=limit of detection.

B3(b)(ii) Expression levels of PAT (*pat*) protein

MON 87419 PAT (*pat*) protein levels were determined in all four tissue types. The results obtained from immunoassay are summarized in Table 17. The mean PAT (*pat*) protein levels were determined across five sites treated with dicamba and glufosinate. The individual PAT (*pat*) protein levels in MON 87419 across all samples analyzed from all sites ranged from 0.56 to 17 µg/g dw. The mean PAT (*pat*) protein level among all tissue types was highest in leaf at 11 µg/g dw and lowest in grain at 0.93 µg/g dw.

Table 17. Summary of PAT (*pat*) Protein Levels in Tissues from MON 87419 Grown in 2013 U.S. Field Trials (Treated with Dicamba and Glufosinate)

Tissue Type	Development Stage[1]	Mean (SD) Range (µg/g fw)[2]	Mean (SD) Range (µg/g dw)[3]	LOQ/LOD (µg/g fw)[4]
Leaf	V3	1.5 (0.35) 1.1-2.4	11 (2.7) 7.0-17	0.094/0.043
Root	V3	0.84 (0.18) 0.49-1.3	7.7 (1.3) 4.7-11	0.094/0.037
Forage	R5	1.6 (0.50) 0.92-2.3	5.0 (1.6) 2.8-8.5	0.094/0.014
Grain	R6	0.85 (0.25) 0.50-1.4	0.93 (0.27) 0.56-1.6	0.094/0.007

[1]The crop development stage each tissue was collected.
[2]PAT protein levels are expressed as the arithmetic mean and standard deviation (SD) as microgram (µg) of protein per gram (g) of tissue on a fresh weight basis (fw). The means, SD, and ranges (minimum and maximum values) were calculated for each tissue across all sites (n=20).
[3]PAT protein levels are expressed as the arithmetic mean and standard deviation (SD) as microgram (µg) of protein per gram (g) of tissue on a dry weight basis (dw). The dry weight values were calculated by dividing the µg/g fw by the dry weight conversion factor obtained from moisture analysis data.
[4]LOQ=limit of quantitation; LOD=limit of detection.

B3(c) Site of expression of all novel substances and levels

Please refer to Section B3(b).

B3(d) Post-translational modifications to the novel protein(s)

Not applicable.

B3(e) Evidence of silencing, if silencing is the method of modification

Not applicable.

B3(f) History of human consumption of novel substances or similarity to substances previously consumed in food

History of Safe Use of MON 87419 DMO and PAT (*pat*) Proteins

History of Safe Use of MON 87419 DMO Protein

As described below, MON 87419 DMO is homologous to proteins that are common in the environment and in the diets of animals and humans. Given the extensive exposure of humans and animals to these homologous oxygenase proteins, it can be concluded that the oxygenase proteins have a history of safe use.

When determining the homology among proteins, both the linear amino acid sequence of the protein as well as the higher order structure of the proteins should be taken into account. Higher order structures are a relevant measure of homology since structure is more conserved than amino acid sequence (Caetano-Anollés *et al.*, 2009). In general, changes in the amino acid sequence of proteins largely occur through evolutionary mechanisms and are mostly conservative, meaning that such changes do not alter the high order structure of the protein and consequently do not alter the functional activity of the protein (Caetano-Anollés *et al.*, 2009; Illergård *et al.*, 2009). The conservation of high order structure is predominant within important functional and structural domains of proteins in similar classes (Illergård *et al.*, 2009). Therefore, it is necessary to understand the structural similarity shared between DMO and other proteins in order to properly assess their homology and determine if homologues of MON 87419 DMO are widely distributed in nature and/or present in foods or feeds consumed by humans or animals.

As described in Section B1(a), DMO is classified as an oxygenase. Oxygenases are enzymes that incorporate one or two oxygen atoms into their substrates and are widely distributed in many universal metabolic pathways (Harayama *et al.*, 1992). Within this large enzymatic class are mono-oxygenases, which incorporate a single oxygen atom as a hydroxyl group with the concomitant production of water and oxidation of NADH (Harayama *et al.*, 1992). Non-heme iron oxygenases, where iron is involved in the catalytic site, are an important class of oxygenases. Within this class are Rieske non-heme iron oxygenases, which contain a Rieske iron-sulfur [2Fe-2S] cluster. All Rieske non-heme iron oxygenases contain two catalytic domains, a non-heme iron domain (nh-Fe) that is a site of oxygen activation, and a Rieske [2Fe-2S] domain which functions by transporting electrons

from ferredoxin to the non-heme iron domain (Ferraro *et al.*, 2005). MON 87419 DMO belongs to this class of oxygenases which are ubiquitous in diverse phyla ranging from bacteria to plants consumed by humans and animals (Ferraro *et al.*, 2005; Schmidt and Shaw, 2001).

The crystal structure of histidine-tagged DMO demonstrated that the quaternary structure of DMO is a trimer, where each individual monomer is in a precise orientation that allows for electron transport between two conserved domains; the Rieske and the non-heme iron domains. Similar to all Rieske non-heme iron oxygenases, DMO monomers contain these two catalytically important and highly conserved domains (D'Ordine *et al.*, 2009; Dumitru *et al.*, 2009; Ferraro *et al.*, 2005). Conservation of these domains ensures that the resulting secondary and tertiary structural domains are in the correct spatial orientation with regard to the non-heme iron and the Rieske [2Fe-2S] domains; which ensures electron transport from ferredoxin and between the monomers of DMO (D'Ordine *et al.*, 2009; Ferraro *et al.*, 2005).

Rieske domains are ubiquitous in numerous bacterial and plant proteins such as the iron-sulfur protein of the cytochrome bc_1 complex, chloroplast cytochrome b_6-*f* complex in spinach, and choline mono-oxygenases (Breyton, 2000; Darrouzet *et al.*, 2004; Gray *et al.*, 2004; Hibino *et al.*, 2002; Rathinasabapathi *et al.*, 1997; Russell *et al.*, 1998). The presence of two conserved domains, a Rieske [2Fe-2S] domain and a non-heme iron domain, suggests that all Rieske type non-heme iron oxygenases share the same reaction mechanism, by which the Rieske domain transfers electrons from the ferredoxin to the non-heme iron to allow catalysis (Chakraborty *et al.*, 2005; Dumitru *et al.*, 2009; Ferraro *et al.*, 2005). The conservation of these important structural domains required for enzymatic activity is further evidence of the evolutionary relation of all Rieske non-heme iron oxygenases to each other (Nam *et al.*, 2001; Rosche *et al.*, 1997; Werlen *et al.*, 1996). Therefore, enzymes with structural homology and functional similarity to MON 87419 DMO have been described in plants and bacteria and have been extensively consumed by both humans and animals.

Additionally, a FASTA alignment search of publicly-available databases using the MON 87419 DMO+12 protein sequence as a query yielded homologous sequences from many different species, predominantly bacteria, with amino acid sequence identity ranging up to approximately 43%. Alignments of MON 87419 DMO+12 with plant proteins revealed homologous oxygenases present in crops, such as canola (*Brassica napus*), soy (*Glycine max*), corn (*Zea mays*), pea (*Pisum sativum*), and rice (*Orysa sativa*), which were determined to have sequence identities up to approximately 24% (Table 18). The highest homology was observed to proteins that are involved in chlorophyll metabolism. Pheophorbide A oxygenase (Accession numbers: ABD60316.1 for Canola, ABA40832.1 for soybean, and ACG28057.1 for corn) is a Rieske-type oxygenase that plays a key role in the overall regulation of chlorophyll degradation in plants (Rodoni *et al.*, 1997). Pheophorbide A oxygenase is constitutively present in all green tissues and, at slightly lower levels, in etiolated and non-photosynthetic tissues including seeds (Yang *et al.*, 2004). As a Rieske-type oxygenase, Pheophorbide A oxygenase is expected to have high degree of secondary and tertiary structure homology to similar structural elements in DMO as described above. The

presence of these conserved structural domains in these plant proteins is further evidence that exposure to a structural homolog of MON 88701 DMO has occurred through consumption of these crops. Chlorophyllide A oxygenase (Accession number: ACG42449.1 for corn) is also a Rieske-type oxygenase that is required for the formation of chlorophyll *b,* which is present in all plants (Tanaka *et al.*, 1998). The presence of these conserved structural domains in these plant proteins is further evidence that exposure to a structural homolog of MON 87419 DMO has occurred through consumption of these crops.

Therefore, MON 87419 DMO shares structural homologies with a wide variety of oxygenases present in bacteria and plants that are widely prevalent in the environment and consumed by humans and animals without any reports of adverse effects due to the protein.

Table 18. Amino Acid Sequence Identity between MON 87419 DMO and Other Proteins Present in Plants

Protein	Accession Number[1]	Scientific Name	Common Name	Sequence Identity (%)[2]
Chloroplast pheophorbide a oxygenase	ABD60316.1	*Brassica napus*	Canola	24.13
Rieske iron-sulfur protein Tic55	CAA04157.1	*Pisum sativum*	Pea	23.64
Lethal leaf spot 1-like protein*	ABA40832.1	*Glycine max*	Soybean	23.56
Pheophorbide a oxygenase	ACG28057.1	*Zea mays*	Corn	23.40
Chlorophyllide a oxygenase	ACG42449.1	*Zea mays*	Corn	22.38
Rieske domain containing protein	ABF99438.1	*Oryza sativa Japonica Group*	Rice	20.84
Pheophorbide a oxygenase, partial	CAR82238.1	*Pisum sativum*	Pea	19.95
Choline mono-oxygenase precursor	AAB52509.1	*Spinacia oleracea*	Spinach	19.36
Sparse inflorescence1	ACI43576.1	*Zea mays*	Corn	19.20
Flavonoid 3'-hydroxylase	AAV74195.1	*Sorghum bicolor*	Sorghum	18.78
Choline mono-oxygenase	CAE17671.1	*Oryza sativa Japonica Group*	Rice	17.87
Beta-carotene hydroxylase	AAX45523.1	*Zea mays*	Corn	17.50
Rieske domain containing protein	ACG43734.1	*Zea mays*	Corn	15.77

*Later identified as Pheophorbide A Oxygenase (Yang *et al.*, 2004).

[1] The accession numbers shown are from the NCBI GenBank database (accessed May 5, 2015).

[2] Percent identity was established through pairwise comparisons of MON 87419 DMO+12 to each of the given sequences using the glsearch36 function of FASTA package version 36.3.5e. This algorithm was applied using an E-score cutoff of 100 with the BLOSUM50 protein scoring matrix to search the given database for optimum global:local alignments with the most optimal hit being retained.

History of Safe Use of PAT (*pat*) Protein

The PAT (*pat*) protein expressed in MON 87419 is 100% homologous to the wild type PAT protein encoded by *S. viridochromogenes*, with the exception of the first methionine that is removed during a co-translational process in MON 87419. N-terminal methionine cleavage occurs naturally in the vast majority of proteins (Meinnel and Giglione, 2008) and has no effect on the physicochemical characteristics, immunoreactivity, functional activity, and/or specificity of the MON 87419-produced PAT (*pat*) protein (see Section B1(b)).

The PAT (*pat*) protein is expressed in numerous commercial glufosinate tolerant crops including soybean, canola, and maize (e.g. T25, TC1507 and DAS-59122-7). The safety of the PAT protein has been well established in the scientific literature based on protein safety literature (Hérouet *et al.*, 2005) and biotech-derived crop safety literature (He *et al.*, 2008; MacKenzie *et al.*, 2007; Malley *et al.*, 2007; Rhee *et al.*, 2005). The EPA has issued a tolerance exemption for PAT proteins regardless of the encoding gene or crop (U.S. EPA, 1997). As a result, the safety of PAT proteins has been favorably assessed following extensive reviews by regulatory agencies in 11 different countries for more than 38 biotechnology-derived events in eight different species (ILSI-CERA, 2011). The lack of any documented reports of adverse effects resulting from PAT-containing crops since their introduction in 1995 (Duke, 2005) further confirms the safety of the MON 87419 PAT (*pat*) protein. Therefore, PAT has a history of safe use (Hérouet *et al.*, 2005; ILSI-CERA, 2011).

B4 Assessment of Potential Toxicity

The assessment of the potential toxicity of an introduced protein takes into account several aspects of its biochemical characteristics (Delaney *et al.*, 2008). A protein introduced into maize is not likely to be associated with toxicity if: 1) the protein lacks any structural similarity to known toxins or other biologically-active proteins that could cause adverse effects in humans or animals; 2) the protein is structurally and functionally related to proteins with a history of safe consumption; and 3) the protein is readily inactivated or degraded in response to common food processing conditions (*e.g.*, heating) and/or digestive enzymes. The lack of any effects in an acute oral mammalian toxicity study performed at dose levels substantially greater than anticipated human exposure levels can provide further confirmation that an introduced protein is unlikely to pose a significant risk to human or animal health.

B4(a) Bioinformatic comparison (aa) of novel protein(s) to toxins

Structural Similarity of MON 87419 DMO and PAT (*pat*) to Known Toxins

The assessment of the potential for protein toxicity includes bioinformatic analysis of the amino acid sequence of the introduced protein. The goal of the bioinformatic analysis is to ensure that the introduced protein does not share homology to known toxins or anti-nutritional proteins associated with adverse health effects.

Potential structural similarities shared between the MON 87419 DMO and PAT (*pat*) proteins with sequences in a protein database were evaluated using the FASTA sequence alignment tool. The FASTA program directly compares amino acid sequences (*i.e.*, primary, linear protein structure) and the alignment data may be used to infer shared higher order structural similarities between two sequences (*i.e.*, secondary and tertiary protein structures). Proteins that share a high degree of similarity throughout the entire sequence are often homologous. Homologous proteins often have common secondary structures, common three-dimensional configuration, and, consequently, may share similar functions (Caetano-Anollés *et al.*, 2009; Illergård *et al.*, 2009).

FASTA bioinformatic alignment searches using the MON 87419 DMO amino acid sequence and the PAT (*pat*) amino acid sequence were performed with the toxin database to identify possible homology with proteins that may be harmful to human and animal health. The toxin database, TOX_2014, is a subset of sequences derived from the PRT_2014 database, that was selected using a keyword search and filtered to remove likely non-toxin proteins and proteins that are not relevant to human or animal health. The TOX_2014 database contains 10,419 sequences.

An *E*-score acceptance criteria of $1x10^{-5}$ or less for any alignment was used to identify proteins from the TOX_2014 database with potential for significant shared structural similarity and function with MON 87419 DMO and PAT (*pat*) proteins. As described above, the *E*-score is a statistical measure of the likelihood that the observed similarity score could have occurred by chance in a search. A larger *E*-score indicates a lower degree of

similarity between the query sequence and the sequence from the database. Typically, alignments between two sequences require an *E*-score of 1×10^{-5} or less to be considered to have sufficient sequence similarity to infer homology. The results of the search comparisons showed that no relevant alignments were observed against proteins in the TOX_2014 database.

The results of the bioinformatic analyses demonstrated that no structurally relevant similarity exists between the MON 87419 DMO protein and any sequence in the TOX_2014 database, as no alignments displaying an *E*-score < 1e-5 were observed. Using PAT (*pat*) as the query sequence to search the TOX_2014 database, 17 alignments displayed *E*-scores of less than or equal to 1e-5 with the toxin component of the GNAT (GCN5-related N-acetyltransferase) toxin-antitoxin system of bacteria. As expected these data reveal structural similarities between the PAT (*pat*) sequence and the toxin component of the GNAT toxin-antitoxin system of bacteria. Bacterial toxin-antitoxin systems are widespread; they are involved in the maintenance of low copy plasmids (Makarova *et al.*, 2009) and are only toxic when produced intracellularly in bacteria. Alignments with bacterial toxin-antitoxin system proteins do not provide any indication that PAT (*pat*) protein would adversely impact human or animal health if consumed. This is comparable with previously published safety assessments of PAT protein (Hérouet *et al.*, 2005).

For details, please refer to [redacted], 2014 (MSL0025907).

B4(b) Stability to heat or processing and/or degradation in gastric model

B4(b)(i) Digestive fate of the MON 87419 DMO and PAT (*pat*) proteins

Digestive Fate of the MON 87419 DMO Protein

Proteins introduced into crops using biotechnology are evaluated for their safety for human and animal consumption. The majority of ingested dietary proteins undergo hydrolytic degradation and/or proteolytic degradation to their constituent amino acids or small peptides, which are then absorbed and used for synthesis of proteins or other glucogenic or ketogenic metabolites by the body (Delaney *et al.*, 2008). Therefore, evaluating a protein's intrinsic sensitivity to proteolytic degradation with enzymes of the gastrointestinal tract is a key aspect to understanding the safety of any introduced proteins in GM crops. One characteristic of protein toxins and many allergens is their ability to withstand proteolytic degradation by enzymes present in the gastrointestinal tract (Astwood *et al.*, 1996; Moreno *et al.*, 2005; Vassilopoulou *et al.*, 2006; Vieths *et al.*, 1999). Allergenic proteins or their fragments, when presented to the intestinal immune system, can lead to a variety of gastrointestinal and systemic manifestations of immune-mediated allergy. The complete enzymatic degradation of an ingested protein by exposure to gastric pepsin and intestinal pancreatic proteases makes it highly unlikely that either the intact protein or protein fragment(s) will reach the absorptive epithelial cells of the small intestine where antigen processing cells reside (Moreno *et al.*, 2005). To reach these cells, protein or protein fragment(s) must first pass through the stomach where they are exposed to pepsin and then the duodenum where they are exposed to pancreatic fluid containing a mixture of enzymes called pancreatin. Therefore, the

susceptibility of MON 87419 DMO protein to degradation by pepsin and pancreatin was assessed.

A correlation between the resistance to protein degradation by pepsin and the likelihood of the protein being an allergen has been previously assessed with a group of proteins consisting of both allergens and non-allergens (Astwood *et al.*, 1996; Codex Alimentarius, 2009), but this correlation is not absolute (Fu *et al.*, 2002). A standardized protocol to compare the relative resistance of proteins to degradation by pepsin has been established based on results obtained from an international, multi-laboratory study (Thomas *et al.*, 2004). The multi-laboratory study showed that the results of *in vitro* pepsin degradation assays were reproducible when a standard protocol was followed. Using this standardized *in vitro* pepsin degradation protocol, the susceptibility of MON 87419 DMO protein to pepsin degradation was assessed.

Incubation of test proteins with pancreatin is also used to assess the susceptibility of the protein to proteolytic degradation (Okunuki *et al.*, 2002; Yagami *et al.*, 2000). The relationship between protein allergenicity and susceptibility to pancreatin degradation is limited for several reasons. Namely, the protein has not been first exposed to the acidic, and proteolytic denaturing condition of the stomach, as would be the case *in vivo* (Helm, 2001). Using an established protocol, the susceptibility of MON 87419 DMO to pancreatin degradation was assessed.

Degradation of MON 87419 DMO by Pepsin

The degradation of *E. coli*-produced MON 87419 DMO (test substance) by pepsin was assessed using two methods: visual analysis of a Brilliant Blue G-Colloidal stained SDS-PAGE gel and visual analysis of a western blot probed with an anti-DMO polyclonal antibody.

Degradation of *E. coli*-produced DMO by pepsin in solution was evaluated over time by analyzing reaction mixtures incubated for targeted time intervals. For SDS-PAGE analysis, approximately 1 µg of total protein was analyzed for each time point (Figure 28). The apparent molecular weights of pepsin (~38 kDa) and MON 87419 DMO (~39 kDa) are similar (Figure 28, lanes 2 and 3, respectively); therefore, it is difficult to distinguish between the two proteins on an SDS-PAGE gel. However, the intensity of the combined band at Pepsin Treated T0 appears to be the combination of the intensity of both proteins run separately (Figure 28, lane 4). After 0.5 min incubation (Pepsin Treated T1), the intensity of the combined bands was reduced to approximately the same level as observed for pepsin alone (0 min No Test Protein Control; Figure 28, compare lanes 2 and 5) suggesting that the intact DMO protein was degraded. A peptide fragment of ~3 kDa was observed at the 0.5 and 2 min time points but was not observed at the 5 min time point (Figure 28, lanes 5-7)), which is likely a result of a partially digested production.

No change in the DMO protein band intensity was observed in the absence of pepsin in the 0 min No Pepsin Control and 60 min No Pepsin Control (Figure 28, lanes 3 and 12). This indicates that the degradation of the DMO protein was due to the proteolytic activity of

pepsin and not due to instability of the protein while incubated in 2 mg/ml NaCl, 10 mM HCl, pH ~1.2 at 37 ± 2°C for 60 min.

The 0 min No Test Protein Control and 60 min No Test Protein Control (Figure 28, lanes 2 and 13) demonstrated that the pepsin is stable throughout the experimental phase.

A separate SDS-PAGE gel to estimate the LOD of the DMO protein was run concurrently with the SDS-PAGE for the degradation assessment (data not shown). Because intact DMO protein and pepsin are difficult to resolve by SDS-PAGE, the LOD of DMO protein on Brilliant Blue G-colloidal stained gel could not be determined, therefore, the percent degradation of intact DMO protein was not estimated on Brilliant Blue G-colloidal stained gels, but it is reasonable to conclude that DMO was completely degraded by pepsin within 5 minutes.

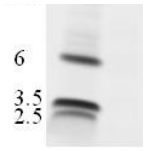

Figure 28. Brilliant Blue G-Colloidal Stained SDS-PAGE Gel Showing the Degradation of Purified *E. coli*-Produced MON 87419 DMO Protein by Pepsin

Brilliant Blue G-Colloidal stained SDS-PAGE gels were used to assess the degradation of DMO protein by pepsin. Molecular weights (kDa) are shown on the left of the gel, and correspond to the markers loaded. In the gel, DMO protein migrated to approximately 39 kDa and pepsin to approximately 38 kDa. Blank lane 15 was cropped from the images. Based on total pre-reaction protein concentrations, 1 µg of test substance was loaded in each lane containing DMO protein. Lane designations are as follows:

Lane	Sample	Incubation Time (min)
1	Mark 12 MWM	-
2	0 min No Test Protein Control	0
3	0 min No Pepsin Control	0
4	Pepsin Treated T0	0
5	Pepsin Treated T1	0.5
6	Pepsin Treated T2	2
7	Pepsin Treated T3	5
8	Pepsin Treated T4	10
9	Pepsin Treated T5	20
10	Pepsin Treated T6	30
11	Pepsin Treated T7	60
12	60 min No Pepsin Control	60
13	60 min No Test Protein Control	60
14	Mark 12 MWM	-
15	Blank	-

Two blots were run concurrently, one used for the western blot analysis of the susceptibility of MON 87419 DMO to degradation by pepsin (Figure 29 Panel A) and another used to estimate the LOD of the intact MON 87419 DMO protein for western blot analysis (Figure 29 Panel B). Twenty ng of *E. coli*-produced MON 87419 DMO protein was analyzed by western blot for each time point. No immunoreactive bands were observed in 0 min No Test Protein Control and 60 min No Test Protein Control (Figure 29 Panel A, Lanes 2 and 13). This result indicates that there was no non-specific interaction between the pepsin solution and the DMO-specific antibody under these experimental conditions.

Western blot analysis demonstrated that the *E. coli*-produced MON 87419 DMO protein was degraded below the LOD within 0.5 min of incubation in the presence of pepsin (Figure 29 Panel A, Lane 5). The LOD of the MON 87419 DMO protein was visually estimated to be 0.63 ng (Figure 29 Panel B, Lane 7). The LOD estimated for the MON 87419 DMO protein was used to calculate the maximum amount of intact MON 87419 DMO protein that could remain visually undetected after degradation. This corresponded to approximately 3.2% of the total protein loaded. Based on the western blot LOD for the MON 87419 DMO protein, it can be concluded that within 0.5 min more than 96% (100% - 3.2% = 96.8%) of the intact MON 87419 DMO protein was degraded and no other immunodetected fragments were observed.

No change in the MON 87419 DMO protein band intensity was observed in the absence of pepsin in the 0 min No Pepsin Control and 60 min No Pepsin Control (Figure 29 Panel A, Lanes 3 and 12). This result reaffirms that the MON 87419 DMO protein was stable in the test system without pepsin.

As indicated on the LOD blot, 0.63 ng of *E.coli*-produced MON 87419 DMO test protein was readily detected by the antibody and blotting methods used for this analysis (Figure 29 Panel B, Lane 7). Thus, the 20 ng of test substance loaded per lane represented a heavy loading of the MON 87419 DMO protein for western blot analysis (Figure 29, Panel A); this amount of MON 87419 DMO protein was applied to increase the probability that any intact protein or protein fragments of MON 87419 DMO would be visible. Under these high levels of gel loading conditions, three immunoreactive bands (~75 kDa, ~25 kDa, and ~20 kDa) were visible in addition to the MON 87419 DMO protein in the absence of digestion (Figure 29 Panel A, Lanes 3, 4, and 12). The ~75 kDa band is likely the result of aggregation of MON 87419 DMO protein and ~25 kDa and ~20 kDa are likely the results of a partially digested production.

In summary, the results from western blot analysis demonstrate that greater than 96% of the *E. coli*-produced MON 87419 DMO protein was degraded in the presence of pepsin within 0.5 min and other immunoreactive bands were not detected.

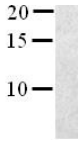

Figure 29. Western Blot Analysis of the Degradation of the Purified *E. coli*-Produced MON 87419 DMO Protein by Pepsin

Western blots probed with an anti-DMO antibody were used to assess the degradation of DMO by pepsin. Molecular weights (kDa) are shown on the left of each gel, and correspond to the markers loaded (cropped from images). Blank lanes were cropped from the images. A 30 sec exposure is shown.
A: DMO protein degradation by pepsin. Based on total pre-reaction protein concentrations, 20 ng of test substance was loaded in each lane containing DMO protein.
B: LOD determination. Indicated amounts of the DMO protein from the Pepsin Treated T0 sample were loaded to estimate the LOD of the DMO protein.

Lane	Sample	Incubation Time (min)
1	Precision Plus MWM	-
2	0 min No Test Protein Control	0
3	0 min No Pepsin Control	0
4	Pepsin Treated T0	0
5	Pepsin Treated T1	0.5
6	Pepsin Treated T2	2
7	Pepsin Treated T3	5
8	Pepsin Treated T4	10
9	Pepsin Treated T5	20
10	Pepsin Treated T6	30
11	Pepsin Treated T7	60
12	60 min No Pepsin Control	60
13	60 min No Test Protein Control	60
14	Precision Plus MWM	-
15	Blank	-

Lane	Sample	Amount of DMO Protein (ng)
1	Precision Plus MWM	-
2	Pepsin Treated T0	20
3	Pepsin Treated T0	10
4	Pepsin Treated T0	5
5	Pepsin Treated T0	2.5
6	Pepsin Treated T0	1.25
7	Pepsin Treated T0	0.63
8	Pepsin Treated T0	0.31
9	Pepsin Treated T0	0.16
10	Pepsin Treated T0	0.08
11	Precision Plus MWM	-
12	Blank	-
13	Blank	-
14	Blank	-
15	Blank	-

Degradation of MON 87419 DMO Protein by Pancreatin

The degradation of the *E. coli*-produced MON 87419 DMO protein by pancreatin was assessed by western blot (Figure 30). The western blot used to assess the *in vitro* degradation of the MON 87419 DMO protein by pancreatin (Figure 30 Panel A) was run concurrently with a western blot used to estimate the LOD (Figure 30 Panel B) of the intact MON 87419 DMO protein in this assay. Twenty ng of *E. coli*-produced MON 87419 DMO protein was analyzed by western blot for each time point. No immunoreactive bands were observed in controls 0 min No Test Protein Control and 24 hr No Test Protein Control, which represent the pancreatin test system without *E. coli*-produced MON 87419 DMO protein (Figure 30 Panel A, Lanes 2 and 14). This result demonstrates the absence of non-specific antibody interactions with the pancreatin test system.

Although no obvious change in the intact MON 87419 DMO (~ 39 kDa) band intensity was observed in the absence of pancreatin in the 0 min No Pancreatin Control and 24 hr No Pancreatin Control (Figure 30 Panel A, Lanes 3 and 13), an increase in intensity of bands at ~72, ~76 and ~140 kDa was observed. These higher order proteins are most likely multimers of the 39 kDa monomeric form of DMO that formed during the 24 hr incubation without pancreatin, since all of these bands are immuno-detected by the anti-DMO antibodies. This indicates that the degradation of all immunoreactive forms of the DMO protein was due to the proteolytic activity of pancreatin and not due to instability of the protein when incubated in the pancreatin test system over the course of the experiment.

Western blot analysis demonstrated that the full-length *E. coli*-produced MON 87419 DMO protein was degraded to a level below the LOD within 5 min of incubation in the presence of pancreatin (Figure 30 Panel A, Lane 5), the first time point assessed. The LOD of the MON 87419 DMO protein was visually estimated to be approximately 0.31 ng protein loaded (Figure 30 Panel B, Lane 8). This LOD was used to calculate the maximum amount of MON 87419 DMO protein that could remain visually undetected after degradation, which corresponded to approximately 1.6% of the total protein loaded. Therefore, based on the LOD, more than 98% (100% - 1.6% = 98.4%) of the full-length MON 87419 DMO protein was degraded in the presence of pancreatin within 5 min. Two peptide fragments of ~12 and ~21 kDa were observed at the 5 min time point, but were gone by 15 min (Figure 30 Panel A, Lanes 5 and 6). The ~12 kDa and ~21 kDa bands are likely the results of a partially digested production. No other immunoreactive bands were detected in any other tested specimens.

In summary, the results from this analysis demonstrate that greater than 98% of the full-length *E. coli*-produced MON 87419 DMO protein was degraded in the presence of pancreatin within 5 min.

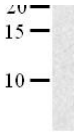

Figure 30. Western Blot Analysis of the Degradation of the Purified *E. coli*-Produced MON 87419 DMO Protein by Pancreatin

Western blots probed with an anti-DMO antibody were used to assess the degradation of DMO by pancreatin. Molecular weights (kDa) are shown on the left of each gel, and correspond to the markers loaded (cropped from images). Blank lanes were cropped from the images. A 10 sec exposure is shown.
A: DMO protein degradation by pancreatin. Based on total pre-reaction protein concentrations, 20 ng of test substance was loaded in each lane containing DMO protein.
B: LOD determination. Indicated amounts of the DMO protein from the Pancreatin Treated T0 sample were loaded to estimate the LOD of the DMO protein.

Lane	Sample	Incubation Time
1	Precision Plus MWM	-
2	0 min No Test Protein Control	0
3	0 min No Pancreatin Control	0
4	Pancreatin Treated T0	0
5	Pancreatin Treated T1	5 min
6	Pancreatin Treated T2	15 min
7	Pancreatin Treated T3	30 min
8	Pancreatin Treated T4	1 hr
9	Pancreatin Treated T5	2 hr
10	Pancreatin Treated T6	4 hr
11	Pancreatin Treated T7	8 hr
12	Pancreatin Treated T8	24 hr
13	24 hr No Pancreatin Control	24 hr
14	24 hr No Test Protein Control	24 hr
15	Precision Plus MWM	-

Lane	Sample	Amount of DMO Protein (ng)
1	Precision Plus MWM	-
2	Pancreatin Treated T0	20
3	Pancreatin Treated T0	10
4	Pancreatin Treated T0	5
5	Pancreatin Treated T0	2.5
6	Pancreatin Treated T0	1.25
7	Pancreatin Treated T0	0.63
8	Pancreatin Treated T0	0.31
9	Pancreatin Treated T0	0.16
10	Pancreatin Treated T0	0.08
11	Precision Plus MWM	-
12	Blank	-
13	Blank	-
14	Blank	-
15	Blank	-

Digestive Fate of the MON 87419 DMO Protein – Conclusions

Degradation of the MON 87419 DMO protein was evaluated in the presence of pepsin and pancreatin. The results of the study demonstrate that greater than 96% of the *E. coli*-produced MON 87419 DMO protein was degraded in the presence of pepsin within 0.5 min, when analyzed by western blot using a DMO-specific antibody. Additionally, more than 98% of the MON 87419 DMO protein was degraded within 5 min during incubation in the presence of pancreatin.

Results from these experiments show that *E. coli*-produced MON 87419 DMO protein is rapidly degraded by pepsin and pancreatin. Rapid degradation of the *E. coli*-produced MON 87419 DMO protein in the presence of pepsin and pancreatin supports the conclusion that the MON 87419 DMO protein is highly unlikely to pose a safety concern to human and animal health.

Please also refer to [redacted], 2014 (MSL0026364).

Degradation of PAT (*pat*) Protein by Pepsin

The degradation of *E. coli*-produced PAT (*pat*) (test substance) by pepsin was assessed using two methods: visual analysis of a Brilliant Blue G-Colloidal stained SDS-PAGE gel and visual analysis of a western blot probed with an anti-PAT (*bar*) polyclonal antibody. For this assessment, a separate SDS-PAGE gel containing dilutions of the pre-reaction test substance was run concurrently to estimate the limit of detection (LOD) of the *E. coli*-produced PAT (*pat*) protein.

Degradation of *E. coli*-produced PAT (*pat*) by pepsin in solution was evaluated over time by analyzing reaction mixtures incubated for targeted time intervals. For SDS-PAGE analysis, approximately 1 µg of total protein was analyzed for each time point (Figure 31 Panel A). The controls, 0 min No Test Protein Control and 60 min No Test Protein Control (Figure 31 Panel A, Lanes 2 and 13), which evaluate the susceptibility of the pepsin in the test system lacking the PAT (*pat*) protein, demonstrated that the pepsin was observed as a stained protein band at ~38 kDa throughout the experimental phase.

No change in the PAT (*pat*) protein band intensity was observed over time in the absence of pepsin (compare 0 min No Pepsin Control to 60 min No Pepsin Control; Figure 31 Panel A, Lanes 3 and 12) indicating that the degradation of the PAT (*pat*) protein was due to the proteolytic activity of pepsin present in test system and not due to instability of the protein while incubated at pH ~1.2 at ~37 °C for 60 min.

Visual examination of SDS-PAGE data showed that the intact PAT (*pat*) protein was completely degraded within 0.5 min of incubation in the presence of pepsin (Figure 31 Panel A, Lane 5). For the SDS-PAGE analysis, the LOD of the PAT (*pat*) protein was visually estimated to be approximately 3.6 ng (Figure 31 Panel B, Lane 8). This LOD used to calculate the maximum amount of intact PAT (*pat*) protein that could remain visually undetected after degradation, which corresponded to approximately 0.4% of the total protein loaded. Based on that LOD, more than 99.6% (100% - 0.4% = 99.6%) of the intact PAT (*pat*) protein was degraded within 0.5 min of incubation in the presence of pepsin. A peptide fragment of ~3 kDa was observed for the first 5 min of pepsin treatment with the staining intensity decreasing over time and it was completely degraded within 10 min of incubation. This ~3 kDa peptide fragment is likely a result of a partially digested production. This is comparable with previously published safety assessments of PAT protein (Hérouet *et al.*, 2005).

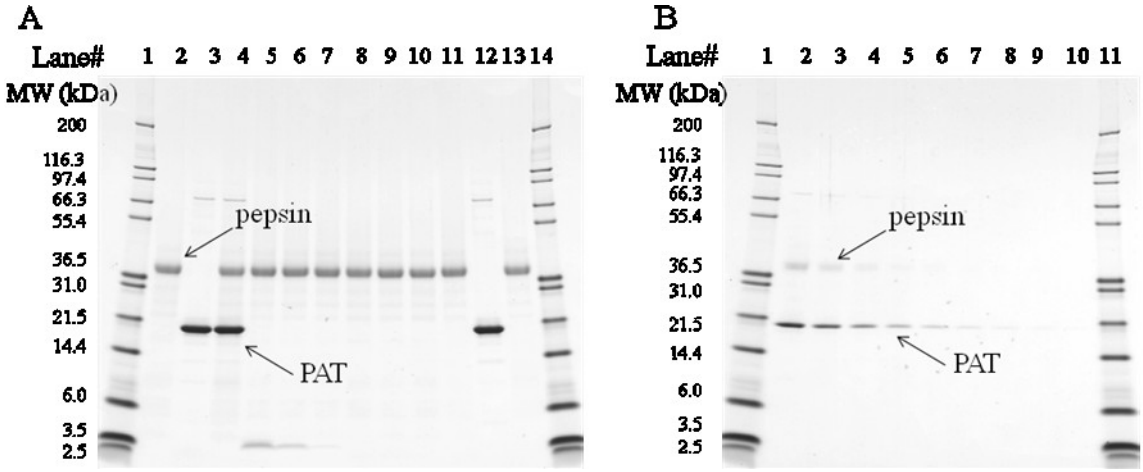

Figure 31. Brilliant Blue G-Colloidal Stained SDS-PAGE Gel Showing the Degradation of Purified *E. coli*-Produced PAT (*pat*) Protein by Pepsin

Brilliant Blue G-Colloidal stained SDS-PAGE gels were used to assess the degradation of PAT (*pat*) protein by pepsin. Molecular weights (kDa) are shown on the left of each gel, and correspond to the markers loaded. In each gel, PAT (*pat*) protein migrated to approximately 21 kDa and pepsin to approximately 38 kDa. Blank lanes were cropped from the images.
A: PAT (*pat*) protein degradation by pepsin. Based on total pre-reaction protein concentrations, 1 µg of test substance was loaded in each lane containing PAT (*pat*) protein.
B: LOD determination. Indicated amounts of the PAT (*pat*) protein from the Pepsin Treated T0 sample were loaded to estimate the LOD of the PAT (*pat*) protein. Lane designations are as follows:

Lane	Sample	Incubation Time (min)
1	Mark 12 MWM	-
2	0 min No Test Protein Control	0
3	T 0 min No Pepsin Control	0
4	Pepsin T0	0
5	Pepsin T1	0.5
6	Pepsin T2	2
7	Pepsin T3	5
8	Pepsin T4	10
9	Pepsin T5	20
10	Pepsin T6	30
11	Pepsin T7	60
12	60 min No Pepsin Control	60
13	60 min No Test Protein Control	60
14	Mark 12 MWM	-

Lane	Sample	Amount of PAT (*pat*) Protein (ng)
1	Mark 12 MWM	-
2	Pepsin T0	230
3	Pepsin T0	115
4	Pepsin T0	57.5
5	Pepsin T0	28.8
6	Pepsin T0	14.4
7	Pepsin T0	7.2
8	Pepsin T0	3.6
9	Pepsin T0	1.8
10	Pepsin T0	0.9
11	Mark 12 MWM	-

Two blots were run concurrently, one used for the western blot analysis of the susceptibility of PAT (*pat*) to degradation by pepsin (Figure 32 Panel A) and another used to estimate the LOD of the PAT (*pat*) protein (Figure 32 Panel B). Twenty ng of total protein was analyzed by western blot for each time point. No immunoreactive bands were observed in controls, 0 min No Test Protein Control and 60 min No Test Protein Control (Figure 32 Panel A, Lanes 2 and 13). This result indicates that non-specific interactions between the test system components and the PAT-specific antibody did not occur under these experimental conditions.

No change in the intact PAT (*pat*) protein band intensity was observed in the absence of pepsin (compare 0 min No Pepsin Control to 60 min No Pepsin Control, Figure 32 Panel A, Lanes 3 and 12). This result reaffirms that the PAT (*pat*) protein was stable in the test system without pepsin.

Western blot analysis demonstrated that the *E. coli*-produced PAT (*pat*) protein was degraded below the LOD within 0.5 min of incubation in the presence of pepsin (Figure 32 Panel A, Lane 5). The LOD of the PAT (*pat*) protein was visually estimated to be approximately 0.36 ng (Figure 32 Panel B, Lane 7). The LOD estimated for the PAT (*pat*) protein was used to calculate the maximum amount of PAT (*pat*) protein that could remain visually undetected after degradation, which corresponded to approximately 1.8% of the total protein loaded. Based on the western blot LOD for the PAT (*pat*) protein, the conclusion was that more than 98% (100% - 1.8% = 98.2%) of the intact PAT (*pat*) protein was degraded within 0.5 min. No other immunoreactive peptide fragments were detected by the western blot analysis at any other time points. This is comparable with previously published safety assessments of PAT (*pat*) protein (Hérouet *et al.*, 2005).

In summary, the results from western blot analysis demonstrate that greater than 98% of the *E. coli*-produced PAT (*pat*) protein was degraded in the presence of pepsin within 0.5 min and other immunoreactive bands were not detected.

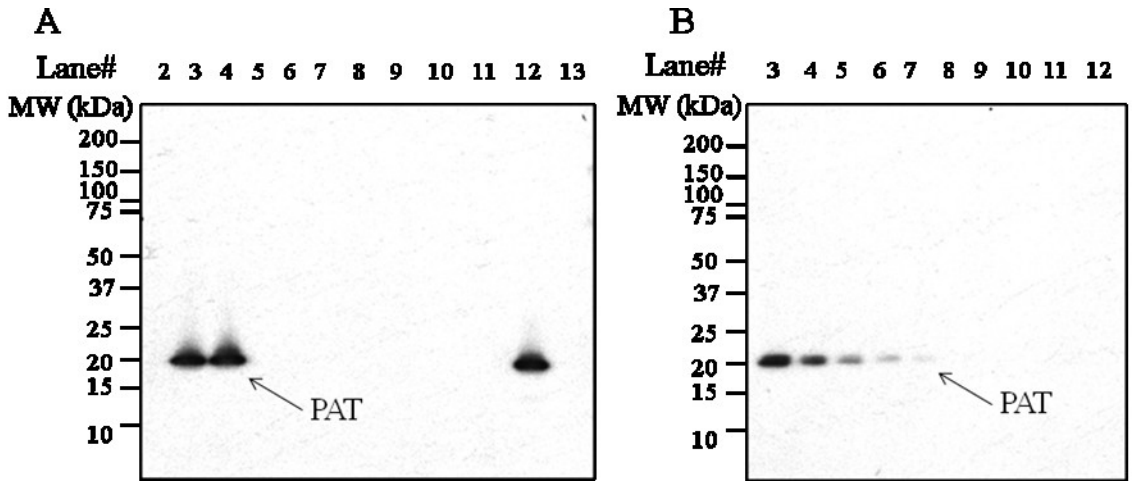

Figure 32. Western Blot Analysis of the Degradation of the Purified *E. coli*-Produced PAT (*pat*) Protein by Pepsin

Western blots probed with an anti-PAT (*bar*) antibody were used to assess the degradation of PAT (*pat*) by pepsin. Molecular weights (kDa) are shown on the left of each gel, and correspond to the markers loaded (cropped from images). Blank lanes were cropped from the images. A 20 sec exposure is shown.

A: PAT (*pat*) protein degradation by pepsin. Based on total pre-reaction protein concentrations, 20 ng of test substance was loaded in each lane containing PAT (*pat*) protein.

B: LOD determination. Indicated amounts of the PAT (*pat*) protein from the Pepsin Treated T0 sample were loaded to estimate the LOD of the PAT (*pat*) protein. Lane designations are as follows:

Lane	Sample	Incubation Time (min)
1	Precision Plus MWM	-
2	0 min No Test Protein Control	0
3	0 min No Pepsin Control	0
4	Pepsin T0	0
5	Pepsin T1	0.5
6	Pepsin T2	2
7	Pepsin T3	5
8	Pepsin T4	10
9	Pepsin T5	20
10	Pepsin T6	30
11	Pepsin T7	60
12	60 min No Pepsin Control	60
13	60 min No Test Protein Control	60
14	Precision Plus MWM	-

Lane	Sample	Amountof PAT (*pat*) Protein (ng)
1	Precision Plus MWM	-
2	Blank	-
3	Pepsin T0	5.8
4	Pepsin T0	2.9
5	Pepsin T0	1.44
6	Pepsin T0	0.72
7	Pepsin T0	0.36
8	Pepsin T0	0.18
9	Pepsin T0	0.09
10	Pepsin T0	0.045
11	Pepsin T0	0.022
12	Pepsin T0	0.011
13	Blank	-
14	Precision Plus MWM	-

Degradation of PAT (*pat*) Protein by Pancreatin

The degradation of the PAT (*pat*) protein by pancreatin was assessed by western blot (Figure 33). The western blot used to assess the *in vitro* degradation of the PAT (*pat*) protein by pancreatin (Figure 33 Panel A) was run concurrently with a western blot used to estimate the LOD of the intact PAT (*pat*) protein (Figure 33 Panel B) in this assay. The gel used to assess the degradation of the PAT (*pat*) protein by pancreatin by western blot was loaded with 20 ng total protein (based on pre-reaction protein concentrations) for each of the incubation time points. No immunoreactive bands were observed in controls, 0 min No Test Protein Control and 24 hr No Test Protein Control, which represent the pancreatin test system without *E. coli*-produced PAT (*pat*) protein (Figure 33 Panel A, Lanes 2 and 14). This result demonstrates the absence of non-specific antibody interactions with the pancreatin test system.

No change in PAT (*pat*) protein band intensity was observed in the controls, 0 min No Pancreatin Control and 24 hr No Pancreatin Control (Figure 33 Panel A, Lanes 3 and 13), which represent the test system without pancreatin. This result reaffirms that PAT (*pat*) was stable in the test system without pancreatin over the course of the experiment.

Western blot analysis demonstrated that a band corresponding to the PAT (*pat*) protein was degraded to a level below the LOD within 5 min of incubation in the presence of pancreatin (Figure 33 Panel A, Lane 5), the first time point assessed. The LOD was visually estimated to be 0.17 ng (Figure 33 Panel B, Lane 8). This LOD was used to calculate the maximum amount of PAT (*pat*) protein that could remain visually undetected after degradation, which corresponded to approximately 0.9% of total protein loaded. Therefore, based on the LOD, more than 99% (100% - 0.9% = 99.1%) of the PAT (*pat*) protein was degraded in the presence of pancreatin within 5 min. No other immunoreactive bands were detected in any other tested specimens. This is comparable with previously published safety assessments of PAT (*pat*) protein (Hérouet *et al.*, 2005).

In summary, the results from this analysis demonstrate that greater than 99% of the *E. coli*-produced PAT (*pat*) protein was degraded in the presence of pancreatin within 5 min and no other immunoreactive bands were detected.

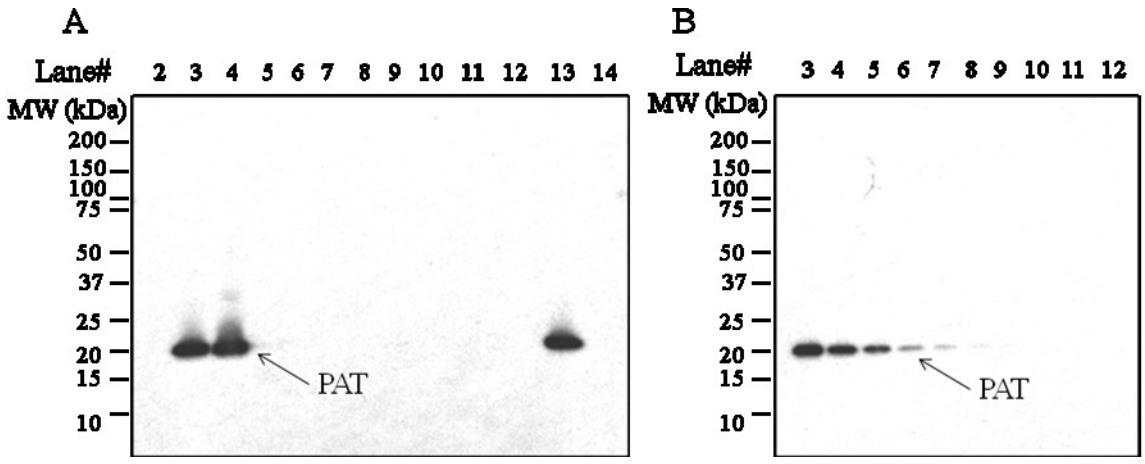

Figure 33. Western Blot Analysis of the Degradation of the Purified *E. coli*-Produced PAT (*pat*) Protein by Pancreatin

Western blots probed with an anti-PAT (*bar*) antibody were used to assess the degradation of PAT (*pat*) by pancreatin. Molecular weights (kDa) are shown on the left of each gel, and correspond to the markers loaded (cropped from images). Blank lanes were cropped from the images. A 15 sec exposure is shown.
A: PAT (*pat*) protein degradation by pancreatin. Based on total pre-reaction protein concentrations, 20 ng of test substance was loaded in each lane containing PAT (*pat*) protein.
B: LOD determination. Indicated amounts of the PAT (*pat*) protein from the Pancreatin Treated T0 sample were loaded to estimate the LOD of the PAT (*pat*) protein. Lane designations are as follows:

Lane	Sample	Incubation Time
1	Precision Plus MWM	-
2	0 min No Test Protein Control	0
3	0 min No Pancreatin Control	0
4	Pancreatin Treated T0	0
5	Pancreatin Treated T1	5 min
6	Pancreatin Treated T2	15 min
7	Pancreatin Treated T3	30 min
8	Pancreatin Treated T4	1 hr
9	Pancreatin Treated T5	2 hr
10	Pancreatin Treated T6	4 hr
11	Pancreatin Treated T7	8 hr
12	Pancreatin Treated T8	24 hr
13	24 hr No Pancreatin Control	24 hr
14	24 hr No Test Protein Control	24 hr
15	Precision Plus MWM	-

Lane	Sample	Amount of PAT (*pat*) Protein (ng)
1	Precision Plus MWM	-
2	Blank	-
3	Pancreatin Treated T0	5.6
4	Pancreatin Treated T0	2.78
5	Pancreatin Treated T0	1.39
6	Pancreatin Treated T0	0.69
7	Pancreatin Treated T0	0.35
8	Pancreatin Treated T0	0.17
9	Pancreatin Treated T0	0.087
10	Pancreatin Treated T0	0.043
11	Pancreatin Treated T0	0.022
12	Pancreatin Treated T0	0.011
13	Blank	-
14	Precision Plus MWM	-

Digestive Fate of PAT (*pat*) Protein – Conclusions

Degradation of the PAT (*pat*) protein was evaluated in the presence of pepsin and pancreatin. Comparable to previously published safety assessment data on PAT (*pat*) protein (Hérouet *et al.*, 2005), the results of this study demonstrate that greater than 98% of the *E. coli*-produced PAT (*pat*) protein was degraded in the presence of pepsin within 0.5 min, when analyzed by Brilliant Blue G-Colloidal stained SDS-PAGE and by western blot using a PAT-(*bar*)-specific antibody. Additionally, at least 99% of the PAT (*pat*) protein was degraded within 5 min during incubation in the presence of pancreatin.

Results from these experiments show that the *E. coli*-produced PAT (*pat*) protein is rapidly degraded by pepsin and pancreatin. Rapid degradation of the *E. coli*-produced PAT (*pat*) protein in the presence of pepsin and pancreatin supports the conclusion that the PAT (*pat*) protein is highly unlikely to pose a safety concern to human and animal health.

Please also refer to [redacted], 2015 (MSL0025998).

B4(b)(ii) Heat Stability of the Purified MON 87419 DMO amd PAT (*pat*) proteins

Heat Susceptibility of the Purified MON 87419 DMO Protein

Temperature can have a profound effect on the structure and function of proteins. Heat treatment is widely used in the preparation of foods derived from maize grain (Hammond and Jez, 2011). It is reasonable that such processing will have an effect on the functional activity and structure of MON 87419 DMO protein when consumed in different food products derived from MON 87419, thus reducing any potential safety concerns posed by the protein. Therefore, an assessment of the effect of heating was conducted as a surrogate for the conditions encountered during the preparation of foods from MON 87419 grain.

The effect of heat treatment on the activity of MON 87419-produced DMO protein was evaluated using the *E. coli*-produced MON 87419 DMO protein. Heat-treated samples and an unheated control sample of *E. coli*-produced MON 87419 DMO protein were analyzed: 1) using a functional assay to assess the impact of temperature on the enzymatic activity of MON 87419 DMO protein; and 2) using SDS-PAGE to assess the impact of temperature on protein integrity.

Aliquots of *E. coli*-produced MON 87419 DMO were heated to 25, 37, 55, 75, and 95 °C for either 15 or 30 minutes, while a separate aliquot of *E. coli*-produced MON 87419 DMO was maintained on ice for the duration of the heat treatments to serve as a temperature control. The effect of heat treatment on the activity of MON 87419 DMO was evaluated using a functional activity assay . The effect of heat treatment on the integrity of the MON 87419 DMO protein was evaluated using SDS-PAGE analysis of the heated and temperature control MON 87419 DMO protein samples.

The effects of heating on the functional activity of *E. coli*-produced MON 87419 DMO are presented in Table 19 and Table 20. The functional activity of MON 87419 DMO was unaffected at 25 ºC and 37 ºC for 15 and 30 minutes. The functional activity of MON 87419 DMO was below the LOQ of the assay following incubation at 55 ºC or higher

for 15 min or more, indicating that the majority of the functional activity of MON 87419 DMO had been lost during heating. These results suggest that temperature has a considerable effect on the activity of MON 87419 DMO.

Analysis by SDS-PAGE stained with Brilliant Blue G-Colloidal demonstrated that the MON 87419 DMO control treatment and reference standard contain a major band at ~39 kDa, corresponding to the MON 87419 DMO protein (Figure 34 and Figure 35, Lanes 7 and 8). No apparent decrease in the intensity of this band was observed in heat-treated MON 87419 DMO at 25, 37, 55, and 75 °C for 15 minutes (Figure 34, Lanes 2–5) and at 25, 37, and 55 °C for 30 minutes (Figure 35, Lanes 2–4). A slight reduction in band intensity at ~ 39 kDa was observed in heat treated MON 87419 DMO protein at 75 °C for 30 minutes (Figure 35, Lane 5) and an apparent decrease in the intensity of this band was observed at 95 ºC for both 15 or 30 minutes (Figure 34 and Figure 35, Lane 6). There was an appearance of higher molecular weight species at heat treatments of 75 and 95 ºC for 15 minutes (Figure 34, Lanes 5-6) or at heat treatments of 55 and 75 ºC for 30 minutes (Figure 35, Lanes 4-5). These higher molecular weight bands are likely the results of aggregation of MON 87419 DMO protein under these heat treatments. When the test sample was heated at 95 ºC for 30 minutes, band intensities of all molecular weight species were reduced (Figure 35, Lane 6).

These data demonstrate that the *E. coli*-produced MON 87419 DMO protein behaves with a predictable tendency toward protein denaturation and loss of functional activity at elevated (>55 °C) temperatures. Heat treatment is widely used in the preparation of foods containing components derived from maize grain. Therefore, it is reasonable to conclude that MON 87419 DMO protein would not be consumed as an active protein in food or feed products due to standard processing practices that include heat treatment.

For details, please refer to [redacted]., 2014 (MSL0025906).

Table 19. DMO Functional Activity of *E. coli*-produced MON 87419 DMO Protein after 15 Minutes at Elevated Temperatures

Temperature	Specific Activity (nmol DCSA × min^{-1} × mg^{-1})[1]	Relative Activity (% of control sample)[2]
0 ºC (control)	215.8	100 %
25 ºC	251.4	117 %
37 ºC	245.7	114 %
55 ºC	Below LOQ[3]	<2.8 %
75 ºC	Below LOQ[3]	<2.8 %
95 ºC	Below LOQ[3]	<2.8 %

[1]Mean specific activity determined from n=3.
[2]DMO protein activity of control sample was assigned 100 % active.
Relative activity = [specific activity of sample/specific activity of control sample] × 100.
[3]The LOQ is 6.03 nmol DCSA × min^{-1} × mg^{-1} *E. coli*-produced MON 87419 DMO protein.

Table 20. DMO Functional Activity of *E. coli*-produced MON 87419 DMO Protein after 30 Minutes at Elevated Temperatures

Temperature	Specific Activity (nmol DCSA × min^{-1} × mg^{-1})[1]	Relative Activity (% of control sample)[2]
0 ºC (control)	215.8	100 %
25 ºC	235.9	109 %
37 ºC	248.1	115 %
55 ºC	Below LOQ[3]	<2.8 %
75 ºC	Below LOQ[3]	<2.8 %
95 ºC	Below LOQ[3]	<2.8 %

[1]Mean specific activity determined from n=3.
[2]DMO protein activity of control sample was assigned 100 % active.
Relative activity = [specific activity of sample/specific activity of control sample] × 100.
[3] The LOQ is 6.03 nmol DCSA × min^{-1} × mg^{-1} *E. coli*-produced MON 87419 DMO protein.

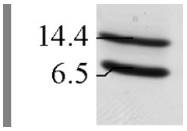

Figure 34. SDS-PAGE of *E. coli*-produced MON 87419 DMO Protein Following Heat Treatment for 15 Minutes

Heat-treated samples of *E. coli*-produced MON 87419 DMO protein (3 µg total protein) were subjected to SDS-PAGE and stained with Brilliant Blue G-Colloidal. Approximate molecular weights (kDa) are shown on the left and correspond to molecular weight markers in lanes 1 and 10. Lane designations are as follows:

Lane	Description	Amount (µg)
1	Broad Range Molecular Weight Markers	4.5
2	*E. coli*-produced MON 87419 DMO Protein 25 ºC	3
3	*E. coli*-produced MON 87419 DMO Protein 37 ºC	3
4	*E. coli*-produced MON 87419 DMO Protein 55 ºC	3
5	*E. coli*-produced MON 87419 DMO Protein 75 ºC	3
6	*E. coli*-produced MON 87419 DMO Protein 95 ºC	3
7	*E. coli*-produced MON 87419 DMO Protein Unheated Control	3
8	*E. coli*-produced MON 87419 DMO Protein Reference 100 % Equivalence	3
9	*E. coli*-produced MON 87419 DMO Protein Reference 10 % Equivalence	0.3
10	Broad Range Molecular Weight Markers	4.5

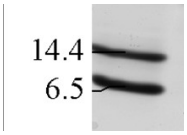

Figure 35. SDS-PAGE of *E. coli*-produced MON 87419 DMO Protein Following Heat Treatment for 30 Minutes

Heat-treated samples of *E. coli*-produced MON 87419 DMO protein (3 µg total protein) were subjected to SDS-PAGE and stained with Brilliant Blue G-Colloidal. Approximate molecular weights (kDa) are shown on the left and correspond to molecular weight markers in lanes 1 and 10. Lane designations are as follows:

Lane	Description	Amount (µg)
1	Broad Range Molecular Weight Markers	4.5
2	*E. coli*-produced MON 87419 DMO Protein 25 ºC	3
3	*E. coli*-produced MON 87419 DMO Protein 37 ºC	3
4	*E. coli*-produced MON 87419 DMO Protein 55 ºC	3
5	*E. coli*-produced MON 87419 DMO Protein 75 ºC	3
6	*E. coli*-produced MON 87419 DMO Protein 95 ºC	3
7	*E. coli*-produced MON 87419 DMO Protein Unheated Control	3
8	*E. coli*-produced MON 87419 DMO Protein Reference 100 % Equivalence	3
9	*E. coli*-produced MON 87419 DMO Protein Reference 10 % Equivalence	0.3
10	Broad Range Molecular Weight Markers	4.5

Heat Susceptibility of the Purified PAT (*pat*) Protein

Temperature can have a profound effect on the structure and function of proteins. Heat treatment is widely used in the preparation of foods derived from maize grain (Hammond and Jez, 2011). It is reasonable that such processing will have an effect on the functional activity and structure of PAT (*pat*) protein when consumed in different food products derived from MON 87419, thus reducing any potential safety concerns posed by the protein. Therefore, an assessment of the effect of heating was conducted as a surrogate for the conditions encountered during the preparation of foods from MON 87419 grain.

The effect of heat treatment on the activity of MON 87419-produced PAT (*pat*) protein was evaluated using the *E. coli*-produced PAT (*pat*) protein. Heat-treated samples and an unheated control sample of *E. coli*-produced PAT (*pat*) protein were analyzed: 1) using a functional assay to assess the impact of temperature on the enzymatic activity of PAT (*pat*) protein; and 2) using SDS-PAGE to assess the impact of temperature on protein integrity.

Aliquots of *E. coli*-produced PAT (*pat*) protein were heated to 25, 37, 55, 75, and 95 °C for either 15 or 30 minutes, while a separate aliquot of *E. coli*-produced PAT (*pat*) protein was maintained on ice for the duration of the heat treatments to serve as a temperature control. The effect of heat treatment on the activity of PAT (*pat*) protein was evaluated using a functional activity assay. The effect of heat treatment on the integrity of the PAT (*pat*) protein was evaluated using SDS-PAGE analysis of the heated and temperature control PAT (*pat*) protein samples.

The effects of heating on the functional activity of *E. coli*-produced PAT (*pat*) are presented in Table 21 and Table 22. The functional activity of PAT (*pat*) protein was unaffected at 25 and 37 ºC for 15 and 30 minutes. The functional activity of the PAT (*pat*) protein was reduced by approximately 90% or greater relative to the activity of control PAT protein whether heated at 55°C and above for 15 or 30 min. These results suggest that temperature has a considerable effect on the functional activity of PAT (*pat*) protein.

Analysis by SDS-PAGE stained with Brilliant Blue G-Colloidal demonstrated that the PAT (*pat*) control treatment and reference standard contain a major band at ~25 kDa, corresponding to the PAT (*pat*) protein (Figure 36 and Figure 37, Lanes 2 and 8). No apparent decrease in the intensity of this band was observed in heat-treated PAT (*pat*) protein at 25, 37, 55, 75 and 95 °C for 15 minutes (Figure 36, Lanes 3-7) or 30 minutes (Figure 37, Lanes 3-7). However, PAT (*pat*) protein heated to 95ºC for 15 and 30 minutes (Figure 36 and Figure 37, Lane 7) showed some appearance of higher molecular weight species, which may be due to slight aggregation of the PAT (*pat*) protein when exposed to high temperatures.

These data demonstrate that PAT (*pat*) protein remains intact, but is deactivated at 55 ºC and above. This is comparable with what has been previously published on the safety assessment of PAT (*pat*) protein (Hérouet *et al.*, 2005). Therefore, it is reasonable to conclude that PAT (*pat*) protein would not be consumed as an active protein in food or feed products due to standard processing practices that include heat treatment.

For details, please refer to [redacted], 2014 (MSL0026345).

Table 21. Functional Activity of PAT (*pat*) Protein after 15 Minutes at Elevated Temperatures

Temperature	Specific Activity ($\mu mol \times minute^{-1} \times mg^{-1}$) [1]	Relative Activity (% of control sample) [2,3]
0 ºC (control)	24.5	100 %
25 ºC	26.7	109 %
37 ºC	26.9	110 %
55 ºC	2.8	11 %
75 ºC	0.9	4 %
95 ºC	1.1	4 %

[1] Mean specific activity determined from n=3.
[2] PAT (*pat*) protein activity of control samples was assigned 100 % active.
[3] Relative Activity = [specific activity of sample/specific activity of control sample] × 100

Table 22. Functional Activity of PAT (*pat*) Protein after 30 Minutes at Elevated Temperatures

Temperature	Specific Activity ($\mu mol \times minute^{-1} \times mg^{-1}$) [1]	Relative Activity (% of control sample) [2,3]
0 ºC (control)	24.5	100 %
25 ºC	31.2	127 %
37 ºC	29.8	122 %
55 ºC	1.0	4 %
75 ºC	1.1	4 %
95 ºC	1.3	5 %

[1] Mean specific activity determined from n=3.
[2] PAT (*pat*) protein activity of control sample was assigned 100 % active.
[3] Relative Activity = [specific activity of sample/specific activity of control sample] × 100

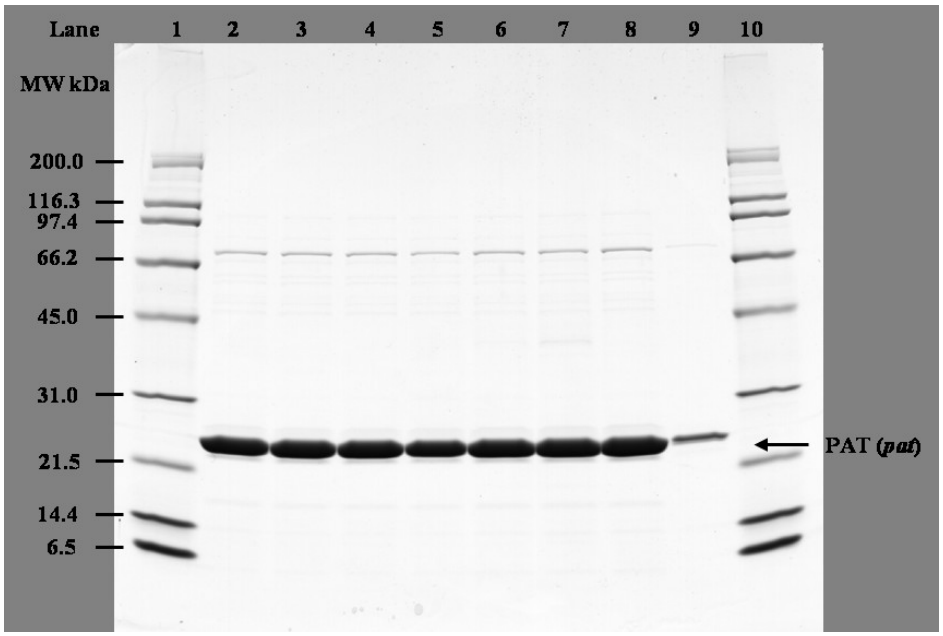

Figure 36. SDS-PAGE of *E. coli*-Produced PAT (*pat*) Protein Following Heat Treatment for 15 Minutes

Heat treated samples of *E. coli*-produced PAT (*pat*) (3.0 µg total protein) separated on a Tris-glycine 4-20 % polyacrylamide gel under denaturing and reducing conditions. The gel was stained with Brilliant Blue G-Colloidal. Approximate molecular weights (kDa) are shown on the left and correspond to molecular weight markers in lanes 1 and 10.

Lane	Description	Amount of Total Protein (µg)
1	Broad Range Molecular Weight Markers	4.5
2	*E. coli*-produced PAT (*pat*) Protein Control	3.0
3	*E. coli*-produced PAT (*pat*) Protein 25 ºC	3.0
4	*E. coli*-produced PAT (*pat*) Protein 37 ºC	3.0
5	*E. coli*-produced PAT (*pat*) Protein 55 ºC	3.0
6	*E. coli*-produced PAT (*pat*) Protein 75 ºC	3.0
7	*E. coli*-produced PAT (*pat*) Protein 95 ºC	3.0
8	*E. coli*-produced PAT (*pat*) Protein Reference 100 % Equivalence	3.0
9	*E. coli*-produced PAT (*pat*) Protein Reference 10 % Equivalence	0.3
10	Broad Range Molecular Weight Markers	4.5

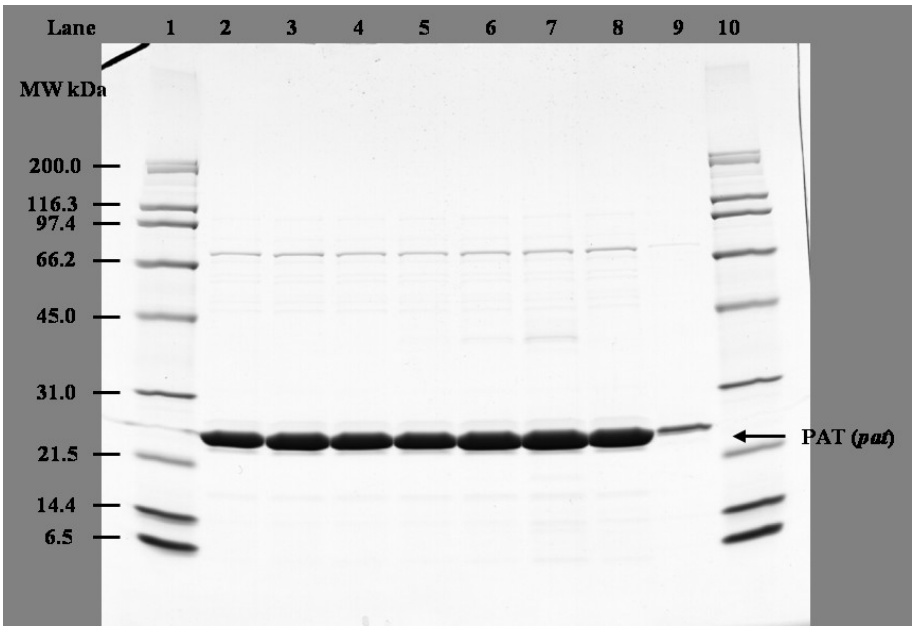

Figure 37. SDS-PAGE of *E. coli*-Produced PAT (*pat*) Protein Following Heat Treatment for 30 Minutes

Heat treated samples of *E. coli*-produced PAT (*pat*) (3.0 µg total protein) separated on a Tris-glycine 4-20 % polyacrylamide gel under denaturing and reducing conditions. The gel was stained with Brilliant Blue G-Colloidal. Approximate molecular weights (kDa) are shown on the left and correspond to molecular weight markers in lanes 1 and 10.

Lane	Description	Amount of Total Protein (µg)
1	Broad Range Molecular Weight Markers	4.5
2	*E. coli*-produced PAT *(pat)* Protein Control	3.0
3	*E. coli*-produced PAT *(pat)* Protein 25 ºC	3.0
4	*E. coli*-produced PAT *(pat)* Protein 37 ºC	3.0
5	*E. coli*-produced PAT *(pat)* Protein 55 ºC	3.0
6	*E. coli*-produced PAT *(pat)* Protein 75 ºC	3.0
7	*E. coli*-produced PAT *(pat)* Protein 95 ºC	3.0
8	*E. coli*-produced PAT *(pat)* Protein Reference 100 % Equivalence	3.0
9	*E. coli*-produced PAT *(pat)* Protein Reference 10 % Equivalence	0.3
10	Broad Range Molecular Weight Markers	4.5

B4(c) Acute oral toxicity study with the DMO and PAT(*pat*) proteins

Acute Oral Toxicity Study with the MON 87419 DMO and PAT (*pat*) Proteins

Acute toxicology studies with DMO and PAT proteins were conducted previously to support applications for other biotech-derived events such as MON 88701, which has been reviewed and has completed a consultation with the FSANZ (A1035). The results of these studies indicate that neither DMO nor PAT caused any adverse effects in mice, with No Observable Adverse Effect Levels (NOAELs) for DMO of 283 mg/kg and for PAT of 1086 mg/kg, the highest doses tested. These acute toxicity study results are applicable to the DMO and PAT proteins expressed in MON 87419 because the DMO and PAT proteins expressed in MON 87419 are identical in structure of the catalytic site, mode of action, and specificity to DMO and PAT proteins expressed in MON 88701 previously assessed with a high degree of amino acid homology.

For details, please refer to [redacted], 2012 (CRO-2011-035) and [redacted], 2012 (CRO-2011-007).

B5 Assessment of Potential Allergenicity

History of safe use of the introduced protein is a key consideration in assessing the potential for allergenicity and toxicity and overall assessment of dietary safety. The history of safe use of MON 87419 DMO and PAT (pat) proteins have been previously addressed in Section B3(f).

Additionally, following the guidelines adopted by the Codex Alimentarius Commission, an assessment of potential allergenicity of introduced proteins has been conducted by comparing the characteristics of the introduced protein to characteristics of known allergens (Codex Alimentarius, 2009). A protein is not likely to be associated with allergenicity if: 1) the protein is from a nonallergenic source, 2) the protein represents only a very small portion of the total plant protein, 3) the protein does not share structural similarities to known allergens based on the amino acid sequence, 4) the protein is rapidly degraded in mammalian gastrointestinal systems, and 5) the protein is not stable to heat treatment. The MON 87419 DMO and PAT (*pat*) proteins in MON 87419 have been assessed for their potential allergenicity according to these safety assessment guidelines.

Taken together, these data support the conclusion that MON 87419 DMO and PAT (*pat*) protein does not pose a significant allergenic risk to humans or animals.

The safety of PAT protein present in biotechnology-derived crops has been extensively assessed (ILSI-CERA, 2011) and in 1997 a tolerance exemption was issued for PAT proteins, including PAT (*pat*) and PAT (*bar*) proteins, by U.S. EPA (1997). Numerous glufosinate-tolerant products including those in cotton, corn, soy, canola, sugar beet, and rice have been reviewed by the FDA (U.S. FDA, 1995a; 1995b; 1996; 1997; 1998b; 1998a; 2000; 2003) with no concerns identified. Further, a comprehensive study on the safety of PAT proteins present in biotechnology-derived crops demonstrated the safety of the donor organism, lack of sequence homology to know allergens, rapid degradation by pepsin and pancreatin and loss of functional activity following heat treatment (Hérouet *et al.*, 2005). Hérouet et al. concluded that there is a reasonable certainty of no harm resulting from the consumption of PAT proteins in human food or animal feed. The data below were generated to confirm the previously documented safety assessments.

B5(a) Source of introduced protein

B5(a)(i) DMO protein

As described in Section A2, the *dmo* gene is derived from the bacterium *S. maltophilia* strain DI-6 (Herman *et al.*, 2005; Palleroni and Bradbury, 1993). *S. maltophilia* is ubiquitous in the environment and is found associated with the rhizosphere of plants (Berg *et al.*, 1999; Echemendia, 2010; Ryan *et al.*, 2009). *S. maltophilia* can be found in a variety of foods and feeds (Echemendia, 2010; Qureshi *et al.*, 2005), and is widespread in the home environment (Denton and Kerr, 1998; Denton *et al.*, 1998). Exposure to *S. maltophilia* is incidental to its presence in food. It has been isolated from "ready to eat" salads, vegetables, frozen fish, milk, and poultry (Qureshi *et al.*, 2005; Ryan *et al.*, 2009). *S. maltophilia* can be found in healthy individuals without causing any harm to human health (Denton and Kerr, 1998) and

infections caused by *S. maltophilia* are extremely uncommon (Cunha, 2009). Strains have been found in the transient flora of hospitalized patients as a commensal organism (Echemendia, 2010) and, similar to the indigenous bacteria of the gastrointestinal tract, *S. maltophilia* can be an opportunistic pathogen (Berg, 1996). As such, *S. maltophilia* is of low virulence in immuno-compromised patients where a series of risk factors (severe debilitation, the presence of indwelling devices such as ventilator tubes or catheters, for prolonged periods of time and prolonged courses of antibiotics) must occur for colonization by *S. maltophilia* in humans (Ryan *et al.*, 2009). Therefore, infections by *S. maltophilia* almost exclusively occur in hospital settings, in which case they are only present in a minimal percentage of infections (Ryan *et al.*, 2009). Finally, *S. maltophilia* has not been reported to be a source of allergens.

The ubiquitous presence of *S. maltophilia* in the environment, the presence in healthy individuals without causing infections, the incidental presence in foods without any adverse safety reports, and the lack of reported allergenicity establish the safety of the donor organism.

B5(a)(ii) PAT (*pat*) protein

As described in Section A2, the *pat* gene is derived from the bacterium *S. viridochromogenes* (Thompson *et al.*, 1987). The ubiquitous presence of *S. viridochromogenes* in the environment, the widespread human exposure without any adverse safety or allergenicity reports, and the successive reviews of several glufosinate-tolerant events by regulatory agencies have identified no safety or allergenicity issues further establish the safety of the donor organism.

B5(b) Bioinformatic comparison (aa) of novel protein(s) to allergens

Structural Similarity of MON 87419 DMO and PAT (*pat*) to Known Allergens

The Codex guidelines for the evaluation of the allergenicity potential of introduced proteins (Codex Alimentarius, 2009) are based on the comparison of amino acid sequences between introduced proteins and allergens, where allergenic cross-reactivity may exist if the introduced protein is found to have at least 35% amino acid identity with an allergen over any segment of at least 80 amino acids. The Codex guideline also recommends that a sliding window search with a scientifically justified peptide size could be used to identify immunologically relevant peptides in otherwise unrelated proteins. Therefore, the extent of sequence similarities between the MON 87419 modified DMO protein with the addition of 12 amino acids from CTP4 and the PAT (*pat*) protein sequences and known allergens, gliadins, and glutenins were assessed using the FASTA sequence alignment tool and an eight-amino acid sliding window search (Codex Alimentarius, 2009; Thomas *et al.*, 2005). The full length MON 87419 DMO was chosen as the query sequence. The data generated from these analyses confirm that the MON 87419 DMO and PAT (*pat*) proteins do not share amino acid sequence similarities with known allergens, gliadins, or glutenins.

The FASTA program directly compares amino acid sequences (*i.e.*, primary, linear protein structure). This alignment data may be used to infer shared higher order structural similarities between two sequences (*i.e.*, secondary and tertiary protein structures). Proteins that share a high degree of similarity throughout the entire sequence are often homologous. By definition, homologous proteins have common secondary structures, and three-dimensional configuration, and, consequently, may share similar functions (Pearson, 2000). The allergen, gliadin, and glutenin sequence database (AD_2014) was obtained from Food Allergy Research and Resource (FARRP, 2014) Program Database and was used for the evaluation of sequence similarities shared between the MON 87419 DMO and PAT (*pat*) proteins with all proteins in AD_2014. The AD_2014 database contains 1,706 sequences. When used to align the sequence of the introduced protein to each protein in the database, the FASTA algorithm produces an *E*-score (expectation score) for each alignment. The *E*-score is a statistical measure of the likelihood that the observed similarity score could have occurred by chance in a search. A larger *E*-score indicates a low degree of similarity between the query sequence and the sequence from the database. Typically, alignments between two sequences which have an *E*-score of less than or equal to 1×10^{-5} are considered to have meaningful homology. Results indicate that the MON 87419 DMO and PAT (*pat*) protein sequences do not share meaningful similarity with sequences in the allergen database. No alignment met nor exceeded the threshold of 35% identity over 80 amino acids recommended by Codex Alimentarius (2009) or had an *E*-score of less than or equal to 1×10^{-5}.

A second bioinformatic tool, an eight-amino acid sliding window search, was used to specifically identify short linear polypeptide matches to known allergens. It is possible that proteins structurally unrelated to allergens, gliadins, and glutenins may contain smaller immunologically meaningful epitopes. An amino acid sequence may have allergenic potential if it has an exact sequence identity of at least eight linearly contiguous amino acids with a potential allergen epitope (Hileman *et al.*, 2002; Metcalfe *et al.*, 1996). Using a sliding window of less than eight amino acids can produce matches containing considerable uncertainty depending on the length of the query sequence (Silvanovich *et al.*, 2006) and are not useful to the allergy assessment process (Thomas *et al.*, 2005). No eight contiguous amino acid identities were detected when the MON 87419 DMO and PAT (*pat*) protein sequences were compared to the proteins in the AD_2014 sequence database.

The bioinformatic results demonstrated there were no biologically relevant sequence similarities to allergens when the MON 87419 DMO and PAT (*pat*) protein sequences were used as a query for a FASTA search of the AD_2014 database. Furthermore, no short (eight amino acid) polypeptide matches were shared between the MON 87419 DMO and PAT (*pat*) protein sequences and proteins in the allergen database. These data show that the MON 87419 DMO and PAT (*pat*) protein sequences lacks both structurally and immunologically relevant similarities to known allergens, gliadins, and glutenins.

For details, please refer to [redacted], 2014 (MSL0025907).

B5(c) Structural properties, including digestion by pepsin, heat treatment

The susceptibility of a protein to heat or its degradation in the presence of pepsin and pancreatin is a factor in the assessment of its potential allergenicity. The degradation of MON 87419 DMO and PAT (*pat*) proteins were evaluated by incubation with solutions containing pepsin and pancreatin, and the results show that both MON 87419 DMO and PAT (*pat*) proteins were readily degraded (Section B4(b), respectively). Exposure to heat during food processing or cooking, and to digestive fluids is likely to have a profound effect on the structure and function of proteins. The effect of heat treatment on the activity of MON 87419 DMO and PAT (*pat*) proteins was evaluated using functional assays to assess the impact of temperature on enzymatic activity, and using SDS-PAGE to assess the impact of temperature on protein integrity. The results show that MON 87419 DMO protein was completely deactivated by heating at 55 ºC or higher for 15 min or more (Section B4(b)) and PAT (*pat*) protein was substantially deactivated by heating at 75 ºC or above for 15 minutes and at 55°C or above for 30 minutes (Section B4(b)). Therefore, it is anticipated that exposure to functionally active MON 87419 DMO or PAT (*pat*) protein from the consumption of MON 87419 or foods derived from MON 87419 is unlikely.

B5(d) Specific serum screening if protein from allergenic source

Not applicable.

B5(e) Protein as a proportion of total protein

The MON 87419 DMO Protein as a Proportion of Total Protein

The MON 87419 DMO protein was detected in all plant tissue types assayed (Table 16). Harvested grain is the most relevant tissue analyzed for an allergenicity assessment because foods derived from maize grain can be consumed directly. The mean level of MON 87419 DMO protein in grain of MON 87419 is 0.19 µg/g dw. The mean percent dry weight of total protein in grain of MON 87419 is 11.52% (or 115200 µg/g). The percentage of MON 87419 DMO protein in MON 87419 grain is calculated as follows:

(0.19 µg/g ÷ 115200 µg/g) × 100% ≈ 0.00016% or 1.6 ppm of total grain protein

Therefore, the MON 87419 DMO protein represents a very small portion of the total protein in the grain of MON 87419. This low percent of MON 87419 DMO in relation to the total protein reduces the potential risk of allergenicity from this protein.

The MON 87419-produced PAT (*pat*) as a Proportion of Total Protein

The PAT (*pat*) protein was detected in all plant tissue types assayed, at a number of time points during the growing season (Table 17). Harvested grain is the most relevant tissue analyzed for an allergenicity assessment because foods derived from maize grain can be consumed directly. The mean level of PAT (*pat*) protein in grain of MON 87419 is 0.93 µg/g dw. The mean percent dry weight of total protein in grain of MON 87419 is 11.52% (or 115200 µg/g). The percentage of PAT (*pat*) protein in MON 87419 grain is calculated as follows:

(0.93 µg/g ÷ 115200 µg/g) × 100% ≈ 0.0008% or 8 ppm of total grain protein

Therefore, the PAT (*pat*) protein represents a very small portion of the total protein in the grain of MON 87419. This low percent of PAT (*pat*) in relation to the total protein reduces the potential risk of allergenicity from this protein.

B6 Toxicity of Novel Herbicide Metabolites in GM Herbicide-Tolerant Plants

MON 87419 contains a demethylase gene from *S. maltophilia* that expresses a dicamba mono-oxygenase (DMO) protein to confer tolerance to dicamba herbicide and the phosphinothricin N-acetyltransferase (*pat*) gene from *Streptomyces viridochromogenes* that expresses the PAT protein to confer tolerance to glufosinate herbicide. DMO is an enzyme that catalyzes the demethylation of dicamba to the non-herbicidal compound 3,6-dichlorosalicylic acid (DCSA) and formaldehyde (Chakraborty *et al.*, 2005). PAT protein acetylates the free amino group of glufosinate to produce non-herbicidal N-acetyl glufosinate, a well known metabolite in glufosinate tolerant plants (2002a).

DCSA is a known soybean, soil and livestock metabolite whose safety has been evaluated by the US EPA (U.S. EPA, 2009a). DCSA is also the primary degradate in soil from dicamba aerobic soil metabolism and is therefore not new to the environment; it is not persistent in the environment and has low potential for leaching to ground water (EFSA, 2007a). DCSA has been evaluated for its toxicity to organisms in the environment. Based on studies using Rainbow trout (*Oncorhynchus mykiss*), *Daphnia*, green algae (*Selenastrum caprinornutum*), *Lemna* and earthworm (*Eisenia fetida*), it was concluded that "the metabolite 3,6-dichlorosalicylic acid (DCSA) was not found to give rise to unacceptable risks" (EFSA, 2007b).

Formaldehyde is a metabolite when dicamba is sprayed on MON 87419 maize. However, formaldehyde is not considered a relevant metabolite in the demethylation of dicamba by U.S. EPA. According to the guidelines published by Office of Prevention, Pesticides and Toxic Substances, United States Environmental Protection Agency (U.S. EPA, 1996), the methoxy side chain that is cleaved from dicamba to form formaldehyde would specifically not be chosen to be labeled in a metabolism study (U.S. EPA, 1996). This is because it is not metabolically stable and would not be considered a significant moiety as it would be readily metabolized and incorporated into the 1-carbon pool of the plant through known pathways. Therefore, formaldehyde was not measured in the residue study when dicamba was applied to MON 87419.

Plants have a large capacity to metabolize formaldehyde naturally produced from internal processes (Hanson and Roje, 2001), and any additional amount of formaldehyde that could be theoretically produced in the plant by dicamba treatment in MON 87419 would be metabolized very quickly. Thus the incremental increase in formaldehyde over and above the levels already presumed to be present in the maize plant would be small and transient and associated with an outdoor application of dicamba herbicide. Further, since current literature supports that formaldehyde is only emitted from foliage under certain conditions (Cojocariu *et al.*, 2005; Cojocariu *et al.*, 2004; Nemecek-Marshall *et al.*, 1995) and that emission rates are low (Nemecek-Marshall *et al.*, 1995), little opportunity exists for formaldehyde to be released from MON 87419 after dicamba treatment. Therefore human safety concerns of formaldehyde released from dicamba-treated MON 87419 are considered to be negligible and the most relevant route of exposure is from repeated inhalation of concentrated levels associated with indoor or occupational environments. USHHS-NTP has already stated that

there is no evidence to suggest that dietary intake of formaldehyde is important, despite NTP's 12th Report on Carcinogens reclassifying formaldehyde as a known human carcinogen (USHHS-NTP, 2011). Therefore, the potential for human exposure to any formaldehyde in dicamba-treated MON 87419 maize is highly unlikely.

Formaldehyde is ubiquitous in the environment; plants and animals are constantly exposed to low levels already present in the environment and the atmosphere from a variety of biogenic (e.g., plant and animal) and anthropogenic (e.g., automotive or industrial emissions) sources. In water, formaldehyde dissipates through biodegradation to low levels in a few days (USHHS-ATSDR, 1999). Aerobic biodegradation half-lives are estimated to be 1-7 days for surface water and 2-14 days for ground water (U.S. EPA, 2008). The half-life of formaldehyde in air is dependent on a number of factors (light intensity, temperature, and location). Through reaction with hydroxyl radical, the half-life of formaldehyde in air varies from 7 to 70 hours (U.S. EPA, 2008) . The photolytic half-life of formaldehyde in air (e.g., in the presence of sunlight) is estimated to be 1.6-6 hours (U.S. EPA, 2008; USHHS-ATSDR, 1999). Formaldehyde is rapidly consumed in the atmosphere through direct photolysis or by oxidation with hydroxyl or nitrate radicals (USHHS-ATSDR, 1999).

Humans are constantly exposed to low levels of formaldehyde. Human exposure to formaldehyde is primarily due to indoor air exposures (USHHS-ATSDR, 1999). Formaldehyde is found in a variety of consumer products such as cosmetics and paints, often as an antimicrobial agent, and is used extensively in urea-formaldehyde "slow-release" fertilizer formulations and adhesives (USHHS-ATSDR, 1999). Indoor formaldehyde air concentrations are generally significantly higher than outdoor air concentrations (USHHS-ATSDR, 1999) as a result of combustion (cooking, heating, tobacco use) and the emission of formaldehyde from a variety of construction materials (e.g., particle board, plywood or foam insulation) as well as permanent press fabrics (e.g., clothing or draperies) (U.S. CPSC, 1997). Formaldehyde present in outdoor air results from a number of sources, and levels of formaldehyde are generally higher in urban areas than in rural areas (USHHS-ATSDR, 1999). Direct contributions of formaldehyde to the atmosphere (i.e., those in the form of formaldehyde itself) from man-made sources are present, but are generally considered to be small relative to natural sources or indirect production of formaldehyde in the atmosphere (WHO, 2002).

Dicamba Metabolism Study

Dicamba, 3,6-dichloro-2-methoxybenzoic acid, is a foliar or soil-applied herbicide in the auxin family and is utilized for the control of many broadleaf weeds in a number of crops including corn, sorghum, small grains, grasses and asparagus.

This summary below describes a metabolism study conducted with [^{14}C]dicamba in dicamba-glufosinate tolerant corn. The study was conducted to support the registration of dicamba for use in dicamba-glufosinate tolerant corn in the United States and other world areas including in Australia in accordance with the requirements of EPA residue chemistry test guideline US EPA OCSPP 860.1300, "Nature of the Residue – Plants, Livestock" and OECD Guideline for the Testing of Chemicals No. 501, "Metabolism in Crops". All phases of the study were

conducted under the U.S. EPA FIFRA Good Laboratory Practice Standards. The purpose of this study was to determine the nature of residues found in/on agricultural commodities of dicamba-glufosinate tolerant corn following preemergence or postemergence treatments with [^{14}C]dicamba.

Metabolism of dicamba in dicamba-glufosinate tolerant corn resulted in a variety of metabolites. The major metabolite identified in corn foliage (thinnings, forage and stover) from the pre- or postemergence treatments (PRE-T or POE-T) was DCSA glucoside constituting 26.94-53.17% of total radioactive residues (TRR). Enzymatic hydrolysis of the major metabolite (DCSA glucoside) indicated that the identified glucosylated metabolites were β-linked D-glucose conjugates. DCSA glucoside was very low in grain (<0.001 mg/kg), where the extractable residue consisted of multiple low-level polar metabolites such as sugars and amino acids that eluted near the column void volume under reverse phase HPLC. Unchanged dicamba ranged from 6.27 to 8.64% of TRR in POE-T forage and stover but was barely present in PRE-T foliage with the exception of PRE-T thinnings (3.42% of TRR). Other minor metabolites identified were DCSA, DCGA glucoside, DCGA pentosylglucoside, 5-hydroxydicamba glucoside, MCTHBA glucoside, DCSA pentoside, MCTHBA cyclic glucoside, DCSA HMGglucoside, DCSA succinylglucoside and 5-hydroxydicamba. Radioactive residues in the hexane extracts of grain were characterized as a mixture of naturally-occurring triglycerides (fatty acids and glycerol) amounting to 4.64 and 5.31% of TRR (0.002 and 0.003 mg/kg) in PRE-T and POE-T respectively.

Metabolism of dicamba in dicamba-glufosinate tolerant corn was similar to the metabolism of dicamba in previously reported metabolism studies of dicamba in dicamba-tolerant crops including soybean and cotton. DCSA is observed as the major aerobic soil metabolite of dicamba, and DCGA is also observed in soil as a minor metabolite. The major metabolic pathway proceeds *via* initial *O*-demethylation of dicamba to DCSA. DCSA is then mainly conjugated to glucose to form DCSA glucoside. As minor pathways, DCSA is conjugated to a pentose to form DCSA pentoside or hydroxylated at the 5-position of the ring to form DCGA which is further glucosylated to form DCGA glucoside. The resultant glucosides are further converted by conjugation or degradation to other low-level metabolites such as DCSA succinylglucoside. In a minor pathway, dicamba is directly hydroxylated to form 5-hydroxydicamba, which is conjugated to glucose to form 5-hydroxydicamba glucoside. Therefore, it was concluded that that the metabolism of dicamba in dicamba-tolerant corn (MON 87419) resulting in DCSA, DCGA, 5-hydroxydicamba and unchanged dicamba is similar to the metabolism of dicamba in soil and other plant species. For details please also refer to [redacted], 2015 (MSL0025703).

Acid hydrolysis was conducted in treated corn matrices to confirm that the primary dicamba-related metabolites identified in this study are converted to the chemophores DCSA, DCGA, 5-hydroxydicamba and unchanged dicamba. It was confirmed that the current residue methodology for dicamba, which incorporates an acid hydrolysis step followed by analysis using LC-MS/MS, would be expected to be adequate for analysis of dicamba residues in

dicamba-glufosinate tolerant corn raw agricultural commodities. For details please also refer to [redacted] 2014 (MSL0026344).

Following the identification of the dicamba metabolites in the metabolism study, a residue study was conducted to determine the levels of residues of dicamba and its principal metabolites in corn grain after application of dicamba formulations to MON 87419. The study utilized a validated analytical method that quantified dicamba, DCSA, DCGA and 5-hydroxydicamba. A petition will be submitted to the U.S. EPA to include DCSA into the current EPA Definition of the Residue (DoR) for dicamba in corn (dicamba and 5-hydroxydicamba) to comprise the majority of the residues in dicamba-tolerant seed following pre- or postemergence treatment of dicamba-tolerant corn with dicamba.

In Australia, dicamba has been registered for use on cereal crops as well as sugar cane by the Australian Pesticides and Veterinary Medicines Authority (APVMA) with maximum residue limits (MRLs) established for cereal grains (0.05 ppm) and sugar cane (0.1 ppm) crop commodities. Dicamba is not registered for use in or on corn in Australia and dicamba MRLs do not exist for corn commodities coming into Australia. The MRL for dicamba in corn in the United States is set at 0.1 ppm and in Japan is set at 0.5 ppm. A petition to establish new tolerances for dicamba in corn will be submitted to Codex to amend the current MRL of 0.01 ppm consisting of dicamba and 5-hydroxydicamba to request an increase to match the EPA MRL and add DCSA to DoR. Consequently, a request will be submitted concurrently with this application to establish an import MRL to cover residues of dicamba on corn into Australia at 0.1 ppm.

In Australia, both the import MRL set by FSANZ and the MRL set by the APVMA for glufosinate in corn is set at 0.2 ppm. The use pattern and rate of glufosinate on MON 87419 will follow the existing glufosinate-tolerant corn uses outlined on the glufosinate herbicide label and the glufosinate residues in MON 87419 treated with commercial glufosinate rates are below the established pesticide residue tolerances for corn. Monsanto will not pursue any changes in the established tolerances for its use on MON 87419 corn, additional data on the identity and levels of herbicide and any metabolites are not given in this application.

Magnitude of Dicamba Residues and Metabolites in MON 87419 Corn after Dicamba Application

A residue study of dicamba applied to MON 87419 maize was conducted at 22 locations in the U.S. in 2013, with a geographic distribution in compliance with US EPA residue chemistry test guidelines. The study was conducted in Pennsylvania (Region 1 – 1 trial), Georgia (Region 2 – 1 trial), North Carolina (Region 2 – 1 trial), Michigan (Region 5 – 1 trial), Kansas (Region 5 – 2 trials), Iowa (Region 5 – 1 trial), Illinois (Region 5 – 6 trials), Indiana (Region 5 – 1 trial), Missouri (Region 5 – 2 trials), Nebraska (Region 5 – 3 trials), South Dakota (Region 5 – 1 trial), Wisconsin (Region 5 – 1 trial), and Texas (Region 6 – 1 trial). The sites were typical of the major maize producing regions of the U.S.

Use of MON 87419 maize in this study was required to generate data that can be used to support regulatory approval of MON 87419 maize.

Control and treated plots were established at each site. The treated plots were 1000 to 5250 square feet in size (planted area). The minimum distance between the control plot and any treated plot was 100 feet. The minimum distance between the treated plots was 50 feet.

There were four separate treatment regimes. All sites contained Treatment 1 (an untreated control plot), and Treatments 2-3, which were treated with a dicamba-based formulation (MON 54140). Three sites also contained an extra plot (Treatment 4) treated with MON 54140 with exaggerated application rates for processing. The target application timings and rates with each treatment are summarized in table below.

Table 23. Target Applications of Dicamba Formulations to MON 87419 Dicamba Tolerant Corn

Trt.	No. of Sites		Growth Stages/Application Rates			
		Preemergence	V2-V4	V4-V6	V8 (~36")	48" (drop)
1	22	—	—	—	—	—
2	22	1.0 lb. a.e./A (1.1 kg a.e./ha)	—	0.5 lb. a.e./A (0.56 kg a.e/ha)	0.5 lb. a.e./A (0.56 kg a.e./ha)	—
3	22	—	0.5 lb. a.e./A (0.56 kg a.e./ha)	0.5 lb. a.e./A (0.56 kg a.e./ha)	0.5 lb. a.e./A (0.56 kg a.e./ha)	0.5 lb. a.e./A (0.56 kg a.e./ha)
4	3	5.0 lb. a.e./A (5.6 kg a.e./ha)	—	2.5 lb. a.e./A (2.8 kg a.e./ha)	2.5 lb. a.e./A (2.8 kg a.e./ha)	—

MON 54140 contains a nominal concentration of 4 lb dicamba acid equivalents per gallon or 480 grams per liter.

Treatment 2 covered the expected range of applications allowed under the proposed label, including a preemergence application of up to 1.0 lb/acre (1.12 kg/ha) and multiple early to late postemergent applications of up to 0.5 lb/acre (0.56 kg/ha) each, with an annual total of up to 2.0 lb/acre (2.24 kg/ha). Actual application rates were within ± 5% of the target rates for all applications at all sites. Spray volumes ranged from 19.0 to 23.6 gallons per acre (GPA) and were within ± 5% of the target spray volumes for all applications at all sites, except one application at the 06KS site where the target GPA was exceeded by 16%. A non-ionic surfactant at a rate of 0.125% v/v (± 5%) was added to the spray mixture for all applications at all sites. At 11 of the 22 sites MON 51806 was also added to the spray solution as a water conditioner at a rate of 2% v/v.

The metabolism study of dicamba in MON 87419 maize above ([redacted], 2015; MSL0025703) demonstrated that dicamba was metabolized mainly to a glucose conjugate of 3,6-dichloro-2-hydroxybenzoic acid (DCSA), with smaller amounts of conjugates of 2,5-dichloro-3,6-dihydroxybenzoic acid (DCGA) and 2,5-dichloro-3-hydroxy-6-methoxybenzoic acid (5-hydroxydicamba). Dicamba was present at very low levels.

Conjugates of the metabolites are very complex molecules which are not readily synthesized to produce analytical reference standards. Because of the difficulty in synthesizing and quantifying the conjugates, an analytical method ([redacted]., 2015; MSL0026344) was developed in which the conjugates are converted by acid hydrolysis to the chemophores DCSA, DCGA and 5-hydroxydicamba in addition to dicamba for residue analysis.

The dicamba analytical method involves the extraction of homogenized raw agricultural commodities with 40% acetonitrile in water containing stable label internal standards. An aliquot of the extract solution is hydrolyzed with 1N hydrochloric acid. After hydrolysis, the hydrolysate is partitioned with 20:80 ethyl acetate:isooctane, dried and re-constituted in a

3:1 water:methanol solution containing 5% phosphoric acid. Analytes are quantitated using LC-MS/MS with electrospray ionization in negative ion mode. The limit of quantitation (LOQ) for dicamba, 5-OH dicamba, DCSA and DCGA (expressed as dicamba equivalents) was determined to be 0.010 ppm (mg/kg).

MON 87419 mature grain samples were analyzed for residues of dicamba and 5-hydroxydicamba, the two analytes that constitute the U.S. EPA Definition of the Residue per 40 CFR §180.227. The method also quantified the residues of DCSA, which will be included in the residue definition to be proposed to the EPA for MON 87419. DCGA was also quantified, but those residues are not part of the U.S. residue definition, and are not included in the total residues reported in this summary. Total residues are expressed as dicamba acid equivalents. None of the residues are corrected for background or recovery. The residue levels in samples collected from Treatment 2 and Treatment 3 were very similar.

Table 24. Summary of Dicamba Residues in MON 87419 Grain

Analyte	Treatment 2			Treatment 3		
	Mean (ppm)	Median[a] (ppm)	Range[b] (ppm)	Mean (ppm)	Median[a] (ppm)	Range[b] (ppm)
Dicamba	<0.0100	<0.0100	<0.0100	<0.0100	<0.0100	<0.0100
5-Hydroxydicamba	<0.0100	<0.0100	<0.0100	<0.0100	<0.0100	<0.0100
DCSA	<0.0111	<0.0100	<0.0100-0.0394	<0.0109	<0.0100	<0.0100-0.0332
DCGA	<0.0105	<0.0100	<0.0100-0.0213	<0.0108	<0.0100	<0.0100-0.0229
Total[c,d]	<0.0311	<0.0100	<0.0300-0.0594	<0.0309	<0.0100	<0.0300-0.0532

[a]Median of residues across all sites in this treatment
[b]Range of residues across all sites in this treatment
[c]Individual analyte residues are expressed as dicamba acid equivalents
[d]Total residues (ppm) = [Dicamba] + [5-hydroxydicamba] + [DCSA] per current U.S. EPA Definition of the Residue in maize grain per 40 CFR §180.227

The residue study indicates that the existing EPA dicamba MRL of 0.1 ppm in maize grain is sufficient to account for the proposed new use of dicamba on MON 87419 tolerant maize with the addition of DCSA to the DoR. Consequently, this application request to establish import MRL of 0.1 ppm to cover residues of dicamba on corn grains into Australia.

For details, please also refer to [redacted], 2015 (MSL0026819).

B7 Compositional Assessment

Safety assessments of biotechnology-derived crops follow the comparative safety assessment process (Codex Alimentarius, 2009) in which the composition of grain and/or other raw agricultural commodities of the biotechnology-derived crop are compared to the appropriate conventional control that has a history of safe use. For maize, assessments are performed using the principles and analytes outlined in the OECD consensus document for maize composition (OECD, 2002c).

A recent review of compositional assessments conducted according to OECD guidelines, encompassing seven biotechnology-derived crop varieties, nine countries and eleven growing seasons, concluded that incorporation of biotechnology-derived agronomic traits has had little impact on natural variation in crop composition. Most compositional variation is attributable to growing region, agronomic practices, and genetic background (Harrigan *et al.*, 2010). Numerous scientific publications have further documented the extensive variability in the concentrations of crop nutrients, anti-nutrients, and secondary metabolites that reflect the influence of environmental and genetic factors as well as extensive conventional breeding efforts to improve nutrition, agronomics, and yield (Harrigan *et al.*, 2010; Harrigan *et al.*, 2009; Ridley *et al.*, 2011; Zhou *et al.*, 2011).

Compositional equivalence between biotechnology-derived and conventional crops supports an "equal or increased assurance of the safety of foods derived from genetically modified plants" (OECD, 2002b). OECD consensus documents on compositional considerations for new crop varieties emphasize quantitative measurements of essential nutrients and known anti-nutrients. These quantitative measurements effectively discern any compositional changes that imply potential nutritional or safety (*e.g.,* anti-nutritional) concerns. Levels of the components in grain and/or other raw agricultural commodities of the biotechnology-derived crop product are compared to: 1) corresponding levels in a conventional control, i.e. a genetically similar conventional line, grown concurrently under similar field conditions, and 2) natural ranges from data published in the scientific literature or documented in the International Life Sciences Institute Crop Composition Database (ILSI-CCDB). The comparison to data published in the literature and the ILSI-CCDB places any potential differences between the assessed new crop variety and its conventional control in the context of the well-documented variation in the concentrations of crop nutrients, anti-nutrients, and secondary metabolites.

This section provides analyses of concentrations of key nutrients, anti-nutrients, and secondary metabolites of MON 87419 compared to that of a conventional control grown and harvested under similar conditions. The production of data for compositional analyses used a sufficient variety of field trial sites, a robust field design, and sensitive analytical methods to allow accurate assessments of compositional characteristics over a range of environmental conditions under which MON 87419 is expected to be grown.

The information provided in this section also addresses the relevant factors in Codex Plant Guidelines, Section 4, paragraphs 44 and 45 for compositional analyses (Codex Alimentarius, 2009).

B7(a) Levels of key nutrients, toxicants and anti-nutrients

Compositional Equivalence of MON 87419 Grain and Forage to Conventional Maize

Grain and forage samples were collected from MON 87419 and a conventional control at five sites grown in the United States during 2013. The field sites were planted in a randomized complete block design with four blocks per site. MON 87419 and the conventional control were grown under agronomic field conditions typical for the different growing regions. MON 87419 plots were treated with dicamba and glufosinate to generate samples under conditions of the intended use of the product.

The evaluation of MON 87419 followed considerations relevant to the compositional quality of maize as defined by the OECD consensus document (OECD, 2002c). Grain samples were analyzed for levels of nutrients including proximates (protein, fat, ash, moisture), amino acids (18 components), fatty acids (22 components), carbohydrates by calculation, acid detergent fiber (ADF), neutral detergent fiber (NDF), total dietary fiber (TDF), minerals (calcium, copper, iron, magnesium, manganese, phosphorus, potassium, sodium, and zinc), and vitamins [A (β-carotene), B1, B2, B6, E (α-tocopherol), niacin, and folic acid]. The anti-nutrients analyzed in grain were phytic acid and raffinose. Secondary metabolites analyzed in grain were furfural, ferulic acid, and p-coumaric acid. Forage samples were analyzed for levels of proximates, carbohydrates by calculation, fiber (ADF, NDF), and minerals (calcium, and phosphorus). In all, 78 different components were analyzed.

Of the 78 measured components, copper, furfural, and 13 fatty acids (caprylic, capric, lauric, myristic, myristoleic, pentadecanoic, pentadecenoic, heptadecanoic, heptadecenoic, gamma linolenic, eicosadienoic, eicosatrienoic, and arachidonic acids) had more than 50% of the observations below the assay limit of quantitation (LOQ) and were excluded from the statistical analyses. Moisture values for grain and forage were measured for conversion of components from fresh to dry weight, but were not statistically analyzed. Therefore, 61 components were statistically analyzed (53 in grain and eight in forage).

The statistical comparison of MON 87419 and the conventional control was based on compositional data combined across all field sites. Statistically significant differences were identified at the 5% level ($\alpha = 0.05$). A statistically significant difference between MON 87419 and the conventional control does not necessarily imply biological relevance from a food and feed perspective. Therefore, statistically significant differences observed between MON 87419 and the conventional control were evaluated further to determine whether the detected difference indicated a biologically relevant compositional change or supported a conclusion of compositional equivalence, as follows:

Step 1 – Determination of the Magnitude of Difference between Test (MON 87419) and Conventional Control Means

The difference in means between MON 87419 and the conventional control was determined for use in subsequent steps. For protein and amino acids only, the relative magnitude of the difference (percent change relative to the control) between MON 87419 and the conventional

control was determined to allow an assessment of any observed difference in amino acids in relation to the difference in protein[4].

Step 2 – Assessment of the Difference in the Context of Natural Variation within the Conventional Control across Multiple Sites

The relative impact of MON 87419 was evaluated in the context of variation within the conventional control germplasm grown across multiple sites (*i.e.,* variation due to environmental influence). This assesses the mean difference between MON 87419 and the conventional control in the context of the individual replicate values for the conventional control (maximum value minus the minimum value). When a mean difference is less than the variability seen due to natural environmental variation within the single, closely related germplasm, the difference is typically not a food or feed safety concern (Venkatesh *et al.*, 2014).

Step 3 – Assessment of the Difference in the Context of Natural Variation Due to Multiple Sources

The relative impact of MON 87419 on composition was evaluated in the context of sources of natural variation such as environmental and germplasm influences. This assessment determined whether the mean value of MON 87419 was within the natural variability defined by the literature values or the ILSI Crop Composition Database (ILSI-CCDB) values. This naturally occurring variability is important in assessing the biological relevance of statistically significant differences in composition between MON 87419 and the conventional control.

These evaluations of natural variation are important as crop composition is known to be greatly influenced by environment and variety (Harrigan *et al.*, 2010). Although used in the comparative assessment process, detection of statistically significant differences between MON 87419 and the conventional control mean values does not necessarily imply a meaningful contribution by MON 87419 to compositional variability. Only if the impact of MON 87419 on levels of components was large relative to natural variation inherent to conventional maize would further assessments be required to establish whether the change in composition would have an impact from a food and feed safety and nutritional perspective. The steps reviewed in this assessment, therefore, describe the process for determining whether the differences between MON 87419 and the conventional control are meaningful from a food and feed perspective or whether they support a conclusion of compositional equivalence.

[4] Since total amino acids measured in a seed analysis are predominately derived from hydrolysis of protein, a change in protein levels would likely result in corresponding changes in amino acids levels. For this reason, the relative magnitudes of difference (percent change relative to the control) for amino acids and protein were determined to allow an assessment of the difference in amino acids in relation to a difference in protein. When the relative magnitudes of difference for amino acids are related to the relative magnitude of difference for protein, then steps 2 and 3 are not discussed for amino acids.

The compositional analysis provided a comprehensive comparative assessment of the levels of key nutrients, anti-nutrients, and secondary metabolites in maize grain and forage of MON 87419 and the conventional control (Tables 25 – 31). Of the 61 components statistically assessed, there were no significant differences in 60 components. Only one component (manganese in grain) showed a significant difference ($p<0.05$) between MON 87419 and the conventional control.

For manganese, the mean value was 6.03 mg/kg dw for MON 87419 and 5.51 mg/kg dw for the conventional control, a difference of 0.52 mg/kg dw (Table 28) (Step 1). This difference was evaluated in the context of the conventional control range value, 2.91 mg/kg dw, calculated from the minimum (4.50 mg/kg dw) and maximum (7.41 mg/kg dw) manganese values. The mean difference in manganese values between MON 87419 and the conventional control was less than the range value of the conventional control, indicating that MON 87419 does not impact levels of manganese more than natural variation within the conventional control grown at multiple locations (Step 2). Additionally, the MON 87419 mean manganese value was also within the range of values observed in the literature and the ILSI-CCDB (Table 32) (Step 3).

These results support the overall conclusion that MON 87419 was not a major contributor to variation in component levels in maize grain and forage and confirmed the compositional equivalence of MON 87419 to the conventional control in levels of these components. These data indicated that the statistically significant difference observed was not compositionally meaningful from a food and feed safety perspective.

For details, please refer to [redacted]., 2014 (MSL0025559).

Table 25. Summary of Maize Grain Protein and Amino Acids for MON 87419 (Treated) and Conventional Control

				Difference (MON 87419 minus Control)		
Component (% dw)[1]	MON 87419 (Treated) Mean (S.E.)[2] Range	Control Mean (S.E.) Range	Control Range Value[3]	Mean (S.E.)	p-Value	% Relative[4]
Protein	11.52 (0.55) 9.14 - 14.60	11.07 (0.55) 9.22 - 14.04	4.82	0.45 (0.26)	0.120	4.10
Alanine	0.92 (0.057) 0.68 - 1.23	0.88 (0.057) 0.71 - 1.17	0.46	0.042 (0.026)	0.151	4.75
Arginine	0.46 (0.014) 0.38 - 0.55	0.45 (0.014) 0.39 - 0.52	0.13	0.010 (0.0076)	0.178	2.33
Aspartic Acid	0.73 (0.036) 0.58 - 0.94	0.70 (0.036) 0.59 - 0.88	0.30	0.029 (0.017)	0.127	4.21
Cystine/Cysteine	0.22 (0.0050) 0.18 - 0.26	0.22 (0.0050) 0.18 - 0.26	0.08	0.0013 (0.0043)	0.767	0.59
Glutamic Acid	2.43 (0.15) 1.80 - 3.26	2.32 (0.15) 1.88 - 3.12	1.24	0.11 (0.070)	0.160	4.69

Table 25 (continued). Summary of Maize Grain Protein and Amino Acids for MON 87419 (Treated) and Conventional Control

				Difference (MON 87419 minus Control)		
Component (% dw)[1]	MON 87419 (Treated) Mean (S.E.)[2] Range	Control Mean (S.E.) Range	Control Range Value[3]	Mean (S.E.)	p-Value	% Relative[4]
Glycine	0.41 (0.011) 0.36 - 0.47	0.40 (0.011) 0.36 - 0.45	0.09	0.0095 (0.0060)	0.118	2.36
Histidine	0.33 (0.011) 0.27 - 0.40	0.32 (0.011) 0.28 - 0.37	0.09	0.0090 (0.0056)	0.114	2.81
Isoleucine	0.42 (0.024) 0.32 - 0.56	0.40 (0.024) 0.33 - 0.53	0.20	0.018 (0.011)	0.123	4.49
Leucine	1.59 (0.11) 1.15 - 2.18	1.51 (0.11) 1.20 - 2.08	0.89	0.078 (0.048)	0.144	5.18
Lysine	0.28 (0.0061) 0.25 - 0.33	0.28 (0.0061) 0.24 - 0.32	0.07	0.0043 (0.0054)	0.431	1.54
Methionine	0.23 (0.0074) 0.19 - 0.27	0.23 (0.0074) 0.18 - 0.28	0.10	0.0015 (0.0054)	0.788	0.64

Table 25 (continued). Summary of Maize Grain Protein and Amino Acids for MON 87419 (Treated) and Conventional Control

				Difference (MON 87419 minus Control)		
Component (% dw)[1]	MON 87419 (Treated) Mean (S.E.)[2] Range	Control Mean (S.E.) Range	Control Range Value[3]	Mean (S.E.)	p-Value	% Relative[4]
Phenylalanine	0.63 (0.040) 0.47 - 0.87	0.61 (0.040) 0.48 - 0.79	0.31	0.028 (0.018)	0.161	4.61
Proline	1.08 (0.044) 0.87 - 1.33	1.04 (0.044) 0.89 - 1.27	0.37	0.041 (0.021)	0.084	3.94
Serine	0.59 (0.032) 0.47 - 0.77	0.57 (0.032) 0.48 - 0.72	0.25	0.023 (0.014)	0.108	4.01
Threonine	0.42 (0.018) 0.34 - 0.53	0.41 (0.018) 0.35 - 0.50	0.15	0.014 (0.0078)	0.074	3.51
Tryptophan	0.070 (0.0017) 0.058 - 0.083	0.069 (0.0017) 0.055 - 0.083	0.03	0.0011 (0.0018)	0.537	1.66
Tyrosine	0.31 (0.018) 0.22 - 0.41	0.30 (0.018) 0.24 - 0.39	0.15	0.0076 (0.0095)	0.429	2.53

Table 25 (continued). Summary of Maize Grain Protein and Amino Acids for MON 87419 (Treated) and Conventional Control

				Difference (MON 87419 minus Control)		
Component (% dw)[1]	MON 87419 (Treated) Mean (S.E.)[2] Range	Control Mean (S.E.) Range	Control Range Value[3]	Mean (S.E.)	p-Value	% Relative[4]
Valine	0.54 (0.025) 0.43 - 0.69	0.52 (0.025) 0.44 - 0.65	0.22	0.020 (0.011)	0.077	3.87

[1]dw = dry weight.

[2]Mean (S.E.) = least-square mean (standard error).

[3]Maximum value minus minimum value for the control maize hybrid.

[4]The relative magnitude of the difference in mean values between MON 87419 (Treated) and the control, expressed as a percent of the control.

Table 26. Summary of Maize Grain Total Fat and Fatty Acids for MON 87419 (Treated) and Conventional Control

Component	MON 87419 (Treated) Mean (S.E.)[2] Range	Control Mean (S.E.) Range	Control Range Value[3]	Difference (MON 87419 minus Control) Mean (S.E.)	Difference (MON 87419 minus Control) p-Value
Total Fat (% dw)[1]	3.40 (0.081) 2.89 - 3.81	3.49 (0.081) 2.80 - 3.98	1.18	-0.093 (0.084)	0.297
16:0 Palmitic[4]	14.51 (0.12) 13.62 - 15.25	14.51 (0.12) 13.80 - 15.56	1.77	0.0065 (0.14)	0.963
16:1 Palmitoleic	0.12 (0.0040) 0.097 - 0.13	0.12 (0.0040) 0.095 - 0.14	0.05	-0.0023 (0.0022)	0.318
18:0 Stearic	1.62 (0.028) 1.45 - 1.77	1.64 (0.028) 1.46 - 1.84	0.37	-0.021 (0.023)	0.366
18:1 Oleic	21.86 (0.20) 20.52 - 23.24	22.37 (0.20) 20.83 - 24.72	3.89	-0.50 (0.28)	0.078
18:2 Linoleic	60.08 (0.27) 58.17 - 62.44	59.52 (0.27) 57.68 - 61.91	4.23	0.56 (0.38)	0.150
18:3 Linolenic	1.00 (0.027) 0.83 - 1.18	1.02 (0.027) 0.84 - 1.16	0.32	-0.021 (0.024)	0.397

Table 26 (continued). Summary of Maize Grain Total Fat and Fatty Acids for MON 87419 (Treated) and Conventional Control

Component	MON 87419 (Treated) Mean (S.E.)[2] Range	Control Mean (S.E.) Range	Control Range Value[3]	Difference (MON 87419 minus Control) Mean (S.E.)	p-Value
20:0 Arachidic	0.40 (0.0079) 0.35 - 0.43	0.41 (0.0079) 0.37 - 0.45	0.08	-0.0072 (0.0057)	0.211
20:1 Eicosenoic	0.27 (0.0049) 0.24 - 0.29	0.27 (0.0049) 0.25 - 0.33	0.08	-0.0056 (0.0063)	0.381
22:0 Behenic	0.14 (0.0070) 0.065 - 0.17	0.15 (0.0070) 0.061 - 0.18	0.11	-0.0021 (0.0074)	0.781

[1]dw = dry weight.
[2]Mean (S.E.) = least-square mean (standard error).
[3]Maximum value minus minimum value for the control maize hybrid.
[4]Expressed as % total fatty acid. Prefix numbers refer to number of carbon atoms and number of carbon-carbon double bonds in the fatty acid molecule; 16:0 means sixteen carbon atoms and zero double bonds. Numbers are not included in text discussion for reasons of clarity. The following fatty acids with more than 50% of observations below the assay LOQ were excluded from statistical analysis: caprylic acid, capric acid, lauric acid, myristic acid, myristoleic acid, pentadecanoic acid, pentadecenoic acid, heptadecanoic acid, heptadecenoic acid, gamma linolenic acid, eicosadienoic acid, eicosatrienoic acid, and arachidonic acid.

Table 27. Summary of Maize Grain Carbohydrates by Calculation and Fiber for MON 87419 (Treated) and Conventional Control

				Difference (MON 87419 minus Control)	
Component (% dw)[1]	MON 87419 (Treated) Mean (S.E.)[2] Range	Control Mean (S.E.) Range	Control Range Value[3]	Mean (S.E.)	p-Value
Carbohydrates by Calculation	83.57 (0.54) 80.87 - 86.28	84.04 (0.54) 81.36 - 85.93	4.57	-0.47 (0.36)	0.231
Acid Detergent Fiber	3.97 (0.12) 3.42 - 5.13	4.04 (0.12) 3.20 - 5.20	2.00	-0.068 (0.13)	0.608
Neutral Detergent Fiber	9.70 (0.11) 9.14 - 10.53	9.42 (0.11) 8.98 - 10.01	1.03	0.28 (0.15)	0.099
Total Dietary Fiber	9.18 (0.23) 7.15 - 11.78	8.97 (0.23) 7.21 - 10.64	3.43	0.21 (0.31)	0.514

[1]dw = dry weight.

[2]Mean (S.E.) = least-square mean (standard error).

[3]Maximum value minus minimum value for the control maize hybrid.

Table 28. Summary of Maize Grain Ash and Minerals for MON 87419 (Treated) and Conventional Control

Component	MON 87419 (Treated) Mean (S.E.)[2] Range	Control Mean (S.E.) Range	Control Range Value[3]	Difference (MON 87419 minus Control) Mean (S.E.)	p-Value
Ash (% dw)[1]	1.39 (0.021) 1.27 - 1.48	1.38 (0.021) 1.30 - 1.51	0.21	0.0066 (0.016)	0.686
Calcium (% dw)	0.0031 (0.00017) 0.0020 - 0.0042	0.0029 (0.00017) 0.0022 - 0.0054	0.003	0.00016 (0.00019)	0.427
Iron (mg/kg dw)	16.83 (0.54) 13.02 - 21.56	16.57 (0.55) 13.39 - 18.71	5.31	0.27 (0.43)	0.536
Magnesium (% dw)	0.13 (0.0019) 0.12 - 0.15	0.12 (0.0019) 0.086 - 0.14	0.05	0.0045 (0.0026)	0.092
Manganese (mg/kg dw)	6.03 (0.45) 4.81 - 8.72	5.51 (0.45) 4.50 - 7.41	2.91	0.52 (0.18)	0.019
Phosphorus (% dw)	0.36 (0.0059) 0.32 - 0.40	0.35 (0.0059) 0.25 - 0.40	0.15	0.0098 (0.0077)	0.204

Table 28 (continued). Summary of Maize Grain Ash and Minerals for MON 87419 (Treated) and Conventional Control

Component	MON 87419 (Treated) Mean (S.E.)[2] Range	Control Mean (S.E.) Range	Control Range Value[3]	Difference (MON 87419 minus Control) Mean (S.E.)	Difference (MON 87419 minus Control) p-Value
Potassium (% dw)	0.36 (0.0081) 0.32 - 0.41	0.36 (0.0081) 0.33 - 0.40	0.07	0.0012 (0.0048)	0.802
Sodium (mg/kg dw)	5.45 (1.92) 0.36 - 24.28	5.63 (1.92) 0.36 - 35.05	34.69	-0.18 (2.65)	0.945
Zinc (mg/kg dw)	22.10 (1.13) 17.21 - 29.83	21.18 (1.13) 16.40 - 26.70	10.30	0.93 (0.67)	0.175

[1]dw = dry weight.

[2]Mean (S.E.) = least-square mean (standard error).

[3]Maximum value minus minimum value for the control maize hybrid.

Table 29. Summary of Maize Grain Vitamins for MON 87419 (Treated) and Conventional Control

Component (mg/kg dw)[1]	MON 87419 (Treated) Mean (S.E.)[2] Range	Control Mean (S.E.) Range	Control Range Value[3]	Difference (MON 87419 minus Control) Mean (S.E.)	p-Value
Folic Acid	0.65 (0.035) 0.41 - 1.03	0.66 (0.035) 0.48 - 0.89	0.41	-0.0063 (0.035)	0.859
Niacin	10.22 (0.41) 8.06 - 12.18	10.20 (0.41) 8.23 - 11.97	3.74	0.028 (0.46)	0.952
Vitamin A	5.44 (0.45) 3.67 - 11.11	5.47 (0.45) 3.66 - 8.19	4.53	-0.030 (0.48)	0.950
Vitamin B1	2.46 (0.12) 1.94 - 3.25	2.48 (0.12) 1.80 - 3.34	1.54	-0.018 (0.095)	0.850
Vitamin B2	2.18 (0.13) 1.52 - 3.47	2.16 (0.13) 1.54 - 3.43	1.89	0.018 (0.18)	0.917
Vitamin B6	5.42 (0.22) 3.45 - 6.62	5.43 (0.22) 2.82 - 7.61	4.79	-0.016 (0.32)	0.959

Table 29 (continued). Summary of Maize Grain Vitamins for MON 87419 (Treated) and Conventional Control

Component (mg/kg dw)[1]	MON 87419 (Treated) Mean (S.E.)[2] Range	Control Mean (S.E.) Range	Control Range Value[3]	Difference (MON 87419 minus Control) Mean (S.E.)	p-Value
Vitamin E	11.56 (0.43) 9.28 - 13.37	11.07 (0.43) 8.65 - 12.76	4.11	0.49 (0.28)	0.085

[1]dw = dry weight.

[2]Mean (S.E.) = least-square mean (standard error).

[3]Maximum value minus minimum value for the control maize hybrid.

Table 30. Summary of Maize Grain Anti-nutrients and Secondary Metabolites for MON 87419 (Treated) and Conventional Control

Component	MON 87419 (Treated) Mean (S.E.)[2] Range	Control Mean (S.E.) Range	Control Range Value[3]	Difference (MON 87419 minus Control) Mean (S.E.)	Difference (MON 87419 minus Control) p-Value
Anti-nutrients (% dw[1])					
Phytic Acid	0.99 (0.031) 0.80 - 1.20	0.93 (0.031) 0.71 - 1.37	0.65	0.065 (0.038)	0.087
Raffinose	0.28 (0.010) 0.23 - 0.34	0.28 (0.010) 0.24 - 0.35	0.11	0.0039 (0.0070)	0.591
Secondary Metabolites (µg/g dw)					
Ferulic Acid	2352.80 (45.66) 2165.31 - 2652.33	2289.17 (45.66) 1882.22 - 2508.79	626.58	63.63 (37.49)	0.097
p-Coumaric Acid	196.51 (12.40) 149.01 - 282.91	187.70 (12.40) 132.56 - 254.88	122.32	8.81 (6.67)	0.194

[1]dw = dry weight.

[2]Mean (S.E.) = least-square mean (standard error).

[3]Maximum value minus minimum value for the control maize hybrid.

Table 31. Summary of Maize Forage Proximates, Fiber and Minerals for MON 87419 (Treated) and Conventional Control

Component (% dw)[1]	MON 87419 (Treated) Mean (S.E.)[2] Range	Control Mean (S.E.) Range	Control Range Value[3]	Difference (MON 87419 minus Control) Mean (S.E.)	p-Value
Ash	3.86 (0.54) 2.28 - 5.34	3.89 (0.54) 2.27 - 5.70	3.43	-0.029 (0.10)	0.778
Carbohydrates by Calculation	87.12 (0.85) 83.54 - 89.84	87.15 (0.85) 83.47 - 90.85	7.38	-0.024 (0.29)	0.935
Protein	7.40 (0.36) 5.54 - 9.32	7.27 (0.36) 5.43 - 8.78	3.35	0.12 (0.19)	0.521
Total Fat	1.59 (0.17) 0.49 - 2.73	1.68 (0.17) 0.66 - 3.84	3.18	-0.091 (0.21)	0.664
Acid Detergent Fiber	26.52 (1.15) 20.80 - 33.33	26.72 (1.15) 20.79 - 40.90	20.10	-0.19 (1.13)	0.865
Neutral Detergent Fiber	41.28 (1.40) 36.10 - 56.57	41.16 (1.40) 32.32 - 47.52	15.20	0.12 (1.10)	0.917

Table 31 (continued). Summary of Maize Forage Proximates, Fiber, and Minerals for MON 87419 (Treated) and Conventional Control

Component (% dw)[1]	MON 87419 (Treated) Mean (S.E.)[2] Range	Control Mean (S.E.) Range	Control Range Value[3]	Difference (MON 87419 minus Control) Mean (S.E.)	p-Value
Calcium	0.21 (0.021) 0.12 - 0.28	0.22 (0.021) 0.13 - 0.33	0.20	-0.014 (0.012)	0.267
Phosphorus	0.20 (0.018) 0.093 - 0.37	0.21 (0.018) 0.13 - 0.32	0.18	-0.013 (0.015)	0.389

[1]dw = dry weight.
[2]Mean (S.E.) = least-square mean (standard error).
[3]Maximum value minus minimum value for the control maize hybrid.

Table 32. Literature and ILSI-CCDB Database Ranges for Components in Maize Forage and Grain

Grain Tissue Components[1]	Literature Range[2]	ILSI Range[3]
Grain Nutrients		
Proximates (% dw)		
Ash	1.17 – 2.01[a]; 1.27 – 1.63[b]	0.616 – 6.282
Carbohydrates by calculation	81.31 – 87.06[a]; 82.10 – 85.98[b]	77.4 – 89.5
Fat, total	2.95 – 4.40[a]; 3.18 – 4.23[b]	1.742 – 5.900
Protein	8.27 – 13.33[a]; 9.17 – 12.19[b]	6.15 – 17.26
Fiber (% dw)		
Acid detergent fiber	1.82 – 4.48[a]; 1.83 – 3.39[b]	1.82 – 11.34
Neutral detergent fiber	6.51 –12.28[a]; 6.08 – 10.36[b]	5.59 – 22.64
Total dietary fiber	10.65 – 16.26[a]; 10.57 – 14.56[b]	9.01 – 35.31
Amino Acids (% dw)		
Alanine	0.60 – 1.04[a]; 0.68 – 0.96[b]	0.44 - 1.39
Arginine	0.34 – 0.52[a]; 0.34 – 0.50[b]	0.12 - 0.64
Aspartic acid	0.52 – 0.78[a]; 0.59 – 0.76[b]	0.33 – 1.21
Cystine	0.19 – 0.26[a]; 0.20 – 0.26[b]	0.13 – 0.51
Glutamic acid	1.54 – 2.67[a]; 1.71 – 2.44[b]	0.97 – 3.54
Glycine	0.33 – 0.43[a]; 0.33 – 0.42[b]	0.18 – 0.54
Histidine	0.25 – 0.37[a]; 0.27 – 0.34[b]	0.14 – 0.43
Isoleucine	0.30 – 0.48[a]; 0.32 – 0.44[b]	0.18 – 0.69
Leucine	1.02 – 1.87[a]; 1.13 – 1.65[b]	0.64 – 2.49
Lysine	0.26 – 0.33[a]; 0.28 – 0.31[b]	0.17 – 0.67
Methionine	0.17 – 0.26[a]; 0.16 – 0.30[b]	0.12 – 0.47
Phenylalanine	0.43 – 0.72[a]; 0.45 – 0.63[b]	0.24 – 0.93
Proline	0.74 – 1.21[a]; 0.78 – 1.11[b]	0.46 – 1.63
Serine	0.39 – 0.67[a]; 0.43 – 0.60[b]	0.24 – 0.77
Threonine	0.29 – 0.45[a]; 0.31 – 0.39[b]	0.22 – 0.67
Tryptophan	0.047 – 0.085[a]; 0.042 – 0.070[b]	0.027 – 0.215
Tyrosine	0.13 – 0.43[a]; 0.12 – 0.41[b]	0.10 – 0.64
Valine	0.42 – 0.62[a]; 0.45 – 0.58[b]	0.27 – 0.86
Fatty Acids (% Total FA)		
16:0 Palmitic	8.80 – 13.33[a]; 9.84 – 12.33[b]	7.94 – 20.71
16:1 Palmitoleic	0.059 – 0.23[a]	0.095 – 0.447
18:0 Stearic	1.36 – 2.14 [a]; 1.30 – 2.10[b]	1.02 – 3.40
18:1 Oleic	19.50 – 33.71[a]; 19.59 – 29.13[b]	17.4 – 40.2
18:2 Linoleic	49.31 – 64.70[a]; 56.51 – 65.65[b]	36.2 – 66.5
18:3 Linolenic	0.89 – 1.56[a]; 1.03 – 1.38[b]	0.57 – 2.25
20:0 Arachidic	0.30 – 0.49[a]; 0.30 – 0.41[b]	0.279 – 0.965
20:1 Eicosenoic	0.17 – 0.29[a]; 0.17 – 0.27[b]	0.170 – 1.917
22:0 Behenic	0.069 – 0.28[a]; 0.059 – 0.18[b]	0.110 – 0.349
Minerals		
Calcium (% dw)	0.0036 – 0.0068[a]; 0.0035 – 0.0070[b]	0.00127 – 0.02084
Copper (mg/kg dw)	0.85-3.54[c]	0.73 – 18.50
Iron (mg/kg dw)	14.17 – 23.40[a]; 15.90 – 24.66[b]	10.42 – 49.07

Table 32 (continued). Literature and ILSI Database Ranges for Components in Maize Forage and Grain

Grain Tissue Components[1]	Literature Range[2]	ILSI Range[3]
Magnesium (% dw)	0.091 – 0.14[a]; 0.10 – 0.14[b]	0.0594 – 0.194
Manganese (mg/kg dw)	4.83 – 8.34[a]; 4.78 – 9.35[b]	1.69 – 14.30
Phosphorus (% dw)	0.24 – 0.37[a]; 0.27 – 0.38[b]	0.147 – 0.533
Potassium (% dw)	0.29 – 0.39[a]; 0.36 – 0.43[b]	0.181 – 0.603
Sodium (mg/kg dw)	ND	0.17 – 731.54
Zinc (mg/kg dw)	16.78 – 28.17[a]; 18.25 – 30.44[b]	6.5 – 37.2
Vitamins (mg/kg dw)		
Folic acid	0.19 – 0.35[a]; 0.23 – 0.42[b]	0.147 – 1.464
Vitamin A [β–Carotene]	0.14 – 11.27[d]	0.19 – 46.81
Vitamin B_1 [Thiamine]	2.33 – 4.17[a]; 2.71 – 4.33[b]	1.26 – 40.00
Vitamin B_2 [Riboflavin]	0.94 – 2.42[a]; 1.64 – 2.81[b]	0.50 – 2.36
Vitamin B_3 [Niacin]	15.07 – 32.38[a]; 13.64 – 42.06[b]	10.37 – 46.94
Vitamin B_6 [Pyridoxine]	4.93 – 7.53[a]; 4.97 – 8.27[b]	3.68 – 11.32
Vitamin E [α–Tocopherol]	5.96 – 18.44[a]; 2.84 – 15.53[b]	1.537 – 68.672
Grain Anti–Nutrients (% dw)		
Phytic acid	0.69 – 1.09[a]; 0.60 – 0.94[b]	0.111 – 1.570
Raffinose	0.079 – 0.22[a]; 0.061 – 0.15[b]	0.020 – 0.320
Grain Secondary Metabolites (µg/g dw)		
Ferulic acid	1205.75 – 2873.05[a]; 1011.40 – 2539.86[b]	291.9 – 3885.8
p–Coumaric acid	94.77 – 327.39[a]; 66.48 – 259.68[b]	53.4 – 576.2

Forage Tissue Components[1]	Literature Range[2]	ILSI Range[3]
Forage Nutrients		
Proximates (% dw)		
Ash	2.67 – 8.01[a]; 4.59 – 6.90[b]	1.527 – 9.638
Carbohydrates by calculation	81.88 – 89.26[a]; 84.11 – 87.54[b]	76.4 – 92.1
Fat, total	1.28 – 3.62[a]; 0.20 – 1.76[b]	0.296 – 4.570
Protein	5.80 – 10.24[a]; 5.56 – 9.14[b]	3.14 – 11.57
Fiber (% dw)		
Acid detergent fiber	19.11 – 30.49[a]; 20.73 – 33.39[b]	16.13 – 47.39
Neutral detergent fiber	27.73 – 49.62[a]; 31.81 – 50.61[b]	20.29 – 63.71
Minerals (% dw)		
Calcium	0.12 – 0.33[a]; 0.21 – 0.41[b]	0.07139 – 0.57679
Phosphorus	0.090 – 0.26[a]; 0.13 – 0.21[b]	0.09362 – 0.37041

[1]dw=dry weight; FA = fatty acids; ND = not detected.

[2]Literature range references: [a]US and [b]Chile (Harrigan *et al.*, 2009), [c](Ridley *et al.*, 2011), [d](Egesel *et al.*, 2003).

[3]ILSI range is from ILSI Crop Composition Database, 2011 [Accessed 9 May 2014] (ILSI, 2011).

Compositional Assessment of MON 87419 Conclusion

Compositional analysis was conducted on grain and forage of MON 87419 treated with dicamba and glufosinate and a conventional control grown at five sites in the U.S. during 2013. Of the 61 components statistically assessed, 60 showed no statistically significant differences between MON 87419 and the conventional control. One component (manganese in grain) showed a statistically significant difference between MON 87419 and the conventional control. For this one component, the mean difference in the component values between MON 87419 and the conventional control was less than the range value of the conventional control. The MON 87419 mean component value was also within the range of values observed in the literature and the ILSI-CCDB. These data indicated that the statistically significant difference for manganese in grain was not compositionally meaningful from a food and feed safety perspective.

These results support the overall conclusion that MON 87419 was not a major contributor to variation in component levels in maize grain and forage and confirmed that food and feed derived from MON 87419 and its progeny are as safe and nutritious as food and feed derived from conventional maize.

B7(b) Levels of other GM-influenced constituents

Not applicable.

B7(c) Levels of naturally-occurring allergenic proteins

Not applicable.

C. NUTRITIONAL IMPACT

C1 Data on Nutritional Impact of Compositional Changes

Not Applicable.

C2 Data from an Animal Feeding Study, if Available

The data and information presented in this submission demonstrate that the food and feed derived from MON 87419 are as safe and nutritious as those derived from commercially-available, conventional maize for which there is an established history of safe consumption. Therefore, animal feeding studies do not add value to the safety of MON 87419.

PART 3 STATUTORY DECLARATION – AUSTRALIA

I, Nina McCormick, declare that the information provided in this application fully sets out the matters required and that the same are true to the best of my knowledge and belief, and that no information has been withheld that might prejudice this application.

Signature: _____

Declared before me ……

This ……7th…….. day of ……August…….. 2015.

PART 4 REFERENCES

Adrian-Romero, M., G. Blunden, B.G. Carpenter and E. Tyihák. 1999. HPLC quantification of formaldehyde, as formaldemethone, in plants and plant-like organisms. Chromatographia 50: 160-166.

Astwood, J.D., J.N. Leach and R.L. Fuchs. 1996. Stability of food allergens to digestion in vitro. Nature Biotechnology 14: 1269-1273.

Barker, R.F., K.B. Idler, D.V. Thompson and J.D. Kemp. 1983. Nucleotide sequence of the T-DNA region from the *Agrobacterium tumefaciens* octopine Ti plasmid pTi15955. Plant Molecular Biology 2: 335-350.

Barry, G.F., G.M. Kishore, S.R. Padgette and W.C. Stallings. 2001. Glyphosate-tolerant 5-enolpyruvylshikimate-3-phosphate synthases. Patent 6,248,876, U.S. Patent Office, Washington, D.C.

Behrens, M.R., N. Mutlu, S. Chakraborty, R. Dumitru, W.Z. Jiang, B.J. LaVallee, P.L. Herman, T.E. Clemente and D.P. Weeks. 2007. Dicamba resistance: Enlarging and preserving biotechnology-based weed management strategies. Science 316: 1185-1188.

Berg, G., P. Marten and G. Ballin. 1996. *Stenotrophomonas maltophilia* in the rhizosphere of oilseed rape - Occurrence, characterization and interaction with phytopathogenic fungi. Microbiological Research 151: 19-27.

Berg, G., N. Roskot and K. Smalla. 1999. Genotypic and phenotypic relationships between clinical and environmental isolates of *Stenotrophomonas maltophilia*. Journal of Clinical Microbiology 37: 3594-3600.

Berg, G., N. Roskot, A. Steidle, L. Eberl, A. Zock and K. Smalla. 2002. Plant-dependent genotypic and phenotypic diversity of antagonistic rhizobacteria isolated from different *Verticillium* host plants. Applied and Environmental Microbiology 68: 3328-3338.

Berg, R.D. 1996. The indigenous gastrointestinal microflora. Trends in Microbiology 4: 430-435.

Bevan, M., W.M. Barnes and M.-D. Chilton. 1983. Structure and transcription of the nopaline synthase gene region of T-DNA. Nucleic Acids Research 11: 369-385.

Biron, D.G., C. Brun, T. Lefevre, C. Lebarbenchon, H.D. Loxdale, F. Chevenet, J.-P. Brizard and F. Thomas. 2006. The pitfalls of proteomics experiments without the correct use of bioinformatics tools. Proteomics 6: 5577-5596.

Breyton, C. 2000. The cytochrome b_6f complex: Structural studies and comparison with the bc_1 complex. Biochimica et Biophysica Acta 1459: 467-474.

Buchanan, B.B., W. Gruissem and R.L. Jones. 2000. Phenylpropanoid and phenylpropanoid-acetate pathway metabolites. Pages 1286-1289 in Biochemistry and Molecular Biology of Plants. American Society of Plant Biologists, Rockville, Maryland.

Caetano-Anollés, G., M. Wang, D. Caetano-Anollés and J.E. Mittenthal. 2009. The origin, evolution and structure of the protein world. Biochemical Journal 417: 621-637.

Chakraborty, S., M. Behrens, P.L. Herman, A.F. Arendsen, W.R. Hagen, D.L. Carlson, X.-Z. Wang and D.P. Weeks. 2005. A three-component dicamba *O*-demethylase from *Pseudomonas maltophilia*, strain DI-6: Purification and characterization. Archives of Biochemistry and Biophysics 437: 20-28.

Clark, S.E. and G.K. Lamppa. 1992. Processing of the precursors for the light-harvesting chlorophyll-binding proteins of photosystem II and photosystem I during import and in an organelle-free assay. Plant Physiology 98: 595-601.

Codex Alimentarius. 2009. Foods derived from modern biotechnology. Second Edition. Codex Alimentarius Commission, Joint FAO/WHO Food Standards Programme, Food and Agriculture Organization of the United Nations, Rome, Italy.

Cojocariu, C., P. Escher, K.-H. Häberle, R. Matyssek, H. Rennenberg and J. Kreuzwieser. 2005. The effect of ozone on the emission of carbonyls from leaves of adult *Fagus sylvatica*. Plant Cell and Environment 28: 603-611.

Cojocariu, C., J. Kreuzwieser and H. Rennenberg. 2004. Correlation of short-chained carbonyls emitted from *Picea abies* with physiological and environmental parameters. New Phytologist 162: 717-727.

Cross, T. 1989. Other genera. Pages 2586-2615 in Bergey's Manual of Systematic Bacteriology. Volume 4. S.T. Williams and M.E. Sharpe (eds.). Williams & Wilkins, Balitmore, Maryland.

Cunha, B.A. 2009. *Stenotrophomonas maltophilia*. WebMD, LLC, New York, New York. http://www.emedicine.com/med/topic3457.htm [Accessed January 2, 2010].

D'Ordine, R.L., T.J. Rydel, M.J. Storek, E.J. Sturman, F. Moshiri, R.K. Bartlett, G.R. Brown, R.J. Eilers, C. Dart, Y. Qi, S. Flasinski and S.J. Franklin. 2009. Dicamba monooxygenase: Structural insights into a dynamic Rieske oxygenase that catalyzes an exocyclic monooxygenation. Journal of Molecular Biology 392: 481-497.

Darrouzet, E., J.W. Cooley and F. Daldal. 2004. The cytochrome bc_1 complex and its homologue the b_6f complex: Similarities and differences. Photosynthesis Research 79: 25-44.

Delaney, B., J.D. Astwood, H. Cunny, R.E. Conn, C. Herouet-Guicheney, S. MacIntosh, L.S. Meyer, L. Privalle, Y. Gao, J. Mattsson and M. Levine. 2008. Evaluation of protein safety in the context of agricultural biotechnology. Food and Chemical Toxicology 46: S71-S97.

della-Cioppa, G., S.C. Bauer, B.K. Klein, D.M. Shah, R.T. Fraley and G.M. Kishore. 1986. Translocation of the precursor of 5-*enol*pyruvylshikimate-3-phosphate synthase into chloroplasts of higher plants *in vitro*. Proceedings of the National Academy of Sciences of the United States of America 83: 6873-6877.

Denton, M. and K.G. Kerr. 1998. Microbiological and clinical aspects of infection associated with *Stenotrophomonas maltophilia*. Clinical Microbiology Reviews 11: 57-80.

Denton, M., N.J. Todd, K.G. Kerr, P.M. Hawkey and J.M. Littlewood. 1998. Molecular epidemiology of *Stenotrophomonas maltophilia* isolated from clinical specimens from patients with cystic fibrosis and associated environmental samples. Journal of Clinical Microbiology 36: 1953-1958.

Depicker, A., S. Stachel, P. Dhaese, P. Zambryski and H.M. Goodman. 1982. Nopaline synthase: Transcript mapping and DNA sequence. Journal of Molecular and Applied Genetics 1: 561-573.

DuBose, A.J., S.T. Lichtenstein, N. Narisu, L.L. Bonnycastle, A.J. Swift, P.S. Chines and F.S. Collins. 2013. Use of microarray hybrid capture and next-generation sequencing to identify the anatomy of a transgene. Nucleic Acids Research 41: e70.

Duke, S.O. 2005. Taking stock of herbicide-resistant crops ten years after introduction. Pest Management Science 61: 211-218.

Dumitru, R., W.Z. Jiang, D.P. Weeks and M.A. Wilson. 2009. Crystal structure of dicamba monooxygenase: A Rieske nonheme oxygenase that catalyzes oxidative demethylation. Journal of Molecular Biology 392: 498-510.

Earle, F.R. and J.J. Curtis. 1946. Composition of the component parts of the maize kernel. Cereal Chemistry 23: 504-511.

Echemendia, Y. 2010. Microorganism of the month: *Stenotrophomonas maltophilia*. Environmental Microbiology Laboratory, Inc., Cherry Hill, New Jersey. http://www.emlab.com/s/sampling/env-report-07-2007.html [Accessed August 10, 2010].

Edgerton, M.D. 2009. Increasing crop productivity to meet global needs for feed, food, and fuel. Plant Physiology 149: 7-13.

EFSA. 2007a. Environmental fate and behaviour. Draft assessment report: Initial risk assessment provided by the rapporteur Member State Denmark for the existing active substance dicamba of the third stage (part B) of the review programme referred to in Article 8(2) of Council Directive 91/414/EEC. European Food Safety Authority, Brussels, Belgium.

EFSA. 2007b. Ecotoxicology. Draft assessment report: Initial risk assessment provided by the rapporteur Member State Denmark for the existing active substance dicamba of the third stage (part B) of the review programme referred to in Article 8(2) of Council Directive 91/414/EEC. European Food Safety Authority, Brussels, Belgium.

Egesel, C.O., J.C. Wong, R.J. Lambert and T.R. Rocheford. 2003. Gene dosage effects on carotenoid concentration in maize grain. Maydica 48: 183-190.

FAO-WHO. 2011a. Pesticide residues in food 2010: Joint FAO/WHO meeting on pesticide residues. FAO Plant Production and Protection Paper 200. Food and Agriculture Organization of the United Nations, World Health Organization, Rome, Italy.

FAO-WHO. 2011b. Summary report: Acceptable daily intakes, acute reference doses, short-term and long-term dietary intakes, recommended maximum residue limits and supervised trials median residue values recorded by the 2011 meeting. Food and Agriculture Organization of the United Nations, World Health Organization, Geneva, Switzerland.

FARRP. 2014. Allergen database, version 14. University of Nebraska, Food Allergy Research and Resource Program, Lincoln, Nebraska. http://www.allergenonline.org/.

Ferraro, D.J., L. Gakhar and S. Ramaswamy. 2005. Rieske business: Structure-function of Rieske non-heme oxygenases. Biochemical and Biophysical Research and Communications 338: 175-190.

Fling, M.E., J. Kopf and C. Richards. 1985. Nucleotide sequence of the transposon Tn*7* gene encoding an aminoglycoside-modifying enzyme, 3"(9)-*O*-nucleotidyltransferase. Nucleic Acids Research 13: 7095-7106.

Fraley, R.T., S.G. Rogers, R.B. Horsch, P.R. Sanders, J.S. Flick, S.P. Adams, M.L. Bittner, L.A. Brand, C.L. Fink, J.S. Fry, G.R. Galluppi, S.B. Goldberg, N.L. Hoffmann and S.C. Woo. 1983. Expression of bacterial genes in plant cells. Proceedings of the National Academy of Sciences of the United States of America 80: 4803-4807.

Fu, T.-J., U.R. Abbott and C. Hatzos. 2002. Digestibility of food allergens and nonallergenic proteins in simulated gastric fluid and simulated intestinal fluid - A comparative study. Journal of Agricultural and Food Chemistry 50: 7154-7160.

Gasser, C.S., J.A. Winter, C.M. Hironaka and D.M. Shah. 1988. Structure, expression, and evolution of the 5-enolpyruvylshikimate-3-phosphate synthase genes of petunia and tomato. Journal of Biological Chemistry 263: 4280-4287.

Giza, P.E. and R.C.C. Huang. 1989. A self-inducing runaway-replication plasmid expression system utilizing the Rop protein. Gene 78: 73-84.

Goodfellow, M. and S.T. Williams. 1983. Ecology of actinomycetes. Annual Review of Microbiology 37: 189-216.

Goodman, M.M. 1988. The history and evolution of maize. Critical Reviews in Plant Sciences 7: 197-220.

Gray, J., E. Wardzala, M. Yang, S. Reinbothe, S. Haller and F. Pauli. 2004. A small family of LLS1-related non-heme oxygenases in plants with an origin amongst oxygenic photosynthesizers. Plant Molecular Biology 54: 39-54.

Hammond, B.G. and J.M. Jez. 2011. Impact of food processing on the safety assessment for proteins introduced into biotechnology-derived soybean and corn crops. Food and Chemical Toxicology 49: 711-721.

Hanson, A.D. and S. Roje. 2001. One-carbon metabolism in higher plants. Annual Review of Plant Physiology and Plant Molecular Biology 52: 119-137.

Harayama, S., M. Kok and E.L. Neidle. 1992. Functional and evolutionary relationships among diverse oxygenases. Annual Review of Microbiology 46: 565-601.

Harrigan, G.G., D. Lundry, S. Drury, K. Berman, S.G. Riordan, M.A. Nemeth, W.P. Ridley and K.C. Glenn. 2010. Natural variation in crop composition and the impact of transgenesis. Nature Biotechnology 28: 402-404.

Harrigan, G.G., W.P. Ridley, K.D. Miller, R. Sorbet, S.G. Riordan, M.A. Nemeth, W. Reeves and T.A. Pester. 2009. The forage and grain of MON 87460, a drought-tolerant corn hybrid, are compositionally equivalent to that of conventional corn. Journal of Agricultural and Food Chemistry 57: 9754-9763.

He, X.Y., K.L. Huang, X. Li, W. Qin, B. Delaney and Y.B. Luo. 2008. Comparison of grain from corn rootworm resistant transgenic DAS-59122-7 maize with non-transgenic maize grain in a 90-day feeding study in Sprague-Dawley rats. Food and Chemical Toxicology 46: 1994-2002.

Helm, R.M. 2001. Topic 5: Stability of known allergens (digestive and heat stability). Joint FAO/WHO expert consultation on foods derived from biotechnology. Food and Agriculture Organization of the United Nations, Rome, Italy.

Herman, P.L., M. Behrens, S. Chakraborty, B.M. Chrastil, J. Barycki and D.P. Weeks. 2005. A three-component dicamba *O*-demethylase from *Pseudomonas maltophilia*, strain DI-6: Gene isolation, characterization, and heterologous expression. Journal of Biological Chemistry 280: 24759-24767.

Hérouet, C., D.J. Esdaile, B.A. Mallyon, E. Debruyne, A. Schulz, T. Currier, K. Hendrickx, R.-J. van der Klis and D. Rouan. 2005. Safety evaluation of the phosphinothricin acetyltransferase proteins encoded by the *pat* and *bar* sequences that confer tolerance to glufosinate-ammonium herbicide in transgenic plants. Regulatory Toxicology and Pharmacology 41: 134-149.

Herrmann, K.M. 1995. The shikimate pathway: Early steps in the biosynthesis of aromatic compounds. The Plant Cell 7: 907-919.

Hibino, T., R. Waditee, E. Araki, H. Ishikawa, K. Aoki, Y. Tanaka and T. Takabe. 2002. Functional characterization of choline monooxygenase, an enzyme for betaine synthesis in plants. Journal of Biological Chemistry 277: 41352-41360.

Hileman, R.E., A. Silvanovich, R.E. Goodman, E.A. Rice, G. Holleschak, J.D. Astwood and S.L. Hefle. 2002. Bioinformatic methods for allergenicity assessment using a comprehensive allergen database. International Archives of Allergy and Immunology 128: 280-291.

Hochuli, E., W. Bannwarth, H. Döbeli, R. Gentz and D. Stüber. 1988. Genetic approach to facilitate purification of recombinant proteins with a novel metal chelate adsorbent. Nature Biotechnology 6: 1321-1325.

Hunt, A.G. 1994. Messenger RNA 3' end formation in plants. Annual Review of Plant Physiology and Plant Molecular Biology 45: 47-60.

Illergård, K., D.H. Ardell and A. Elofsson. 2009. Structure is three to ten times more conserved than sequence - A study of structural response in protein cores. Proteins 77: 499-508.

ILSI-CERA. 2011. A review of the environmental safety of the PAT protein. International Life Sciences Institute, Center for Environmental Risk Assessment, Washington, D.C.

ILSI. 2011. Crop Composition Database, Version 4.2. International Life Sciences Institute, Washington, D.C. http://www.cropcomposition.org/.

Janas, K.M., M. Cvikrová, A. Palągiewicz and J. Eder. 2000. Alterations in phenylpropanoid content in soybean roots during low temperature acclimation. Plant Physiology and Biochemistry 38: 587-593.

Joung, Y.H. and K. Kamo. 2006. Expression of a polyubiquitin promoter isolated from *Gladiolus*. Plant Cell Reports 25: 1081-1088.

Juhnke, M.E. and E. des Jardin. 1989. Selective medium for isolation of *Xanthomonas maltophilia* from soil and rhizosphere environments. Applied and Environmental Microbiology 55: 747-750.

Juhnke, M.E., D.E. Mathre and D.C. Sands. 1987. Identification and characterization of rhizosphere-competent bacteria of wheat. Applied and Environmental Microbiology 53: 2793-2799.

Kämpfer, P. 2006. The family *Streptomycetaceae*, Part I: Taxonomy. Pages 538-604 in The Prokaryotes. A Handbook on the Biology of Bacteria: Archaea. Bacteria: Firmicutes, Actinomycetes. Volume 3. M.Dworkin, S. Falkow, E. Rosenberg, K.-H. Schleifer, and E. Stackebrandt (eds.). Springer+ Business Media, LLC., New York, New York.

Kiesselbach, T.A. 1980. Development and structure of vegetative parts. Pages 10-37 in The Structure and Reproduction of Corn. University of Nebraska Press, Lincoln, Nebraska.

Klee, H.J., Y.M. Muskopf and C.S. Gasser. 1987. Cloning of an *Arabidopsis thaliana* gene encoding 5-enolpyruvylshikimate-3-phosphate synthase: Sequence analysis and manipulation to obtain glyphosate-tolerant plants. Molecular and General Genetics 210: 437-442.

Kovalic, D., C. Garnaat, L. Guo, Y. Yan, J. Groat, A. Silvanovich, L. Ralston, M. Huang, Q. Tian, A. Christian, N. Cheikh, J. Hjelle, S. Padgette and G. Bannon. 2012. The use of next generation sequencing and junction sequence analysis bioinformatics to achieve molecular characterization of crops improved through modern biotechnology. The Plant Genome 5: 149-163.

Krause, E., H. Wenschuh and P.R. Jungblut. 1999. The dominance of arginine-containing peptides in MALDI-derived tryptic mass fingerprints of proteins. Analytical Chemistry 71: 4160-4165.

Krueger, J.P., R.G. Butz, Y.H. Atallah and D.J. Cork. 1989. Isolation and identification of microorganisms for the degradation of dicamba. Journal of Agricultural and Food Chemistry 37: 534-538.

Kutzner, H.J. 1981. The family streptomycetaceae. Pages 2028-2090 in The Prokaryotes: A Handbook on Habitats, Isolation, and Identification of Bacteria. Volume 2. M.P. Starr, H. Stolp, H.G. Trüper, A. Balows, and H.G. Schlegel (eds.). Springer-Verlag, Berlin, Germany.

Lambert, B., F. Leyns, L. Van Rooyen, F. Gosselé, Y. Papon and J. Swings. 1987. Rhizobacteria of maize and their antifungal activities. Applied and Environmental Microbiology 53: 1866-1871.

Lamppa, G.K., G. Morelli and N.-H. Chua. 1985. Structure and developmental regulation of a wheat gene encoding the major chlorophyll a/b-binding polypeptide. Molecular and Cellular Biology 5: 1370-1378.

Leath, M.N. and L.D. Hill. 1987. Economics of production, marketing, and utilization. Pages 210-219 in Corn: Chemistry and Technology. S.A. Watson and P.E. Ramstad (eds.). American Association of Cereal Chemists, St. Paul, Minnesota.

Lege, K.E., J.T. Cothren and C.W. Smith. 1995. Phenolic acid and condensed tannin concentrations of six cotton genotypes. Environmental and Experimental Botany 35: 241-249.

Locci, R. 1989. Streptomycetes and related genera. Pages 2451-2508 in Bergey's Manual of Systematic Bacteriology. Volume 4. S.T. Williams and M.E. Sharpe (eds.). Williams & Wilkins, Baltimore, Maryland.

MacKenzie, S.A., I. Lamb, J. Schmidt, L. Deege, M.J. Morrisey, M. Harper, R.J. Layton, L.M. Prochaska, C. Sanders, M. Locke, J.L. Mattsson, A. Fuentes and B. Delaney. 2007. Thirteen week feeding study with transgenic maize grain containing event DAS-Ø15Ø7-1 in Sprague-Dawley rats. Food and Chemical Toxicology 45: 551-562.

Maiti, I.B. and R.J. Shepherd. 1998. Isolation and expression analysis of peanut chlorotic streak caulimovirus (PClSV) full-length transcript (FLt) promoter in transgenic plants. Biochemical and Biophysical Research Communications 244: 440-444.

Makarova, K.S., Y.I. Wolf and E.V. Koonin. 2009. Comprehensive comparative-genomic analysis of Type 2 toxin-antitoxin systems and related mobile stress response systems in prokaryotes. Biology Direct 4: 19.

Malley, L.A., N.E. Everds, J. Reynolds, P.C. Mann, I. Lamb, T. Rood, J. Schmidt, R.J. Layton, L.M. Prochaska, M. Hinds, M. Locke, C.-F. Chui, F. Claussen, J.L. Mattsson and B. Delaney. 2007. Subchronic feeding study of DAS-59122-7 maize grain in Sprague-Dawley rats. Food and Chemical Toxicology 45: 1277-1292.

Manderscheid, R. and A. Wild. 1986. Studies on the mechanism of inhibition by phosphinothricin of glutamine synthetase isolated from *Triticum aestivum* L. Journal of Plant Physiology 123: 135-142.

May, J.B. 1987. Wet milling: Process and products. Pages 377-397 in Corn: Chemistry and Technology. S.A. Watson and P.E. Ramstad (eds.). American Association of Cereal Chemists, St. Paul, Minnesota.

McElroy, D., W. Zhang, J. Cao and R. Wu. 1990. Isolation of an efficient actin promoter for use in rice transformation. The Plant Cell 2: 163-171.

McElwain, E.F. and S. Spiker. 1989. A wheat cDNA clone which is homologous to the 17 kd heat-shock protein gene family of soybean. Nucleic Acids Research 17: 1764.

Meinnel, T. and C. Giglione. 2008. Tools for analyzing and predicting N-terminal protein modifications. Proteomics 8: 626-649.

Metcalfe, D.D., J.D. Astwood, R. Townsend, H.A. Sampson, S.L. Taylor and R.L. Fuchs. 1996. Assessment of the allergenic potential of foods derived from genetically engineered crop plants. Critical Reviews in Food Science and Nutrition 36: S165-S186.

Moreno, F.J., F.A. Mellon, M.S.J. Wickham, A.R. Bottrill and E.N.C. Mills. 2005. Stability of the major allergen Brazil nut 2S albumin (Ber e 1) to physciologically relevant *in vitro* gastrointestinal digestion. FEBS Journal 272: 341-352.

Morris, M.L. 1998. Overview of the world maize economy. Pages 13-34 in Maize Seed Industries in Devoloping Countries. M.L. Morris (ed.). Lynne Rienner Publishers, Inc., Boulder, Colorado.

Nam, J.-W., H. Nojiri, T. Yoshida, H. Habe, H. Yamane and T. Omori. 2001. New classification system for oxygenase components involved in ring-hydroxylating oxygenations. Bioscience, Biotechnology, and Biochemistry 65: 254-263.

NCGA. 2014. World of corn 2014. National Corn Growers Association, Chesterfield, Missouri.

Nemecek-Marshall, M., R.C. MacDonald, J.J. Franzen, C.L. Wojciechowski and R. Fall. 1995. Methanol emission from leaves: Enzymatic detection of gas-phase methanol and relation of methanol fluxes to stomatal conductance and leaf development. Plant Physiology 108: 1359-1368.

Nunes, F.V. and I.S. de Melo. 2006. Isolation and characterization of endophytic bacteria of coffee plants and their potential in caffeine degradation. Environmental Toxicology 10: 293-297.

OECD. 1999. Consensus document on general information concerning the genes and their enzymes that confer tolerance to phosphinothricin herbicide. ENV/JM/MONO(99)13. Series on Harmonization of Regulatory Oversight in Biotechnology No.11. Organisation for Economic Co-operation and Development, Paris, France.

OECD. 2002a. Module II: Herbicide biochemistry, herbicide metabolism and the residues in glufosinate-ammonium (Phosphinothricin)-tolentant transgenic plants. ENV/JM/MONO(2002)14. Series on Harmonization of Regulatory Oversight in Biotechnology No. 25. Organisation for Economic Co-operation and Development, Paris, France.

OECD. 2002b. Report of the OECD workshop on the toxicological and nutritional testing of novel foods. SG/ICGB(1998)1/FINAL. Organisation for Economic Co-operation and Development, Paris, France.

OECD. 2002c. Consensus document on compositional considerations for new varieties of maize (*Zea mays*): Key food and feed nutrients, anti-nutrients and secondary plant metabolites. ENV/JM/MONO (2002)25. Series on the Safety of Novel Foods and Feeds, No. 6. Organisation for Economic Co-operation and Development, Paris, France.

Okunuki, H., R. Techima, T. Shigeta, J. Sakushima, H. Akiyama, Y. Goda, M. Toyoda and J. Sawada. 2002. Increased digestibility of two products in genetically modified food (CP4 EPSPS and Cry1Ab) after preheating. Journal of the Food Hygienic Society of Japan 43: 68-73.

Padgette, S.R., D.B. Re, G.F. Barry, D.E. Eichholtz, X. Delannay, R.L. Fuchs, G.M. Kishore and R.T. Fraley. 1996. New weed control opportunities: Development of soybeans with a Roundup Ready™ gene. Pages 53-84 in Herbicide-Resistant Crops: Agricultural, Environmental, Economic, Regulatory and Technical Aspects. S.O. Duke (ed.). CRC Press, Inc., Boca Raton, Florida.

Palleroni, N.J. and J.F. Bradbury. 1993. *Stenotrophomonas*, a new bacterial genus for *Xanthomonas maltophilia* (Hugh 1980) Swings et al. 1983. International Journal of Systematic Bacteriology 43: 606-609.

Pearson, W.R. 2000. Flexible sequence similarity searching with the FASTA3 program package. Methods in Molecular Biology 132: 185-219.

Perry, T.W. 1988. Corn as a livestock feed. Pages 941-963 in Corn and Corn Improvement. Third Edition. G.F. Sprague and J.W. Dudley (eds.). American Society of Agronomy, Inc., Crop Science Society of America, Inc., Soil Science Society of America, Inc., Madison, Wisconsin.

Prado, J.R., G. Segers, T. Voelker, D. Carson, R. Dobert, J. Phillips, K. Cook, C. Cornejo, J. Monken, L. Grapes, T. Reynolds and S. Martino-Catt. 2014. Genetically engineered crops: From idea to product. Annual Review of Plant Biology 65: 769-790.

Qureshi, A., L. Mooney, M. Denton and K.G. Kerr. 2005. *Stenotrophomonas maltophilia* in salad. Emerging Infectious Diseases 11: 1157-1158.

Rademacher, T.W., R.B. Parekh and R.A. Dwek. 1988. Glycobiology. Annual Review of Biochemistry 57: 785-838.

Rathinasabapathi, B., M. Burnet, B.L. Russell, D.A. Gage, P.-C. Liao, G.J. Nye, P. Scott, J.H. Golbeck and A.D. Hanson. 1997. Choline monooxygenase, an unusual iron-sulfur enzyme catalyzing the first step of glycine betaine synthesis in plants: Prosthetic group characterization and cDNA cloning. Proceedings of the National Academy of Sciences of the United States of America 94: 3454-3458.

RFA. 2010. Industry resources: Co-products. Renewable Fuels Association, Washington, D.C. http://www.ethanolrfa.org/pages/industry-resources-coproducts [Accessed February 24, 2011].

Rhee, G.S., D.H. Cho, Y.H. Won, J.H. Seok, S.S. Kim, S.J. Kwack, R.D. Lee, S.Y. Chae, J.W. Kim, B.M. Lee, K.L. Park and K.S. Choi. 2005. Multigeneration reproductive and developmental toxicity study of *bar* gene inserted into genetically modified potato on rats. Journal of Toxicology and Environmental Health, Part A 68: 2263-2276.

Ridley, W.P., G.G. Harrigan, M.L. Breeze, M.A. Nemeth, R.S. Sidhu and K.C. Glenn. 2011. Evaluation of compositional equivalence for multitrait biotechnology crops. Journal of Agricultural and Food Chemistry 59: 5865-5876.

Rodoni, S., W. Mühlecker, M. Anderl, B. Kräutler, D. Moser, H. Thomas, P. Matile and S. Hörtensteiner. 1997. Chlorophyll breakdown in senescent chloroplasts (cleavage of pheophorbide *a* in two enzymic steps). Plant Physiology 115: 669-676.

Rooney, L.W. and S.O. Serna-Saldivar. 1987. Food uses of whole corn and dry-milled fractions. Pages 399-429 in Corn: Chemistry and Technology. S.A. Watson and P.E. Ramstad (eds.). American Association of Cereal Chemists, St. Paul, Minnesota.

Rosche, B., B. Tshisuaka, B. Hauer, F. Lingens and S. Fetzner. 1997. 2-oxo-1,2-dihydroquinoline 8-monooxygenase: Phylogenetic relationship to other multicomponent nonheme iron oxygenases. Journal of Bacteriology 179: 3549-3554.

Russell, B.L., B. Rathinasabapathi and A.D. Hanson. 1998. Osmotic stress induces expression of choline monooxygenase in sugar beet and amaranth. Plant Physiology 116: 859-865.

Ryan, R.P., S. Monchy, M. Cardinale, S. Taghavi, L. Crossman, M.B. Avison, G. Berg, D. van der Lelie and J.M. Dow. 2009. The versatility and adaptation of bacteria from the genus *Stenotrophomonas*. Nature Reviews Microbiology 7: 514-525.

Salomon, S. and H. Puchta. 1998. Capture of genomic and T-DNA sequences during double-strand break repair in somatic plant cells. EMBO Journal 17: 6086-6095.

Schmelz, E.A., J. Engelberth, H.T. Alborn, P. O'Donnell, M. Sammons, H. Toshima and J.H. Tumlinson. 2003. Simultaneous analysis of phytohormones, phytotoxins, and volatile organic compounds in plants. Proceedings of the National Academy of Sciences of the United States of America 100: 10552-10557.

Schmidt, C.L. and L. Shaw. 2001. A comprehensive phylogenetic analysis of Rieske and Rieske-type iron-sulfur proteins. Journal of Bioenergetics and Biomembranes 33: 9-26.

Sidorov, V. and D. Duncan. 2009. *Agrobacterium*-mediated maize transformation: Immature embryos versus callus. Pages 47-58 in Methods in Molecular Biology: Transgenic Maize - Methods and Protocols. M.P. Scott (ed.). Humana Press, Inc, Totowa, New Jersey.

Silvanovich, A., M.A. Nemeth, P. Song, R. Herman, L.Tagliani and G.A. Bannon. 2006. The value of short amino acid sequence matches for prediction of protein allergenicity. Toxicological Sciences 90: 252-258.

Stalker, D.M., C.M. Thomas and D.R. Helinski. 1981. Nucleotide sequence of the region of the origin of replication of the broad host range plasmid RK2. Molecular and General Genetics 181: 8-12.

Sutcliffe, J.G. 1979. Complete nucleotide sequence of the *Escherichia coli* plasmid pBR322. Cold Spring Harbor Symposia on Quantitative Biology 43: 77-90.

Swings, J., P. De Vos, M. Van den Mooter and J. De Ley. 1983. Transfer of *Pseudomonas maltophilia* Hugh 1981 to the genus *Xanthomonas* as *Xanthomonas maltophilia* (Hugh 1981) comb. nov. International Journal of Systematic Bacteriology 33: 409-413.

Tanaka, A., H. Ito, R. Tanaka, N.K. Tanaka, K. Yoshida and K. Okada. 1998. Chlorophyll *a* oxygenase (*CAO*) is involved in chlorophyll *b* formation from chlorophyll *a*. Proceedings of the National Academy of Sciences of the United States of America 95: 12719-12723.

Thomas, K., M. Aalbers, G.A. Bannon, M. Bartels, R.J. Dearman, D.J. Esdaile, T.J. Fu, C.M. Glatt, N. Hadfield, C. Hatzos, S.L. Hefle, J.R. Heylings, R.E. Goodman, B. Henry, C. Herouet, M. Holsapple, G.S. Ladics, T.D. Landry, S.C. MacIntosh, E.A. Rice, L.S. Privalle, H.Y. Steiner, R. Teshima, R. van Ree, M. Woolhiser and J. Zawodny. 2004. A multi-laboratory evaluation of a common in vitro pepsin digestion assay protocol used in assessing the safety of novel proteins. Regulatory Toxicology and Pharmacology 39: 87-98.

Thomas, K., G. Bannon, S. Hefle, C. Herouet, M. Holsapple, G. Ladics, S. MacIntosh and L. Privalle. 2005. In silico methods for evaluating human allergenicity to novel proteins: International Bioinformatics Workshop Meeting Report, 23-24 February 2005. Toxicological Sciences 88: 307-310.

Thompson, C.J., N.R. Movva, R. Tizard, R. Crameri, J.E. Davies, M. Lauwereys and J. Botterman. 1987. Characterization of the herbicide-resistance gene *bar* from *Streptomyces hygroscopicus*. EMBO Journal 6: 2519-2523.

U.S. CPSC. 1997. An update on formaldehyde. U.S. Consumer Product Safety Commission, Washington, D.C.

U.S. EPA. 1996. Residue chemistry test guidelines - Nature of the residue - Plants, livestock. OPPTS 860.1300. U.S. Environmental Protection Agency, Office of Prevention, Pesticides and Toxic Substances, Washington, D.C.

U.S. EPA. 1997. Phosphinothricin acetyltransferase and the genetic material necessary for its production in all plants; Exemption from the requirement of a tolerance on all raw agricultural commodities. Federal Register 62: 17717-17720.

U.S. EPA. 2008. Reregistration eligibility decision for formaldehyde and paraformaldehyde. EPA 739-R-08-004. U.S. Environmental Protection Agency, Office of Pesticide Programs, Washington, D.C.

U.S. EPA. 2009a. Memorandum: Correction to the amendments to the dicamba RED. U.S. Environmental Protection Agency, Office of Prevention, Pesticides, and Toxic Substances, Washington, D.C.

U.S. EPA. 2009b. Reregistration eligibility decision for dicamba and associated salts. U.S. Environmental Protection Agency, Office of Prevention, Pesticides, and Toxic Substances, Washington, D.C.

U.S. FDA. 1995a. AgrEvo BNF No. 23: Oilseed rape: Tolerance to the herbicide glufosinate-ammonium. HCN92. U.S. Food and Drug Administration, Washington, D.C. http://www.accessdata.fda.gov/scripts/fcn/fcnDetailNavigation.cfm?rpt=bioListing&id=8 [Accessed April 2, 2012].

U.S. FDA. 1995b. AgrEvo BNF No. 29: Corn: Tolerance to the herbicide glufosinate-ammonium. T14, T25. U.S. Food and Drug Administration, Washington, D.C. http://www.accessdata.fda.gov/scripts/fcn/fcnDetailNavigation.cfm?rpt=bioListing&id=15 [Accessed April 2, 2012].

U.S. FDA. 1996. Dekalb Genetics BNF No. 28: Corn: Tolerance to the herbicide glufosinate-ammonium. DLL25. U.S. Food and Drug Administration, Washington, D.C. http://www.accessdata.fda.gov/scripts/fcn/fcnDetailNavigation.cfm?rpt=bioListing&id=16 [Accessed April 2, 2012].

U.S. FDA. 1997. AgrEvo BNF No. 46: Canola: Tolerance to the herbicide glufosinate-ammonium. T45. U.S. Food and Drug Administration, Washington, D.C. http://www.accessdata.fda.gov/scripts/fcn/fcnDetailNavigation.cfm?rpt=bioListing&id=30 [Accessed April 2, 2012].

U.S. FDA. 1998a. AgrEvo BNF No. 55: Soybean: Tolerance to the herbicide glufosinate-ammonium. A2704-12, A5547-127. U.S. Food and Drug Administration, Washington, D.C. http://www.accessdata.fda.gov/scripts/fcn/fcnDetailNavigation.cfm?rpt=bioListing&id=38 [Accessed April 2, 2012].

U.S. FDA. 1998b. AgrEvo BNF No. 38: Sugar beet: Tolerance to the herbicide glufosinate-ammonium. T120-7. http://www.accessdata.fda.gov/scripts/fcn/fcnDetailNavigation.cfm?rpt=bioListing&id=43 [Accessed April 2, 2012].

U.S. FDA. 2000. Aventis BNF No. 63: Rice: Tolerance to the herbicide glufosinate-ammonium. LLRICE E06, LLRICE E62. U.S. Food and Drug Administration, Washington, D.C. http://www.accessdata.fda.gov/scripts/fcn/fcnDetailNavigation.cfm?rpt=bioListing&id=50 [Accessed April 2, 2012].

U.S. FDA. 2003. Bayer CropScience BNF No. 86: Cotton: Tolerance to the herbicide glufosinate-ammonium. LLCotton25. U.S. Food and Drug Administration, Washington, D.C. http://www.accessdata.fda.gov/scripts/fcn/fcnDetailNavigation.cfm?rpt=bioListing&id=56 [Accessed April 2, 2012].

USDA-FAS. 2013a. Corn: Production (1000 MT), country. U.S. Department of Agriculture, Foreign Agricultural Service, Washington, D.C. http://apps.fas.usda.gov/psdonline/psdResult.aspx [Accessed January 8, 2014].

USDA-FAS. 2013b. Corn: Production (1000 MT), world. U.S. Department of Agriculture, Foreign Agricultural Service, Washington, D.C. http://apps.fas.usda.gov/psdonline/psdResult.aspx [Accessed January 8, 2014].

USHHS-ATSDR. 1999. Toxicological profile for formaldehyde. U.S. Department of Health and Human Services, Agency for Toxic Substances and Disease Registry, Washington, D.C.

USHHS-NTP. 2011. Report on carcinogens. U.S. Department of Health and Human Services, National Toxicology Program, Washington, D.C.

Vassilopoulou, E., N. Rigby, F.J. Moreno, L. Zuidmeer, J. Akkerdaas, I. Tassios, N.G. Papadopoulos, P. Saxoni-Papageorgiou, R. van Ree and C. Mills. 2006. Effect of *in vitro* gastric and duodenal digestion on the allergenicity of grape lipid transfer protein. Journal of Allergy and Clinical Immunology 118: 473-480.

Venkatesh, T.V., M.L. Breeze, K. Liu, G.G. Harrigan and A.H. Culler. 2014. Compositional analysis of grain and forage from MON 87427, an inducible male sterile and tissue selective glyphosate-tolerant maize product for hybrid seed production. Journal of Agricultural and Food Chemistry 62: 1964-1973.

Vieths, S., J. Reindl, U. Müller, A. Hoffmann and D. Haustein. 1999. Digestibility of peanut and hazelnut allergens investigated by a simple in vitro procedure. European Food Research and Technology 209: 379-388.

Waksman, S.A. and A.T. Henrici. 1943. The nomenclature and classification of the actinomycetes. Journal of Bacteriology 46: 337-341.

Wang, X.-Z., B. Li, P.L. Herman and D.P. Weeks. 1997. A three-component enzyme system catalyzes the O demethylation of the herbicide dicamba in *Pseudomonas maltophilia* DI-6. Applied and Environmental Microbiology 63: 1623-1626.

Watson, S.A. 1988. Corn marketing, processing, and utilization. Pages 881-940 in Corn and Corn Improvement. Third Edition. G.F. Sprague and J.W. Dudley (eds.). American Society of Agronomy, Inc., Crop Science Society of America, Inc., Soil Science Society of America, Inc., Madison, Wisconsin.

Wehrmann, A., A.V. Vliet, C. Opsomer, J. Botterman and A. Schulz. 1996. The similarities of *bar* and *pat* gene products make them equally applicable for plant engineers. Nature Biotechnology 14: 1274-1278.

Werlen, C., H.-P.E. Kohler and J.R. van der Meer. 1996. The broad substrate chlorobenzene dioxygenase and *cis*-chlorobenzene dihydrodiol dehydrogenase of *Pseudomonas* sp. strain P51 are linked evolutionarily to the enzymes for benzene and toluene degradation. Journal of Biological Chemistry 271: 4009-4016.

WHO. 2002. Concise international chemical assessment document 40: Formaldehyde. World Health Organization, Geneva, Switzerland.

Wild, A. and R. Manderscheid. 1984. The effect of phosphinothricin on the assimilation of ammonia in plants. Zeitschrift für Naturforschung C 39: 500-504.

Wishart, D.S. 2010. Human metabolome database. www.hmdb.ca [Accessed June 2, 2010].

Wishart, D.S., C. Knox, A.C. Guo, R. Eisner, N. Young, B. Gautam, D.D. Hau, N. Psychogios, E. Dong, S. Bouatra, R. Mandal, I. Sinelnikov, J. Xia, L. Jia, J.A. Cruz, E. Lim, C.A. Sobsey, S. Shrivastava, P. Huang, P. Liu, L. Fang, J. Peng, R. Fradette, D. Cheng, D. Tzur, M. Clements, A. Lewis, A. De Souza, A. Zuniga, M. Dawe, Y. Xiong, D. Clive, R. Greiner, A. Nazyrova, R. Shaykhutdinov, L. Li, H.J. Vogel and I. Forsythe. 2009. HMDB: A knowledgebase for the human metabolome. Nucleic Acids Research 37: D603-D610.

Wohlleben, W., W. Arnold, I. Broer, D. Hillemann, E. Strauch and A. Pühler. 1988. Nucleotide sequence of the phosphinothricin *N*-acetyltransferase gene from *Streptomyces viridochromogenes* Tü494 and its expression in *Nicotiana tabacum*. Gene 70: 25-37.

Wych, R.D. 1988. Production of hybrid seed corn. Pages 565-607 in Corn and Corn Improvement. Third Edition. G.F. Sprague and J.W. Dudley (eds.). American Society of Agronomy, Inc., Crop Science Society of America, Inc., Soil Science Society of America, Inc., Madison, Wisconsin.

Yagami, T., Y. Haishima, A. Nakamura, H. Osuna and Z. Ikezawa. 2000. Digestibility of allergens extracted from natural rubber latex and vegetable foods. Journal of Allergy and Clinical Immunology 106: 752-762.

Yang, M., E. Wardzala, G.S. Johal and J. Gray. 2004. The wound-inducible *Lls1* gene from maize is an orthologue of the *Arabidopsis Acd1* gene, and the LLS1 protein is present in non-photosynthetic tissues. Plant Molecular Biology 54: 175-191.

Zambryski, P., A. Depicker, K. Kruger and H.M. Goodman. 1982. Tumor induction by *Agrobacterium tumefaciens*: Analysis of the boundaries of T-DNA. Journal of Molecular and Applied Genetics 1: 361-370.

Zhou, J., G.G. Harrigan, K.H. Berman, E.G. Webb, T.H. Klusmeyer and M.A. Nemeth. 2011. Stability in the composition equivalence of grain from insect-protected maize and seed from glyphosate-tolerant soybean to conventional counterparts over multiple seasons, locations, and breeding germplasms. Journal of Agricultural and Food Chemistry 59: 8822-8828.